How many straight-line trajectories for MH370 ?

CAPTIO

V1.0c, 20-Apr-2021

Executive Summary

This study provides positive answers to the question: from Arc2 crossing locations within the range of latitudes [15°N; 3.4°S], is it possible to determine linear trajectories taking advantage of the 3D characteristics of the so-called Inmarsat arcs modulo some small adjustments of the flight parameters?

Millions of numerical estimations of such trajectories have been computed based on Arc2 latitude, track direction and speed limits using discrete sets of crossing locations at each arc.

Numerous such trajectories were found within latitudes within [5.8°N; 3.4°S] fitting all of the Inmarsat constraints i.e. timing, BTOs and BFOs, as well as operational and meteorological constraints and fuel autonomy. They are statistically equivalent to each other and equally probable. They lead to a large latitude span on Arc7 from 31.2°S to 39.3°S as illustrated below.

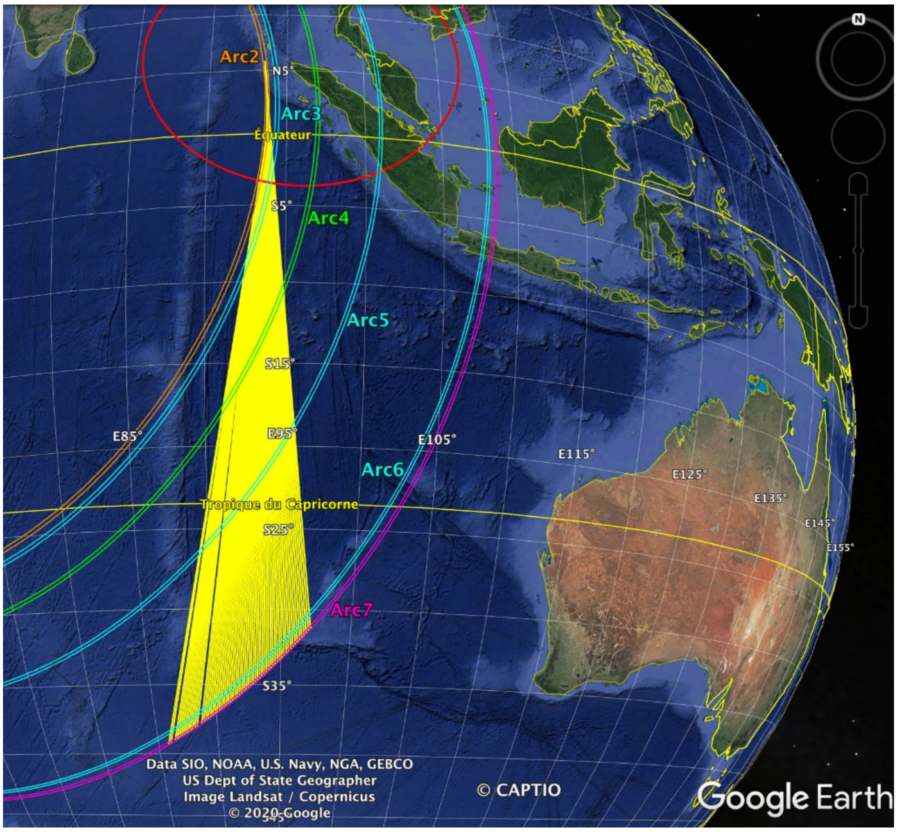

In addition, an analytic one-to-one relation is proposed for computing the best track direction of a straight-line trajectory at any latitude of the Arc2 crossing location.

Contents

1 Objective: 2
2 Preliminary observations about geometry 3
2.1 Geometry of the system under consideration 3
2.2 Shape of the arcs 3
2.3 Relative position of the arcs 5
2.4 Geometry of the "Arc crossing" 5
2.5 The appeal of track 180° 7
3 Fuel modelling 9
4 Analysis 10
4.1 A non-central symmetry 10
4.2 The methodology 11
4.3 The principle 11
4.4 The constraints 12
4.4.1 A gross reduction of the latitude span to be analysed 13
4.4.2 Track direction angular span 13
4.4.3 About the quantisation effect 13
4.4.4 About the wind 13
4.4.5 Recap of all constraints 14
4.5 The Analysis 14
4.5.1 Study based on lower ground speed standard deviation 14
4.5.2 Study based on lower BFOR standard deviation 19
4.5.3 Inmarsat example trajectory 21
5 Conclusions 22
6 References 23
7 Annex 1 23
8 Annex 2 24
9 Annex 3: MH370: Mastering BFO Residuals for Trajectory Selection 25

1 Objective:

The objective of this analysis is five-fold:

1- For each possible ARC2 crossing location, identify a set of linear trajectories exists that fit the Inmarsat signal constraints as well as fuel constraints and an operationally acceptable speed range,
2- Demonstrate that these trajectories are acceptable solutions when simplifying hypotheses are made i.e. flight in straight-line between Arc2 and Arc6, constant flight level and constant Mach number without any human intervention,
3- Demonstrate that such linear trajectories follow a privileged track direction which is a function of the latitude of the Arc2 crossing location,
4- Verify that the Inmarsat-suggested trajectory is one among a large set of other possible trajectories, starting at Arc2 crossing latitude 0°,
5- Demonstrate that the number of acceptable trajectories is very high leading to a large span of end points on Arc7.

2 Preliminary observations about geometry

2.1 Geometry of the system under consideration

The system under consideration (SuC) includes the moving aircraft, the real moving Inmarsat's 3F1 Indian Ocean Region satellite (3F1-IOR) as described in [1], the Inmarsat ground infrastructure and the on-board aircraft Doppler compensation algorithm as described in [2]. In Annex3, CAPTIO has demonstrated the direct relation of the Burst Frequency Offset residuals (BFORs) to the geometry of the system mentioned above and illustrated in Figure 1 below, particularly in respect of the North-South excursion of 3F1-IOR and the fixed position of the perfect satellite used as a reference.

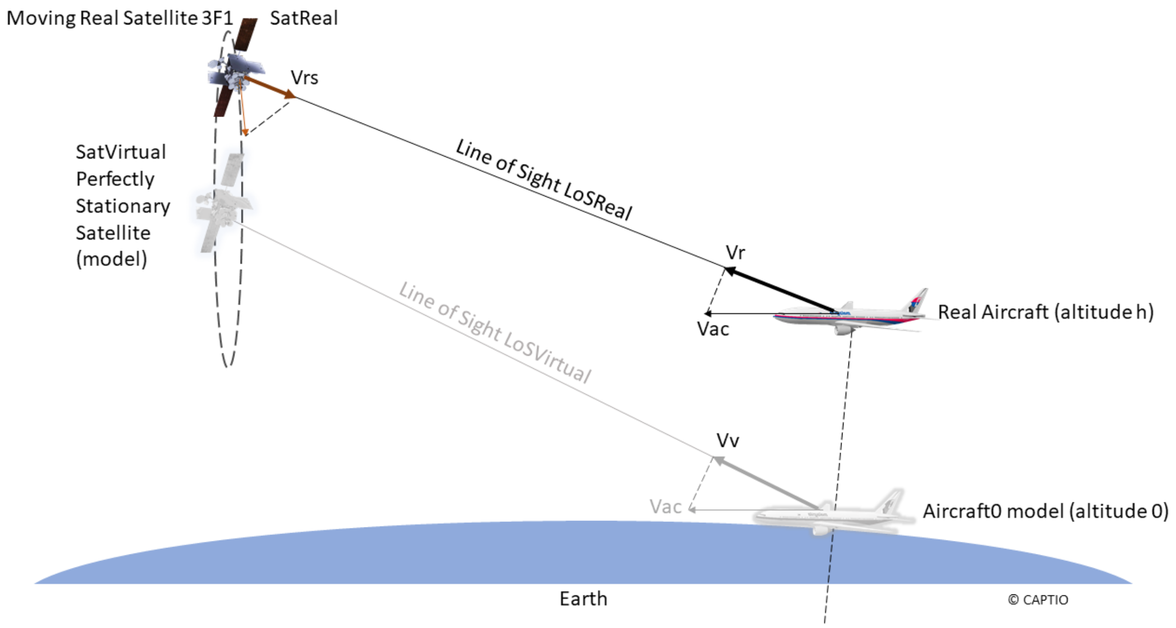

Figure 1: The 4 principal components of the SuC

The important conclusion from these studies to be kept in mind is that two trivial directions (180° and 0°) are intrinsic to the system, independently of the actual trajectory flown by the aircraft. No matter what the geographical location of the aircraft is, the sensitivity of the BFORs to the track angle is very low around these trivial directions offering a vast range of possible track/speed combinations compatible with the +/-7 Hz tolerance defined in [1].

2.2 Shape of the arcs

During the unknown leg of MH370 i.e. the flight path flown after the reboot of the SATCOM at 18h25:27 UTC, Inmarsat recorded Burst Time Offsets - so-called measured BTO - which is a time shift used to estimate the travel time of the signal between the satellite and the aircraft at each so-called arc. The BTOs are used to determine the nominal slant range distance at each arc i.e. the radius of a sphere centred on 3F1-IOR. The marginal error on BTO measurement is about 50µs as indicated by Inmarsat in [1]. In fact, an arc is a volumetric ring limited at its bottom by the Earth ellipsoid at sea level, at its top by the ellipsoid at the maximum flying altitude circa 45000ft and also limited by the two spheres centred on the 3F1-IOR satellite with a radius equal to the distance corresponding to BTO-50µs (inside) and to the distance corresponding to BTO+50µs (outside). A cross-section of the arc ring is sketched by the red dotted lines in Figure 2.

Thus, crossing an arc_i at time t_i means that the aircraft was inside the ring somewhere in the cross-section area limited by the red dotted lines at that particular time without further precision on its exact position in this area. It should be kept in mind that every location within the cross-section is thus a valid crossing point.

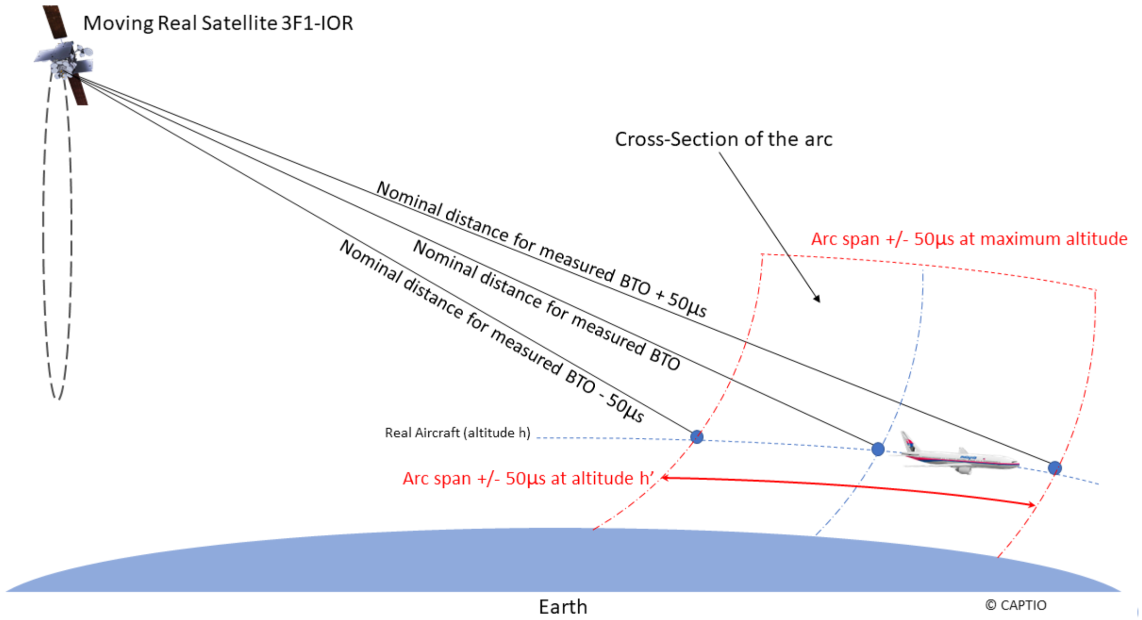

Figure 2: The arc ring shape considering the +/- 50µs uncertainty

The width (in km or Nm) of the cross-section of the arc-band is thus dependent of the BTO: The larger the BTO, the further away is the aircraft from the satellite and thus the lower the elevation of the satellite at the aircraft position which is further decreased in time by the North to South course of the Satellite. This reduces the distance between the limiting inner and outer spheres mentioned above. This explains why, after arc2, each arc is narrower than its predecessor. Figure 3 illustrates an example of a top view of Arc1 to Arc6 for the altitude 35000ft. Additionally Arc5 is also depicted at altitude 5000ft. At 5000ft, Arc5 shift towards the centre is clearly visible as expected (in red).

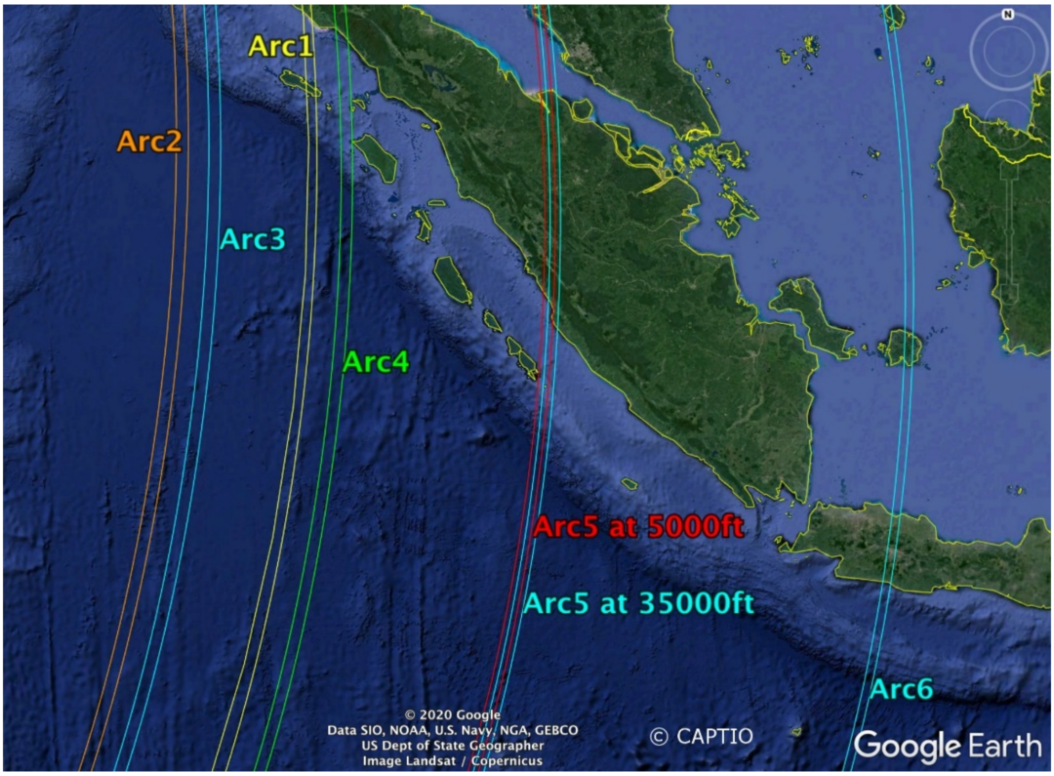

Figure 3: The arcs width at altitude 35000ft considering the +/- 50µs uncertainty
(in red is an example of the shift of Arc5 towards the inside due to a lower altitude)

In addition, as during MH370 flight time the real 3F1-IOR satellite is first moving to the north then to the south, the arc rings are not concentric but distributed along the path followed by the vertical projection of 3F1-IOR on the Earth ellipsoid (cf below Figure 4 Right).

2.3 Relative position of the arcs

Would 3F1-IOR satellite be perfectly geostationary-fixed, the arcs would be concentric like in Figure 4 left. But the real satellite was moving on a quasi-north-south direction – as from 19h41 – thus the arcs centre location shifted with time as shown (not to scale) in Figure 4 right. This particular north-south direction will contribute to the trivial solutions as explained in Annex3 and hereunder.

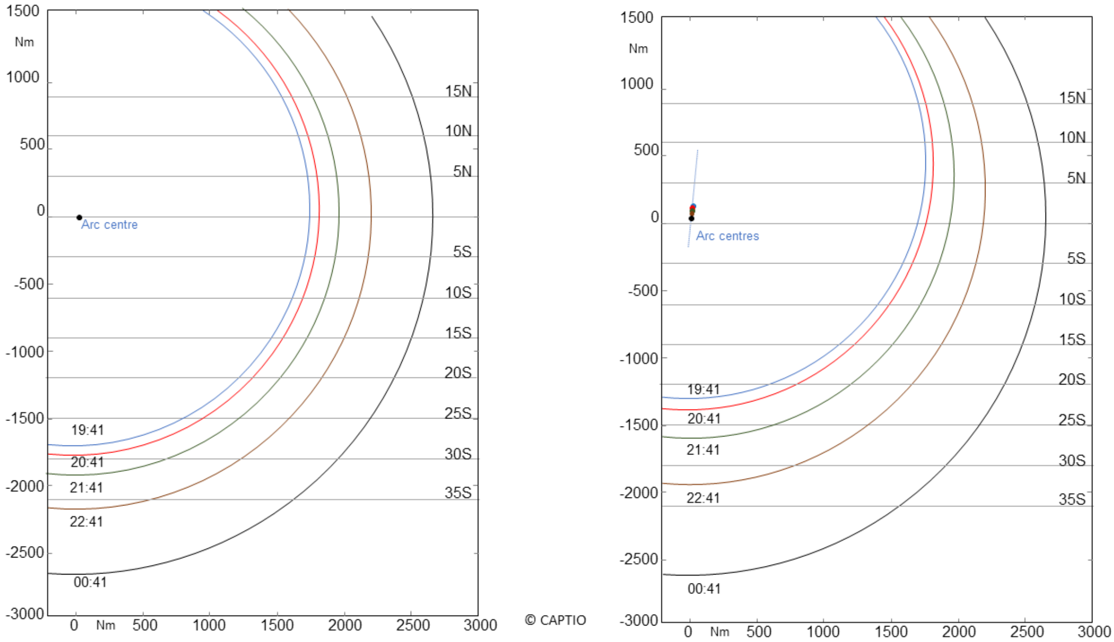

Figure 4: Left: Hypothetical concentric arcs from perfect satellite, Right: Shifted arcs from real moving satellite (not to scale)

2.4 Geometry of the "Arc crossing"

The non-zero width of the arcs brings forward the importance of the track direction of the aircraft versus the arc radius when crossing occurs.

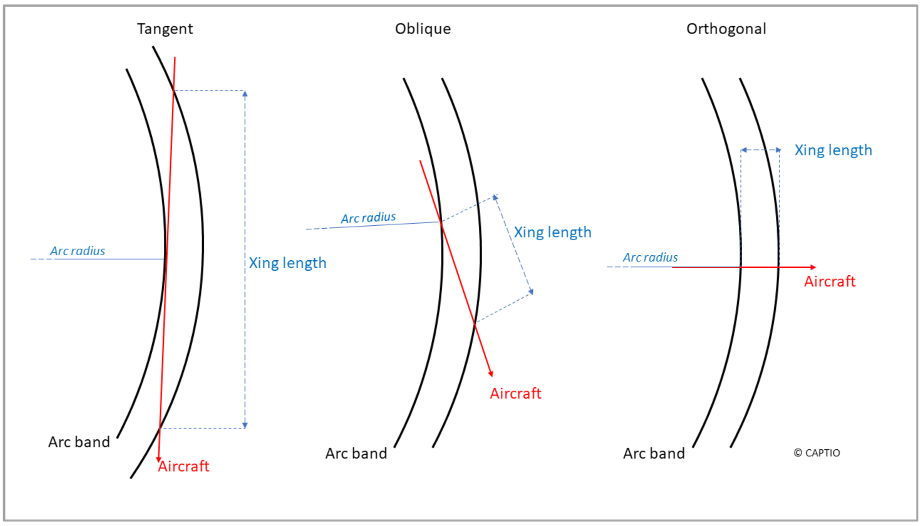

Figure 5: Length of an arc crossing (Xing) as a function of the angle [arc radius; track direction]

As illustrated in Figure 5 by three different examples of track direction, the length of the arcs crossing (called Xing length in the figure) is dependent of the angle between the arc radius and the aircraft track direction at the location of crossing. This is equivalent to saying dependent of the angle between the tangent to the arc and the aircraft track direction since the two angles differ by 90°.

For example, taking one tangent to Arc2 with a track direction of 180° as illustrated by the yellow vertical line in Figure 6, at an altitude of 35000ft, the acceptable crossing locations of Arc2 span from latitude ~5.8°N down to ~ 2.1°S representing a distance of ~850km (~460Nm) because the trajectory is chosen tangent to the inner border of Arc2 maximising the path inside this arc. The subsequent crossing segment of Arc3 in continuation on the same trajectory of 180° is around latitude 5.0°S with an acceptable span of 130km (~70Nm) inside Arc3. Would the track direction be at 90°, the crossing length at Arc2 would be ~28.8km (15.6Nm) and the subsequent crossing length at Arc3 would be 28km (15.1Nm). Table 1 details the figures for these examples.

Arc	Crossing length for track direction			
	180°		90°	
	km	*Nm*	*km*	*Nm*
2	850	460	28.8	15.6
3	130	70	28	15.1
4	59	32	25	13.5
5	43	23	24	13.0
6	29	15.7	20	10.8

Table 1: Successive approximate crossing lengths for examples of linear trajectories on track 180° and 90° at 35000ft

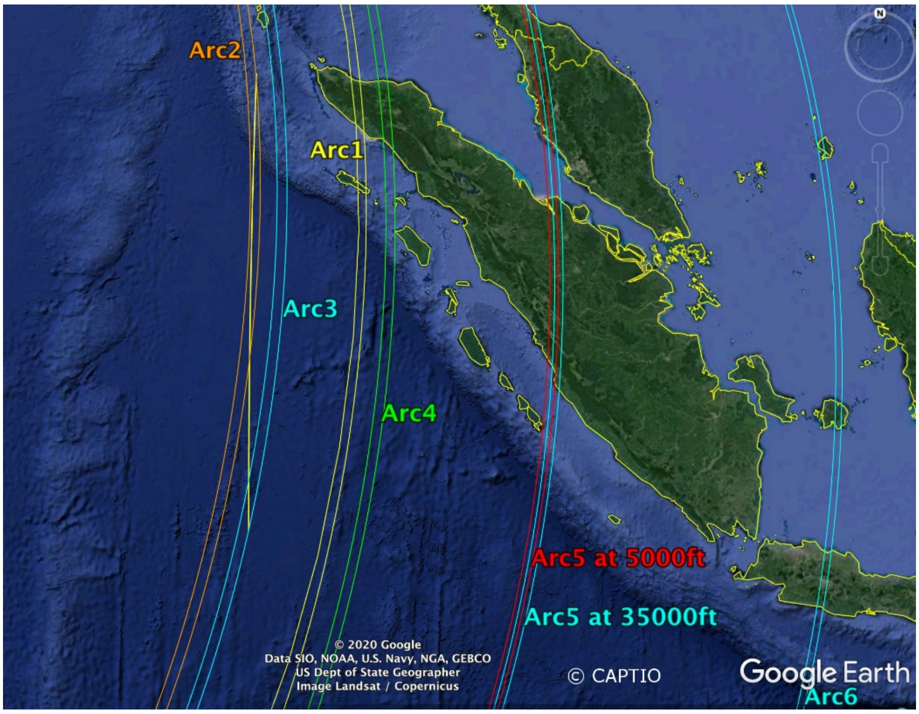

Figure 6: Example of a crossing tangent at Arc2 and subsequently Arc3 with a track at 180° (yellow line)

The probability of finding a trajectory is directly linked to the crossing length. This explains why the first published trajectories were linear trajectories heading south due to their maximising the chance of matching all the constraints, in addition to the choice to minimise variations in the trajectory parameters or variables (i.e. not piloted). At Arc2, the increase of probability is already by a factor 850/29=~29. As there are 4 subsequent arcs (Arcs3-6) under consideration, the probability to find a linear trajectory is further increased approximately by a factor of (130/28) at Arc3, (59/25) at Arc 4, (43/24) at Arc5 and (29/20) at Arc6. Altogether fitting a north/south straight line is simplified by a factor up to ~460 compared to a west/east trajectory without any other consideration.

2.5 The appeal of track 180°

In the early stage of the search for MH370 wreckage, Inmarsat proposed an example of a possible trajectory with the assumption that the trajectory should be as stable as possible (constant heading, constant altitude, constant speed) i.e. including the lowest number of variables as possible.

These assumptions imply that the aircraft was no longer piloted. Thus, a quasi-constant speed is expected, with slight evolutions related to the decreasing fuel weight, to wind variations, and also to some possible automatic flight control adjustments.

As seen in Annex3, the BFORs are very accommodating for the speed range when flying around the trivial 180° direction as illustrated in Figure 7 where any speed in the interval [~345;~492] kts is acceptable for the BFOR to stay within the +/-7Hz tolerance interval. At altitude 35,000 ft, the distance span yielded at each arc leads to acceptable speed variations which are in fact bound by the most constraining Arc5-Arc6 segment. At this altitude, this means that one can choose any constant speed in this speed interval to fit the timing for crossing the arcs while matching the BFORs margins. The selection of the crossing location of Arc2 is subsequently straightforward by a backwards-linear extrapolation from Arc3. Due to the 850km admissible crossing length at Arc2 for a track direction 180°, one is certain to find a crossing location that fits the purpose.

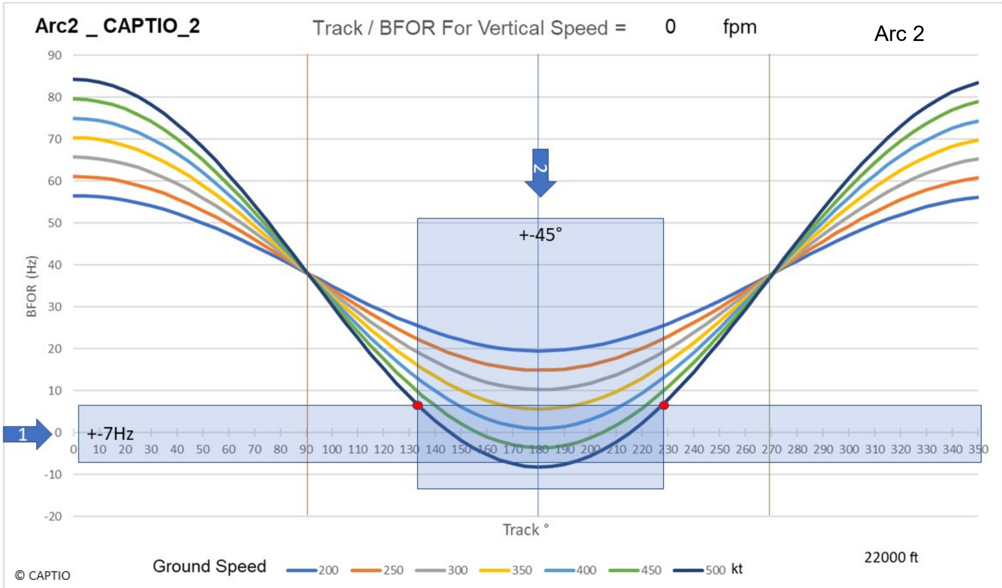

Figure 7: Acceptable aircraft velocity direction interval at Arc 2 CAPTIO

For a given fixed ground speed, the BFORs behaviour versus the track direction is similar for all latitudes along one arc. The shape of the curve as a function of the latitude also confirms that the trivial directions 0° and 180° are inherent characteristics of the system.
Figure 8, Figure 9 and Figure 10 illustrate this BFORs behaviour along Arc2, Arc4 and Arc6 for 490kt ground speed versus the track direction.
More details will be provided by CAPTIO in [5] "MH370: Trajectory Selection based on BFO Residuals".

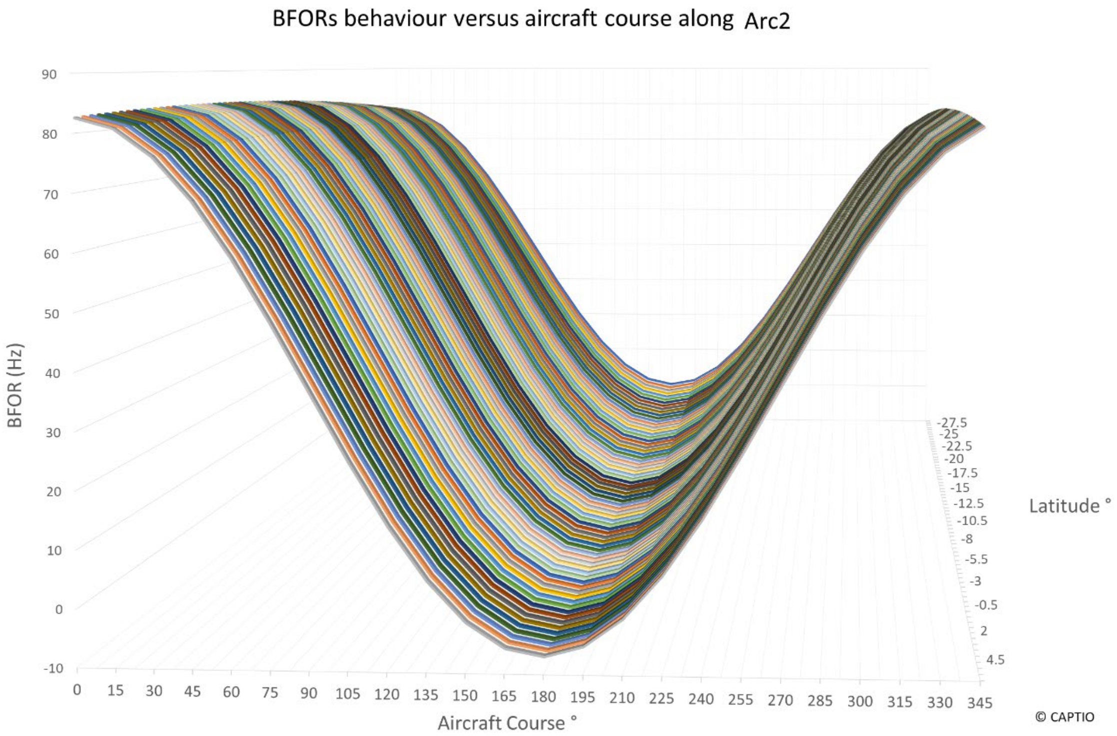

Figure 8: BFORs behaviour along Arc2 versus latitude and aircraft track direction at 490kt GSP

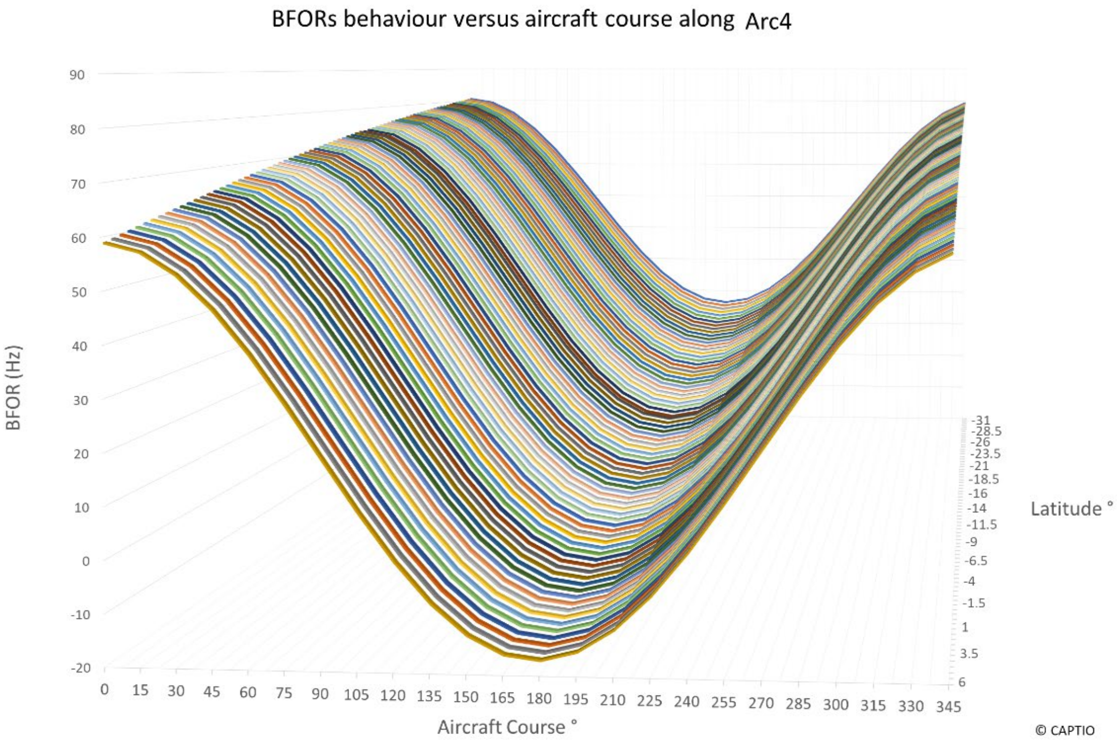

Figure 9: BFORs behaviour along Arc4 versus latitude and aircraft track direction at 490kt GSP

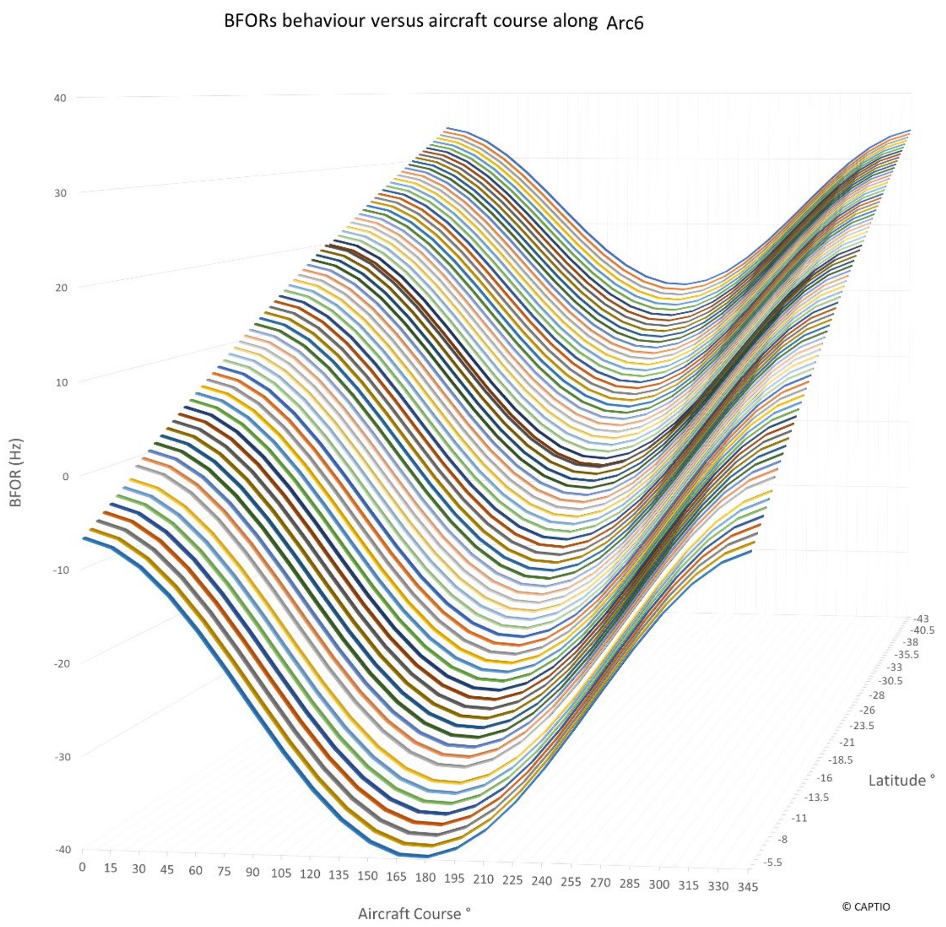

Figure 10: BFORs behaviour along Arc6 versus latitude and aircraft track direction 490kt GSP

3 Fuel modelling

Today, the accuracy of the fuel consumption models is around 4% or 5%. Furthermore, based on these models it is assumed that the fuel weight at Arc2 is around 26.7t. The possible combinations of average speed with distance flown in a timely manner provide a large variety of solutions. Table 2 summarises the limits in distance, altitude and average ground speed computed by our Constraint Assessment Tool (CAT) within which the flight could have occurred (the symbol * means the max or min whichever is obviously appropriate).

Altitude	Arc2-Arc6 Distance *km*	Arc2-Arc6 Distance *Nm*	Average Ground Speed *kt*	Mach[1]
~34000ft	3820	2067	450*	0.777
~40000ft	3975	2146	485*	0.845
~40000ft	4068*	2194	475	0.828

Table 2: Boundaries in distance, average speed and altitude based on fuel weight = 26.7t at Arc2.

Any acceptable linear trajectory will be retained if it fits within these boundaries, which are in full agreement with the information provided in the B777-FCOM document.

[1] *ISA temperature was taken equal to 10°C*

4 Analysis

4.1 A non-central symmetry

From the estimated location of the Arc1 crossing location at 18h25 UTC, and taking a maximum ground speed around 500kts, the latitude of possible locations of crossing Arc2 ranges from ~15.7N to ~3.4S approximately.

In the time interval between 19h30 UTC before Arc2 and 00h11 UTC at Arc6, 3F1-IOR satellite moved from north to south and the related ping rings moved accordingly, as illustrated in Figure 11. This shows that the geometry of the arcs does not hold a central symmetry based on the ping centres. This was studied in details in Annex3.

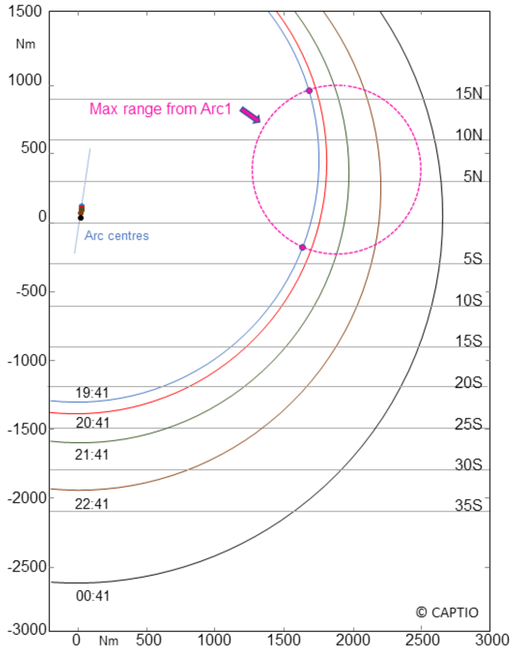

Figure 11: Position of Arcs 2 to 6 and their different centres locations (not to scale)

Thus, for all linear trajectories crossing Arc2 with the same relative track angle but at different latitudes, the distances between the subsequent arc crossing points are not identical from one trajectory to the next after a rotation around Arc2 centre, as illustrated in Figure 12. Thus, if a linear trajectory exists, its track direction will be different at each Arc2 crossing latitude. This demonstrates the influence of the geometry of the system on the very existence of linear trajectories.

Nevertheless, the foundation of this study is to answer the question: Is it possible to determine such a track direction taking into account the thickness of the arcs and small speed variation somehow compensating for this anisotropy within the restricted range of latitudes [15°N; 3.4°S]?

Some initial analyses along great circles have been performed in the past like in [3] and others. This analysis provides a positive answer to this question via systematic numerical estimations of the latitude, great circle from a given track direction at Arc2 and speed boundaries. Numerous linear trajectories fitting the Inmarsat constraints (timing, BTOs and BFOs) can be found. In addition, an analytic relation is identified for computing the best linear trajectory track direction at each latitude of Arc2 crossing within restricted northern and southern boundaries.

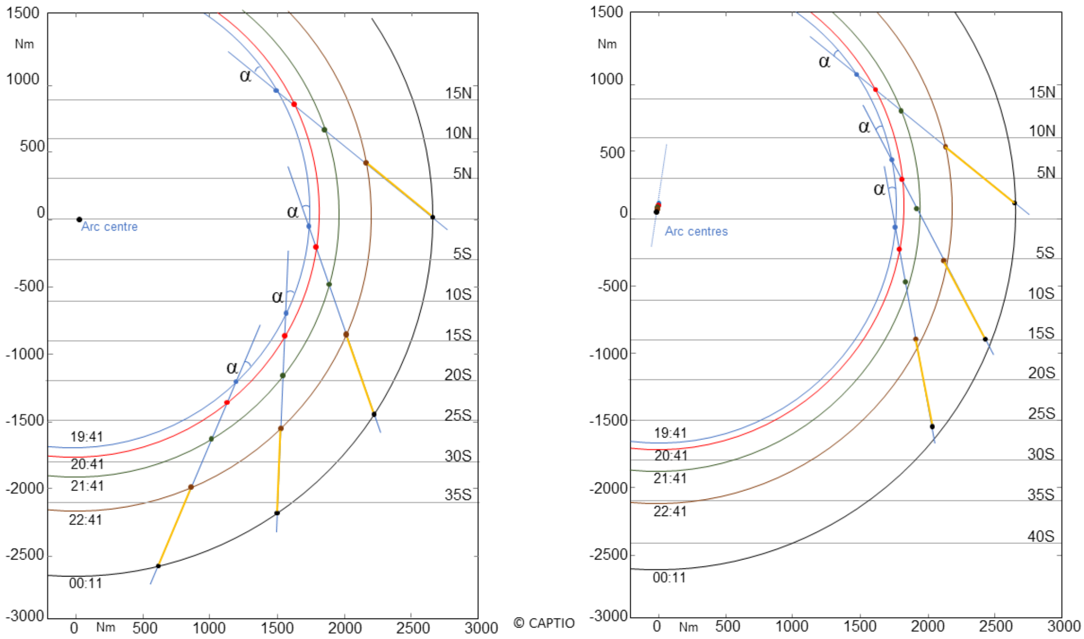

Figure 12: Central symmetry (left) preserves distances by rotation, reality (right) does not preserve distances

4.2 The methodology

Our methodology consists in building aligned “chains” of crossing points at arcs 2 to 6 along a great circle line for digitized initial track directions at Arc2. Arc7 is not an issue because the end of the flight with engine flameout is out of scope of this study. So Arc7 crossing location is arbitrarily chosen in the same track direction from Arc6.

A chain construction is straightforward and follows these steps:

1- Select the central crossing point in Arc2 corresponding to the selected latitude (a unique point) and select an initial track direction
2- Identify a set of points within Arc3 width along the great circle line at regular intervals (predefined odd number of points)
3- Repeat this computation for arcs 4 to 6

Doing so without further limitation would simply lead to billions of trajectories to be computed. For example, considering 20 crossing points per degree of latitude along Arc2 with 17 aligned crossing points per subsequent arc and an initial track direction angular span of 2.5°, this leads to ~1.4 billion trajectories computations for the segment 15°N to 3.4°S on Arc2. Thus, an additional step is required in the algorithm so as to stay within reasonably computable limits:

4- Select the trajectories satisfying a set of a priori constraints

4.3 The principle

The fundamental principle is to consider that any linear trajectory crosses subsequent arc rings, which have a substantial width as illustrated in Figure 13. The trajectory computation requires selecting one of the points inside the arc. Starting from Arc2 until Arc6, the algorithm progresses along all the possible branches of this developing tree. It evaluates the constraints at each arc crossing point and stops if they are not satisfied and so forth until all possible branches have been explored.

In this study, an odd number of points inside each arc is considered. They are regularly spaced along the linear trajectory and symmetrically located around the centre line of the arc. The interval length is deduced from the corresponding even number of intervals encompassed in the arc including a small margin to avoid getting too close to the "unsymmetrical" borders of the arc. The number of points retained as the best trade-off between the ground speed standard deviation precision and the number of trajectories to be evaluated was 17. Thus, from one point crossing the previous arc, there will be 17 legs ending at the next arc leading to 17 different distances and thus 17 different average speeds on these legs and so on. Consequently, 83521 linear trajectories could be potentially computed per track direction from any latitude on Arc2 until Arc6.

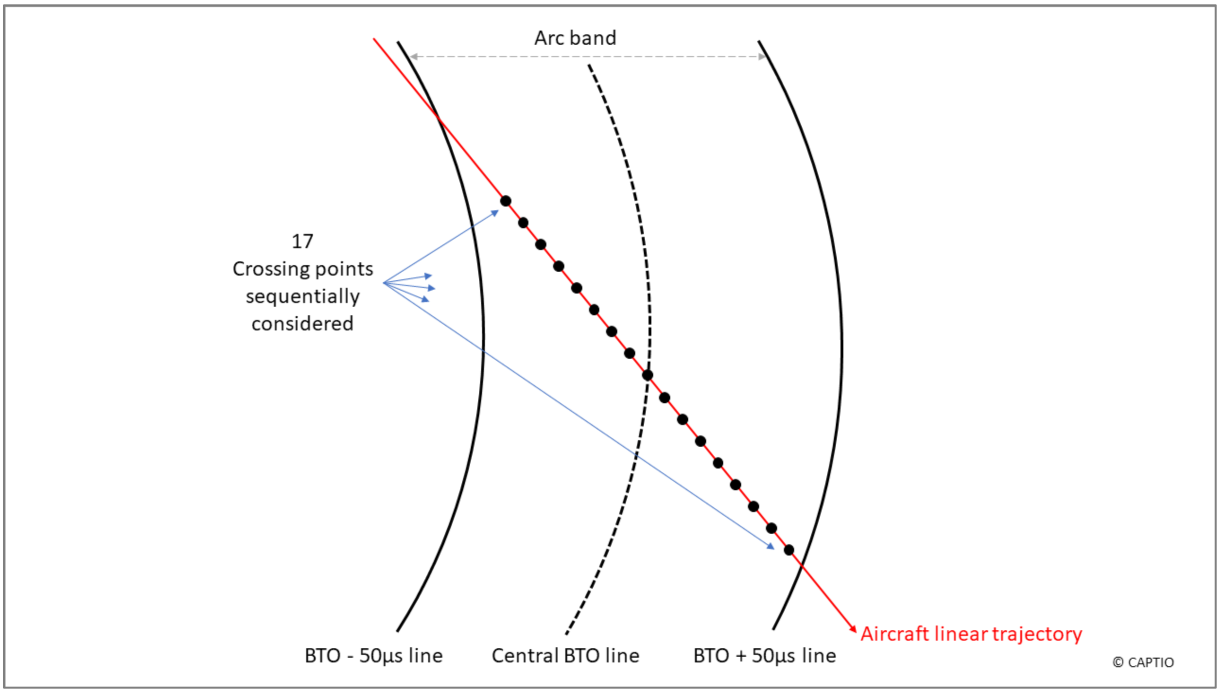

Figure 13: Candidate crossing points evenly located symmetrically from central line used in the computations

The sampling interval length is arc dependent as explained above, an example of which is posted in Table 3 at altitude 35000ft and for a track direction at 180°.

Arc	***Arc width at 180° (km)***	***Sampling Interval "d" including safety margin (km)***
Arc3	130	8.0
Arc4	59	3.6
Arc5	43	2.6
Arc6	29	1.7

Table 3: Table typical interval length inside the arcs at altitude 35000ft and for track direction 180°

4.4 The constraints

Firstly, due to the continuity of the variables under study, the sampling will be chosen to sufficiently describe the phenomenon but also to limit the computational requirements, which are tremendous otherwise.

Two variables need to be sampled: the latitude along Arc2 and the angular search sector of the linear trajectory track direction. Thus, the valid span of latitudes along Arc2 has been identified and an appropriate sampling interval has been selected. The track direction angular sampling interval has been chosen to be representative at the selected Arc2 latitude. The local lower and upper bounds determined a sliding window in order to stay around the best solution (according to a criteria minimisation process). The number of points considered inside each arc between two consecutive legs was found to be best with 17 points per arc. The numerical values of the constraints are posted in Table 5: Constraints imposed on the analysis.

4.4.1 A gross reduction of the latitude span to be analysed

A preliminary gross analysis was performed by using a large sampling interval to determine the northern latitude to start with and the southern latitude to stop at. The 6.3°N limit was the highest northern latitude providing trajectories respecting the +/-7Hz margin in BFO Residuals. The southern limit was reached at 3.35°S which happens to correspond closely to the maximum south-bound range of the aircraft. Boundaries are listed in Table 5.

4.4.2 Track direction angular span

After several trials and an evaluation of the ground speed standard deviation sensitivity, a 2.5° angular sector was adopted to find the local ground speed standard deviation minimum. This was used as a sliding window moving along with the evolution of Arc2 latitude. Inside this angular sector, sampling intervals of either 0.20° or 0.25° were used.

4.4.3 About the quantisation effect

The use of a limited set of crossing points inside each arc is similar to grouping the speed values between two arcs into classes as the only possible distances come from the product $S_i \times S_{i+1}$ of the two sets of points of these consecutive arcs. Thus, only certain fixed distance values are taken into consideration for the speed computation during this leg. Subsequently, a Sheppard's correction must be applied when considering the standard deviation of the speed as a function of the distance taken as a "continuous" variable. Sheppard's correction is $d^2/12$ where d is the sampling interval.
Interval d is dependent of the arc width as illustrated in the example in Table 3. Thus, taking the worst case as a basis, a corrective term can be applied as computed in Table 4 below.

Arc	***Sampling Interval "d"***		***Sheppard's Correction $d^2/12$***
	km	***kt***	***(kt)***
Arc3	**8.0**	**4.3**	**1.6**
Arc4	**3.6**	**1.9**	**0.3**
Arc5	**2.6**	**1.4**	**0.2**
Arc6	**1.7**	**0.9**	**0.1**

Table 4: Sheppard's correction for the most unfavourable case at track direction 180°

4.4.4 About the wind

To be closer to reality, the aloft component of the wind should be taken into account statistically. The analysis did not compute this value along each trajectory. Still, integrating the standard deviation of sampled measurements at representative locations is a practical way of inserting the effect of the wind along the computed trajectories. Table 6: Sampled wind characteristics at altitude 35000ft at track direction 180° is presented in Annex 1 posting representative values of aloft component of the wind for such linear trajectories at altitude 35000ft. Of particular interest is the standard deviation of this component which will be used for limiting the range of possible trajectories to the realistic cases.

The maximum standard deviation value determined for the wind field of interest is given in the last row of Table 6 i.e. σ =5.17 kt. Thus, in the analysis, this upper limit will be added to the max Sheppard's correction.

4.4.5 Recap of all constraints

Table 5 below presents a recapitulation of all the constraints imposed on the analysis detailed in chapter " 4.5 The Analysis":

Variable Name	***Constraints***	***Comments / Example***
Burst Time Offset (BTO) margin	+/-50µs	Inmarsat defined
Burst Frequency Offset Residual (BFOR)	+/-7Hz	Inmarsat defined
Max Arc2 Latitude North	6.3°N	Due to BFO Residuals +/-7 Hz
Min Arc2 Latitude South	3.35°S	Due to BFO Residuals +/-7 Hz coinciding with the aircraft range limit
Arc2 Latitude sampling interval	0.05° to 0.15°	0.15°sufficient for Track direction sampling so used for most of the computations
Flight Track Direction angular span	2.5° (sliding interval)	Ex. at 5°N: 175-177.5, Ex at 3°S: 189-191.5
Track Direction sampling interval	0.20° to 0.25°	0.25 sufficient, used for computation time savings
Ground Speed range	425 to 510 kts	Table 2 ground speed values +/-25kts margin. For Mach number see Table 2.
Flown distance range Arc2-Arc6	3820 – 4068km	See Table 2.
Number of crossing points inside each arc	17	Regularly located on each side of the BTO centre line on the trajectory, best trade-off
Fuel at Arc2	26.7t	Extrapolation from remaining 43.8t at 17h07.
Ground Speed Standard Deviation	6.8 kt	This value is the sum of the Sheppard's correction and of the wind maximum Std Dev.
Typical Altitude	35000ft	Similar to Inmarsat

Table 5: Constraints imposed on the analysis

4.5 The Analysis

The analysis was performed in successive steps. The first one was a systematic linear trajectory computation starting for the Max Arc2 latitude down to the Min Arc2 latitude with a track direction in the angular span of Table 5. Only those trajectories whose BFO Residuals are within the margin defined by Inmarsat were recorded. From the 171 million computed linear trajectories, 43.5 million satisfied this criterion.
Further constraining the selection of trajectories by their ground speed standard deviation in the operationally acceptable limits (cf Table 5), the number of acceptable linear trajectories is reduced to circa 38000 based on the limited set of 63 sampled "root" crossing points on the central BTO line at Arc2. Additionally, this constraint leads also to a decrease of the northern limit Max Arc2 Latitude North to 5.8°N.

The following studies are based on this reduced set of ~38000 linear trajectories.

4.5.1 Study based on lower ground speed standard deviation

The question addressed here is twofold: Are there linear trajectories for every latitude on Arc2 between 5.8°N and 3.35°S matching the constraints? If yes, does a direct link exist between the latitude and the track angle?

The answer to the first part of the question is yes. Within all the constraints, all latitudes on Arc2 between these limits do accept linear trajectories which are thus flyable.

To answer the second part of the question, the best linear trajectory - i.e. with the lower standard deviation of the computed ground speed (GSP) - for each latitude has been selected from the full set. Figure 14 presents the plot of the track direction of the best linear trajectories versus the latitude of the starting point on Arc2. In addition, we remember that the southern limit coming from the BFOR constraint coincides with the aircraft maximum range southern limit. Thus the answer is also yes.

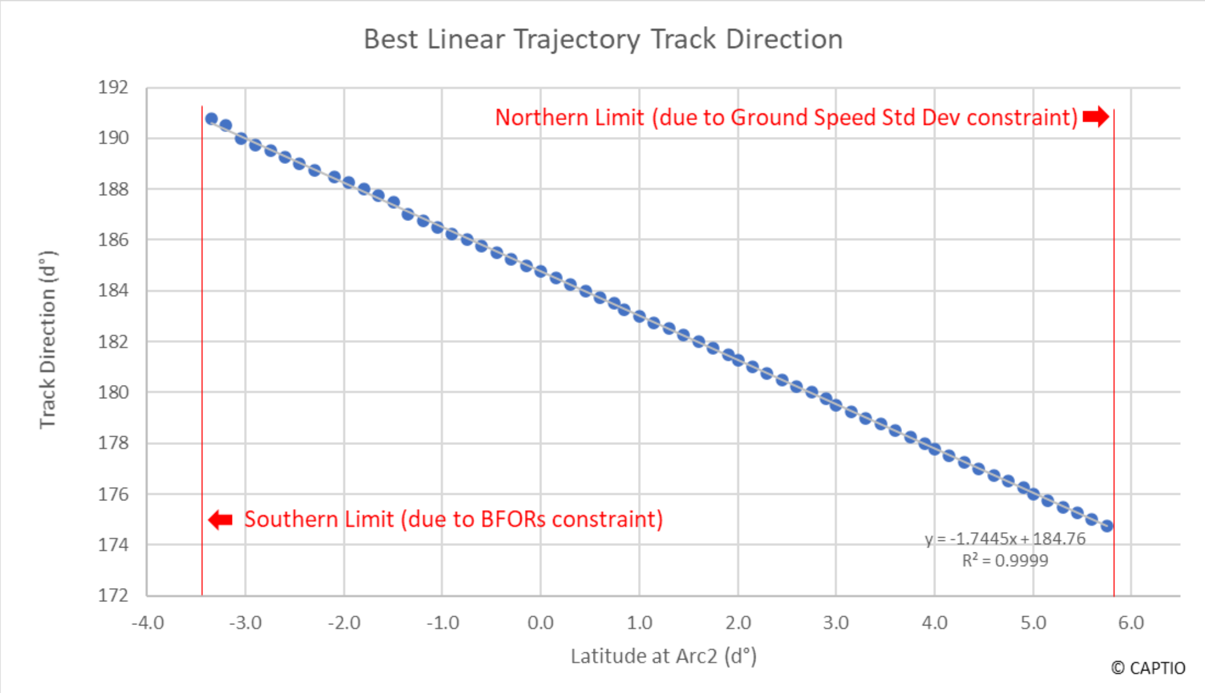

Figure 14: Track direction of the best GSP σ linear trajectories versus Arc2 crossing location latitude

The trend line shows a clear linear relationship between the Arc2 latitude and the linear trajectory track direction with an extremely good correlation coefficient. Consequently, it can be approximated into the following remarkable simple equation using α as the track direction and LatArc2 as Arc2 latitude crossing location between [5.75°N; 3.35°S]:

$$\alpha°(\mathrm{LatArc2}) \cong -1.7445 * LatArc2° + 184.77 \qquad (1)$$

This is a direct way to identify the best linear trajectory at altitude 35000ft[2] from any Arc2 latitude crossing location based on minimum ground speed standard deviation.

Taking the inverse of equation (1), one can infer that for any track direction α in [174.75°;190.75°] there always exists a crossing point at LatArc2 according to this one-to-one relationship:

$$\mathrm{LatArc2}°(\alpha) \cong -0.5732 * [\alpha° - 184.77] \qquad (1bis)$$

The subsequent average ground speed for each of these best trajectories is within the range [474;484] kt. This range is within the computed limits found by the fuel modelling in Table 2. It is plotted versus Arc2 latitude of the initial point in Figure 15. The vertical bars represent the respective standard deviation of the speed during the trajectory. The discontinuity of the curve of the speed points comes from the sampling mechanism of the points at the sampled crossing location of the arcs. The distance between two arcs being digitised, the subsequent speed is consequently digitised also.

[2] The altitude has a minor influence, thus the study is applicable to any altitude leading to minor changes in the coefficients only

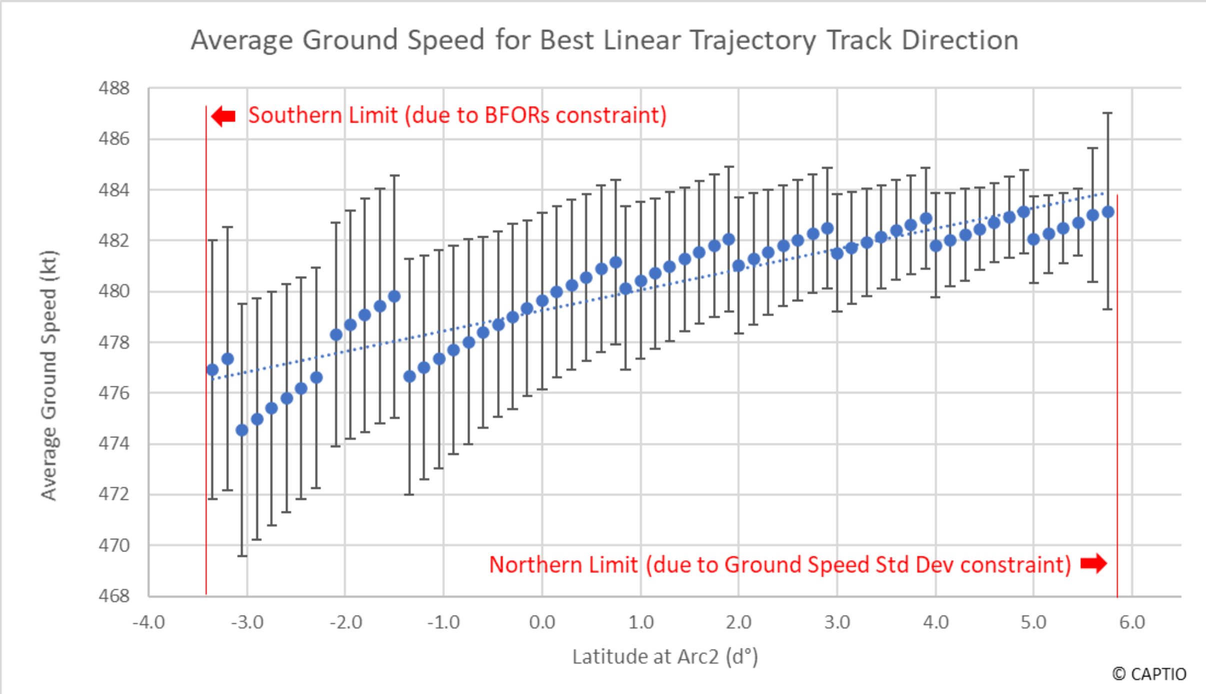

Figure 15: Average Ground Speed of the best linear trajectories versus Arc2 crossing location latitude (The vertical bars represent the respective standard deviation of the speed during the trajectory)

In principle, the selection of the best linear trajectories on minimum ground speed standard deviation does not imply that they would withhold the best performances for BFORs and their associated standard deviation. Nevertheless, thanks to the constraint to stay within the +/-7Hz BFOR margin, the selected trajectories are always compliant with the Inmarsat constraints by construction. Figure 16 shows the curve of the average BFOR which ranges from -2.4Hz to 5.2Hz with a standard deviation of 4.6Hz to 1.8Hz respectively.

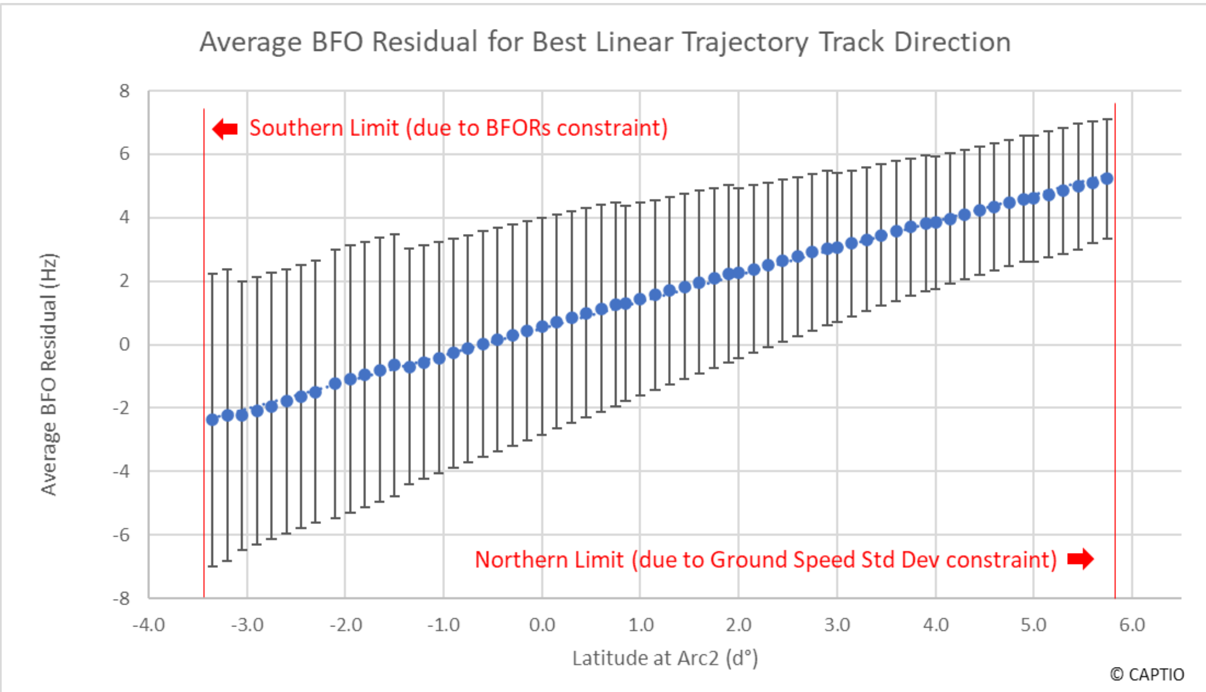

Figure 16: Average BFO Residuals of the best linear trajectories versus the crossing location latitude on Arc2 (The vertical bars represent the respective standard deviation of the BFOR during the trajectory)

As far as the flown distance between Arc2 and Arc6 is concerned, the best linear trajectories length varies from 3953km to 4023km while the full set of acceptable linear trajectories includes lengths between 3935km and 4054km. Thus, they are all within the acceptable limits computed with the fuel model in Table 2.

For the set of the best linear trajectories, the latitude at Arc6 varies between -30.3°S and -38.4°S. If it is assumed that the aircraft flew in the same direction from Arc6 to Arc7, then the latitude of their crossing point at Arc7 ranges from -31.2°S to -39.2°S. This represents a ~890km arc segment length on Arc7.
When considering the full set of acceptable linear trajectories, the range of latitude at Arc6 is from -30°S to -38.5°S.

Table 6 summarises the findings of this study with respect to the extremes (or ranges). Please note that each line of the table characterises the tagged variable only as far as there is no direct relation accross the lines.

Variable	**Across all best trajectories**		**Across all acceptable trajectories**		**Comments**
	Min	Max	Min	Max	
Track Direction *corresponding latitude Arc2*	174.75° *5.75°N*	190.75° *3.35°S*	174.75° *5.75°N*	191° *3.35°S*	
Average Ground Speed (kt)	474.6	484.0	472.8	487.0	
BFOR (Hz) *with BFOR Stand Deviation*	-2.4 *4.6*	5.2 *1.8*	-2.6 *3.8*	-5.3 *1.7*	
Distance Arc2-Arc6 (km)	3953	4023	3935	4054	
Latitude on Arc6	30.3°S	38.4°S	30°S	38.5°S	
Latitude on Arc7	31.2°S	39.2°S	31.2°S	39.3°S	*Same track dir.*

Table 6: Synopsis of variables ranges from the study based on best ground speed standard Deviation

Figure 17 presents a graphic representation of the angular span of the studied 63 best linear trajectories. The red circle represents the maximum range of the aircraft from Inmarsat Arc1 crossing point.

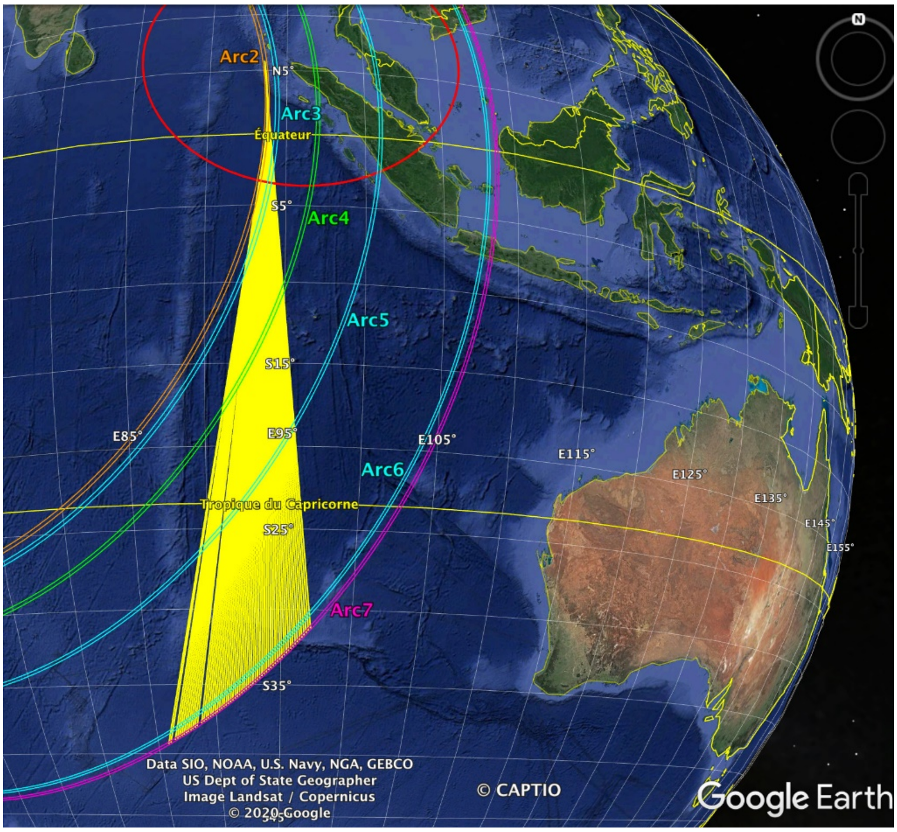

Figure 17: Graphic representation of the discrete set of the best GSP standard Deviation linear trajectories

Figure 18 presents the minimum and maximum ground speed found across the full set of the ~38000 acceptable linear trajectories. From South to North the ground speed span increases encompassing speed compatible with the set of flight modes offered by the aircraft Flight Management System (FMS).

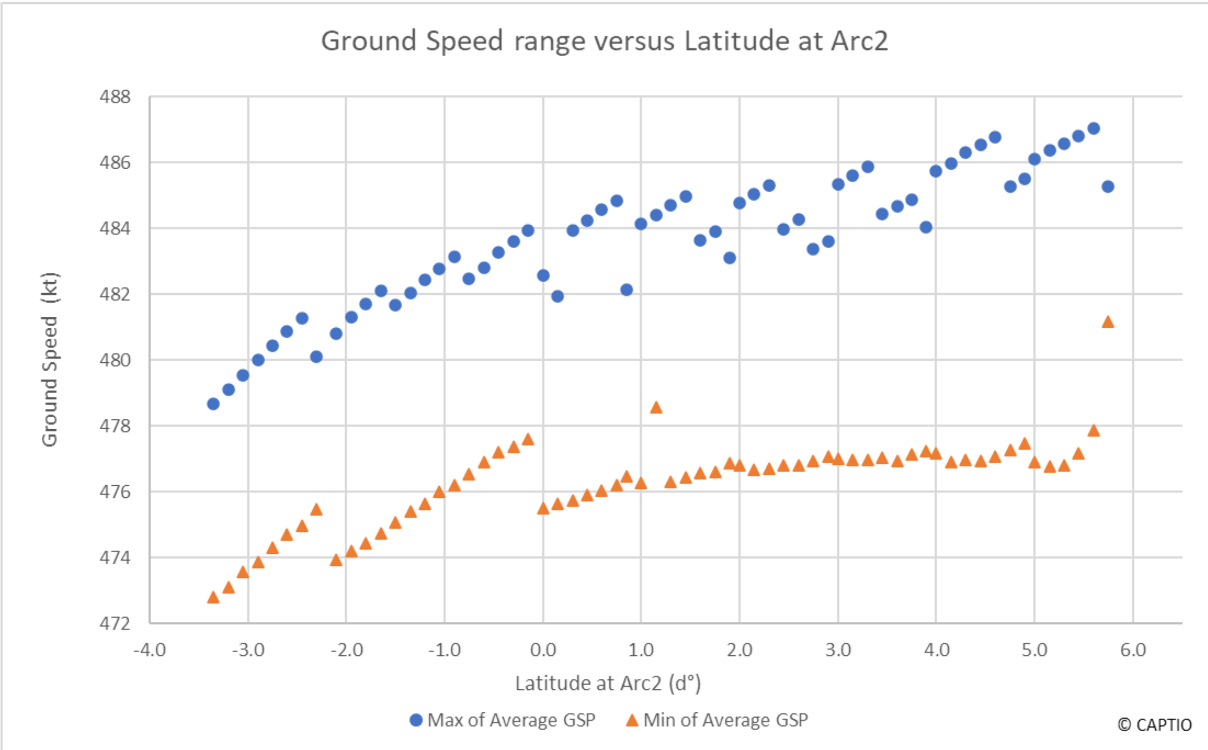

Figure 18: Ground Speed range per Arc2 Latitude over the full set of 38000 acceptable linear trajectories

4.5.2 Study based on lower BFOR standard deviation

A similar analysis was performed considering the BFOR standard deviation as the primary variable in view to evaluate how it would compare with the analysis on ground speed. The full analysis results are provided in Annex 2. For the sake of comparison, the relationship between the track direction and the latitude at Arc2 is provided in Figure 19.

A linear relationship can be approximated with the following remarkable simple equation using α as the track direction and LatArc2 as Arc2 crossing location latitude between [5.75°N;3.35°S]:

$$\alpha°(\mathrm{LatArc2}) \cong -1.7183 * LatArc2° + 184.64 \quad (2)$$

This is a direct way to identify the best linear trajectory at altitude 35000ft from any Arc2 crossing location latitude based on minimum BFOR standard deviation.

Taking the inverse of equation (2), one can infer that for any track direction α [175°; 190.25°] there always exists a crossing point at LatArc2 according to this one-to-one relationship:

$$\mathrm{LatArc2}°(\alpha) \cong -0.5820 * [\alpha° - 184.64] \quad (2bis)$$

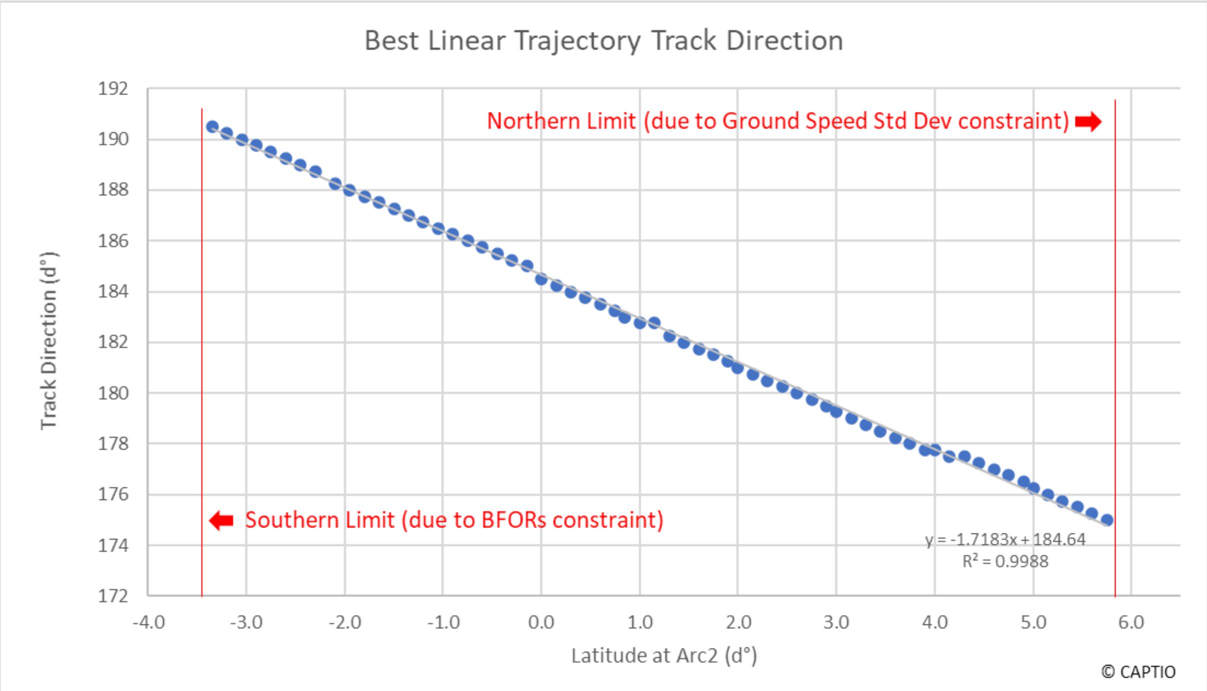

Figure 19: Track direction of the best BFOR linear trajectories versus Arc2 crossing location latitude

In Figure 20, the difference between the track direction curve of Figure 14: Track direction of the best GSP σ linear trajectories versus Arc2 crossing location latitude" and of Figure 19: "Track direction of the best BFOR linear trajectories versus Arc2 crossing location latitude" posts values included within the interval [-0.25°;0.25°] from 5.8°N to 3.05°S which are at the level of the digitisation step of the study. It is at -0.5° or 0.5° at latitudes 3°S to 3.35°S. One can thus consider that the error is within the quantification noise and conclude that the curves are similar except at the southern end marginally.

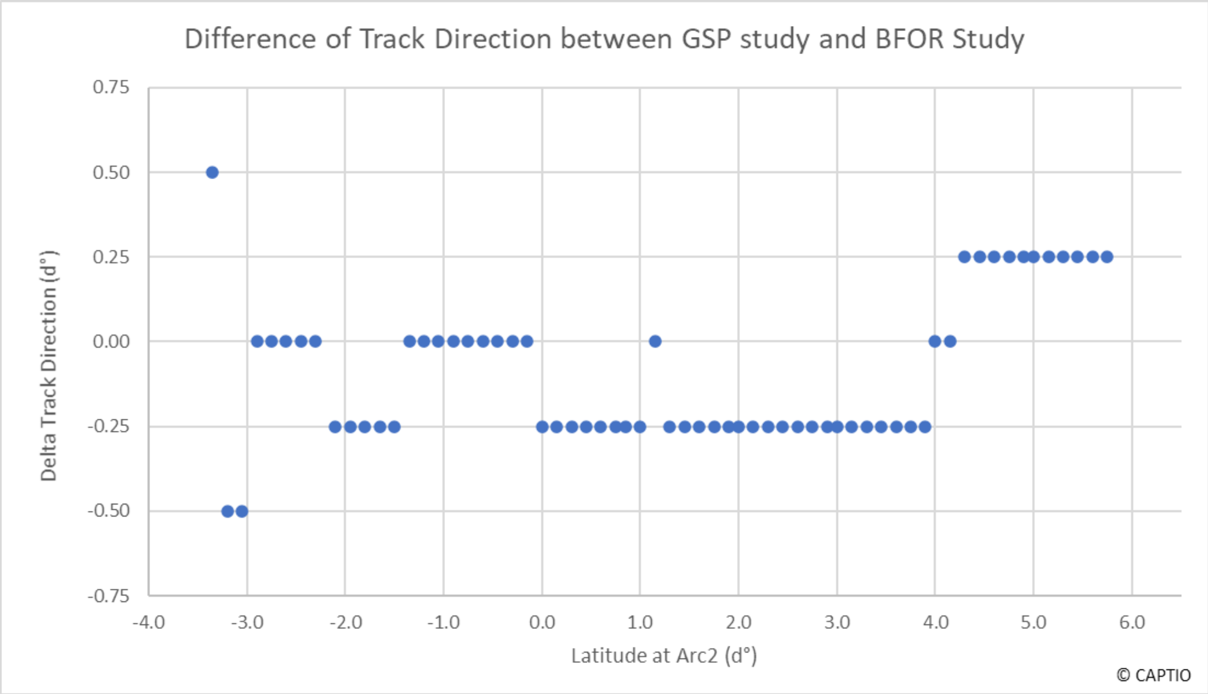

Figure 20: Track direction difference between best GSP linear trajectories and best BFOR linear trajectories versus the same Arc2 crossing location latitude

4.5.3 Inmarsat example trajectory

In table 9 of [1], Inmarsat proposed "Example Reconstructed Flight Path Results" concerning a particular trajectory almost linear from Arc2 to Arc7 flown at a constant speed of 829km/h (447.5kt) from somewhere between Arc1 and Arc2 until Arc7 with σ = 0 km/h. Their chosen Arc2 speed is tabled at 800km/h. The track direction varies between 186° and 179° in a broken line manner to accommodate for the constant speed. The average BFOR is 0Hz with a σ = 2.1Hz. This shows that Inmarsat chose the average BFOR and its standard deviation as primary constraints for their optimisation algorithm while keeping the ground speed at a constant value and letting the track direction as a variable. It should be noted that Inmarsat team did not make provision for wind fluctuations thus no speed fluctuation was allowed.

In section 4.5.1 "Study based on lower ground speed standard deviation", the philosophy was chosen to stay closer to the aircraft automation principles: the trivial parameter to choose as a constant was the track direction in relation to the heading reference provided by the pilot to the auto/pilot. The speed is most likely a variable as the aircraft automation optimises the speed according to the weight of the aircraft and its altitude which normally gets higher during the flight. It should be noted that the ground speed is never used by the pilot, it is only an a posteriori measurement as the pilot inputs KIAS or Mach number.
Thus, the results above concluded that the aircraft average ground speed was above 474kt i.e. 879 km/h and that the track direction is constant, there is no exact match with Inmarsat example. The best linear trajectory starting at Arc2 Latitude 0° posts a constant track direction equal to 184.75° and an average speed of 888 km/h with σ = 6.5km/h. The average BFOR is -0.1Hz with σ = 3.6Hz.
For comparison and considering the best linear trajectory found in 4.5.2 "Study based on lower BFOR standard deviation", the track direction is 184.5° with an average BFOR = 0.4 Hz and σ = 2.7Hz

In order to find a possible trajectory matching Inmarsat example, more than 0.6M trajectories were additionally computed from 5°N down to 2°S with a constant speed but with a slightly varying track direction mimicking Inmarsat "slightly broken" line approach. The ground speed was given a pre-set value in the range [422; 460]kt with 2.5 kt increments and the track direction was scanned with a span of +/- 5° by 0.25° increments at each subsequent arc with only 5 possible equidistant crossing locations at each arc.

Thus, there was a slight difference in the ground speed as 447.5kt was used and not 447kt as well as using 447.5kt at Arc2 too. In total the computation resulted in 1566 acceptable pseudo linear trajectories similar to Inmarsat example with Arc6 crossing point latitude between 33.4°S and 33.6°S. Table 7 presents the closest computed pseudo linear trajectory compared to Inmarsat example.

	Lat°	Long°	Track°	Ground Speed (kt)	BFO Predicted (Hz)	BFO Measured (Hz)	BFOR (Hz)
Arc2	-0.1	93.7	185	447.5	107	111	4
Arc3	-7.5	93.1	182	447.5	144	141	-3
Arc4	-15.0	92.8	178	447.5	171	168	-3
Arc5	-22.5	93.0	179	447.5	204	204	0
Arc6	-33.6	93.3	179	447.5	253	252	-1

Table 7: Computed trajectory mimicking Inmarsat Table 9 example

The BFOR average is -0.7Hz with a σ = 2.7Hz to be compared with Inmarsat reference 0Hz and 2.1Hz respectively. This trajectory can be considered as similar to Inmarsat example due to the quantisation process of the crossing locations and of the track direction angle used during the computation.

5 Conclusions

Looking for a linear trajectory is based on a set of hypotheses that reduces the most the number of flight variables by considering them as all constant but one. For example, on this basis, Inmarsat chose the local track direction as the only variable.

A large number of linear trajectories have been computed and evaluated under Table 5 constraints including the Inmarsat defined constraints among others. Some ground speed variation was allowed in order to accommodate the real flight conditions like meteo conditions especially in the leg Arc6-Arc7 which was under windy conditions.

The influence of the geometry of the system over the existence of linear trajectories is clearly demonstrated by the identified analytical dependency between the Arc2 crossing location latitude and the track direction of the linear trajectory best respecting the constraints.

This means that for a linear trajectory crossing Arc2 at a latitude between [5.75°N; 3.35°S], there always exists a different track direction within the range [174.75°;191°] dependent on the latitude. Arc7 crossing point would thus lay at a latitude within [31.2°S; 39.3°S] which is within the area already searched by Fugro, Go Phenix and Ocean Infinity.

Between these latitudes, every point within Arc7 has an equal chance to be a valid crossing point. This makes a huge number of operationally valid possibilities.

Every flight mode e.g. ECON speed control mode, Long Range Cruise (LRC) or Maximum-Range Cruise (MRC) etc. could be matched by a corresponding linear trajectory thanks to the ground speed range determined during the analysis. Figure 15: "Average Ground Speed of the best linear trajectories versus Arc2 crossing location latitude" shows that for any particular average ground speed at least 4 best linear trajectories are possible to cross Arc2 at four different latitudes in a ~3° interval. But there are much more trajectories than the “best” ones. Thus, the selection method would be first to select a suitable average speed based on these operational preferences and then refer to the set of ~38000 acceptable trajectories to select the possible track directions to get the sub-set of “perfect” linear trajectories for that speed.

6 References

[1] The Search for MH370 , Inmarsat, Chris Ashton, Alan Shuster Bruce, Gary Colledge and Mark Dickinson, The Journal of Navigation (2015), 68, 1–22

[2] Bayesian Methods in the Search for MH370, Samuel Davey, Neil Gordon, Ian Holland, Mark Rutten, Jason Williams, SpringerBriefs in Electrical and Computer Engineering, 2016

[3] https://mh370.radiantphysics.com/2017/10/22/possible-mh370-paths-along-great-circles/

[4] The Final Resting Place of MH370, Bobby Ulich, Richard Godfrey, Victor Iannello and Andrew Banks, 7th March 2020

[5] MH370: Trajectory Selection based on BFO Residuals, CAPTIO, to be published, 2021

7 Annex 1

Sampled wind characteristics along typical linear trajectories at 180°.

Arc	Starting Latitude														
	+5.3			+2			0			-1.5			-3.35		
	Dir	Mod	Eff	Dir	Mod	Eff	Dir	Mod	Eff	Dir	Mod	Eff	Dir	Mod	Eff
	°	*kt*	*kt*	°	*kt*	*kt*	°	*kt*	*kt*	°	*kt*	*kt*	°	*kt*	*kt*
2	*90*	*12*	*0*	*85*	*20*	*1.7*	*90*	*22*	*0*	*85*	*26*	*2.3*	*70*	*19*	*6.5*
3	*75*	*24*	*6.2*	*65*	*11*	*2.1*	*80*	*12*	*2.1*	*90*	*15*	*0*	*85*	*14*	*1.2*
4	*85*	*10*	*0.9*	*75*	*13*	*3.4*	*70*	*17*	*5.8*	*70*	*7*	*2.4*	*60*	*13*	*6.5*
5	*285*	*4*	*1*	*280*	*32*	*5.6*	*275*	*46*	*4*	*280*	*53*	*9.2*	*280*	*57*	*9.9*
6	*275*	*64*	*5.5*	*245*	*35*	*-14.8*	*240*	*30*	*-15*	*235*	*41*	*-23.5*	*245*	*52*	*-22*
σ			**1.68**			**3.38**			**3.34**			**5.09**			**5.17**

Table 8: Sampled wind characteristics at altitude 35000ft at track direction 180°

8 Annex 2

Graphical results of the analysis based on BFOR average and lowest BFOR standard deviation

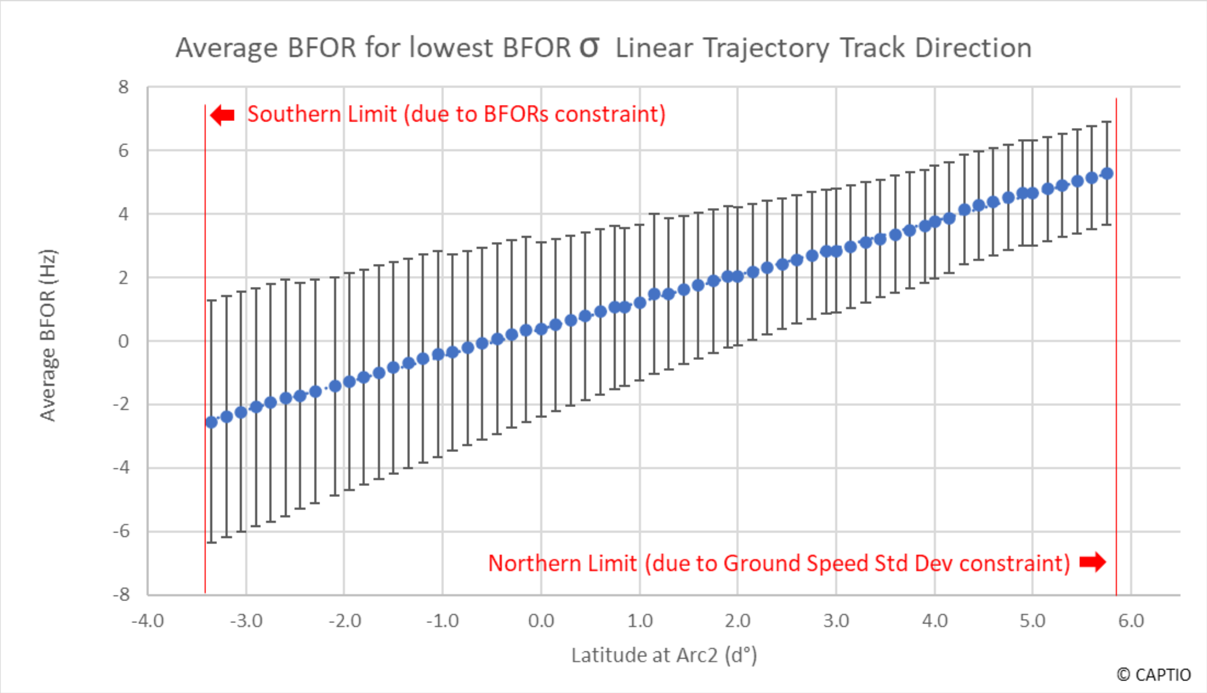

Figure 21: Average BFO Residuals of the best linear trajectories versus the crossing location latitude on Arc2 (The vertical bars represent the respective standard deviation of the BFOR during the trajectory)

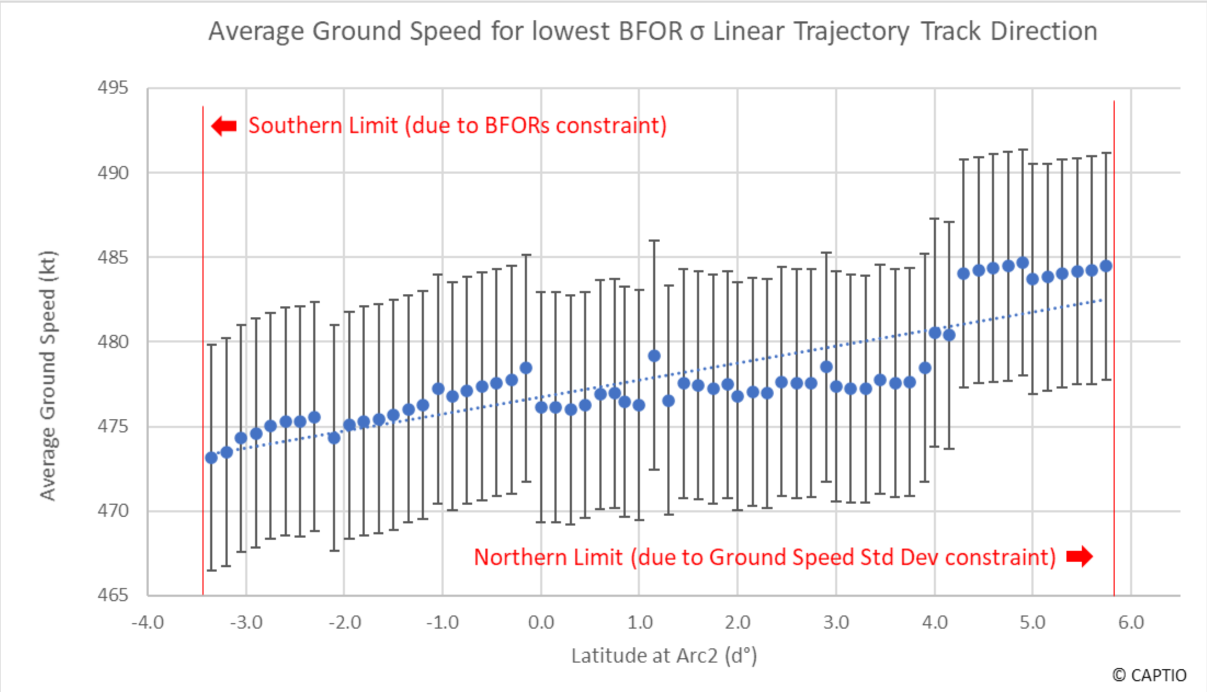

Figure 22: Average Ground Speed of the best linear trajectories versus the starting point latitude on Arc2 (The vertical bars represent the respective standard deviation of the speed during the trajectory)

MH370: Mastering BFO Residuals for Trajectory Selection

CAPTIO, Dec. 2020

Summary

An innovative sensitivity analysis of the Burst Frequency Offset (BFO) residuals (BFOR) which are the differences between the calculated BFO and the measured BFO from [1] has been carried out to explain the BFORs behaviour in function of the true track angle of the aircraft. Computations were made for the crossing points of the Inmarsat "arcs" where BFO measurements are available.

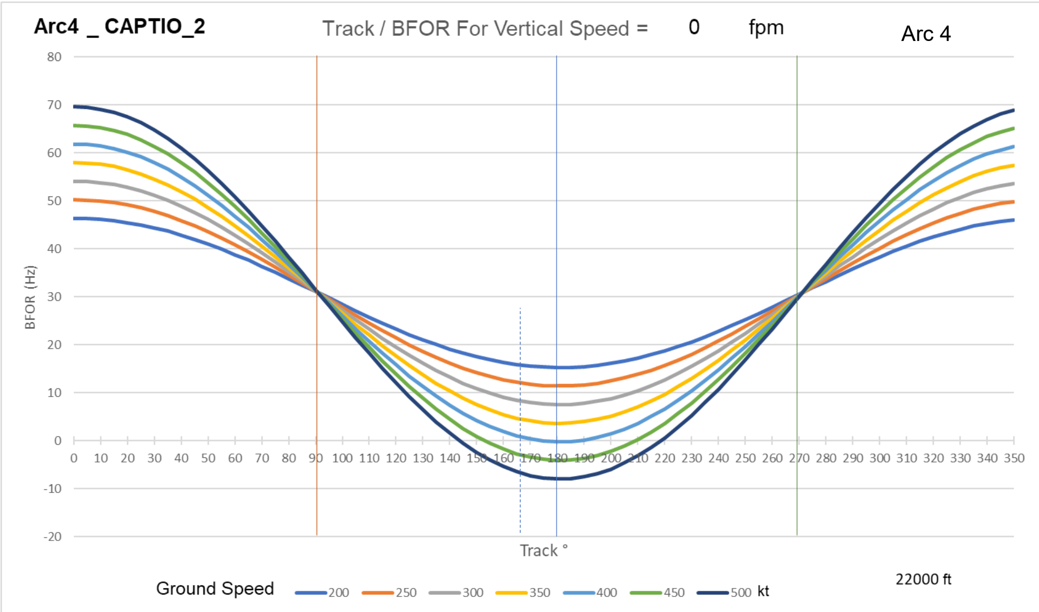

Figure 23: Typical family of BFOR curves for the MH370 flight for horizontal velocity in [200 kt;500 kt] range

It demonstrates that the changing geometry and kinetics of the quadruplet including the aircraft, real satellite, the virtual "perfectly stationary" satellite and the Earth are the driving factors of this behaviour illustrated in Figure 23. These four elements are contributing to the two frequency components *ΔFup* and *δfcomp* of the BFO, which are the only ones to be dependent of the aircraft velocity and of the relative geometry of the aircraft, the satellite and its model.

Results are posted using the true track angle as the input variable taking into account the specificities of the airborne Doppler compensation algorithm used by the onboard satellite communication unit.

It is also shown that the shape of the resulting BFOR curves is similar within the duration of the MH370 flight and also similar within the duration of the preceding MH371 flight but shifted by 180°. At each arc, the families of curves systematically cross each other for basically the same two directions and also post minima and maxima for the same two opposite directions.

The behaviour of the BFORs as a function of the true track, with a fixed speed value, reveals "privileged" trivial directions which could be misinterpreted. They should be considered cautiously when elaborating a MH370 trajectory compatible with Inmarsat pings.

Table of Content

1 BFO: the basics 27

2 The geometry and the kinetics of the System under Consideration 28

2.1 The geometry of the SuC 28

2.2 The kinetics of the SuC 30

2.2.1 Inmarsat Satellite 3F1 ephemerides 30

2.2.2 Aircraft Movement 32

3 Analytic computation of Δfup and δfcomp 33

3.1 Analytic computation of ΔFup: the Doppler affecting the signal passing from the aircraft to the satellite 33

3.2 Analytic computation of δfcomp: the frequency compensation applied by the aircraft 34

4 ΔFup + δfcomp behaviour when the aircraft track varies from 0° to 360° 36

5 BFO & BFOR behaviour versus aircraft velocity and direction 41

6 Sensitivity analysis for MH370 flight 44

7 Sensitivity analysis for MH371 flight 46

8 Hypothetical satellite West-East excursion 49

9 References: 52

10 Annex A: Inmarsat sensitivity analysis complement 53

11 Annex B: Vertical Motion of the Aircraft: 54

12 Annex C: Satellite model and BFO/BTO models 57

1 BFO: the basics

The method to compute the BFO with the six aircraft trajectory parameters from its position and velocity: x, y, z, vx, vy, vz has been explained in details in several documents referenced here under [1], [5], [6] and [7].
In short, a BFO is the sum of six frequency components:

$$BFO = \Delta Fup + \Delta Fdown + \delta fcomp + \delta fsat + \delta fAFC + \delta fbias \quad (1)$$

For this sensitivity analysis and under its specific conditions, it happens that four components are fixed:

$$\Delta Fdown + \delta fsat + \delta fAFC + \delta fbias,$$

And only two components are varying as they are dependent of the aircraft velocity and of the relative geometry of the aircraft and the satellites:
Only two components depend on the aircraft velocity and its position relative to the real and perfectly stationary satellites:

$$\Delta Fup + \delta fcomp$$

ΔFup is the Doppler shift on the signal travelling from the aircraft to the INMARSAT satellite 3F1-IOR (hereafter called SatReal), known by the analytic equations of its inclined elliptical geo-synchronised orbit [8] and the earth modelling [9].
δfcomp is the frequency compensation applied by the aircraft SatCom system including a Satellite Data Unit[3] taking into account the position of the aircraft, but at altitude 0, to a virtual perfectly stationary geo-synchronised satellite in the equatorial plane (called SatVirtual in the analysis below). As the result, the quadruplet [aircraft, SatReal, SatVirtual, aircraft0] constitutes the main part of the System under Consideration (SuC) as depicted in Figure 24.

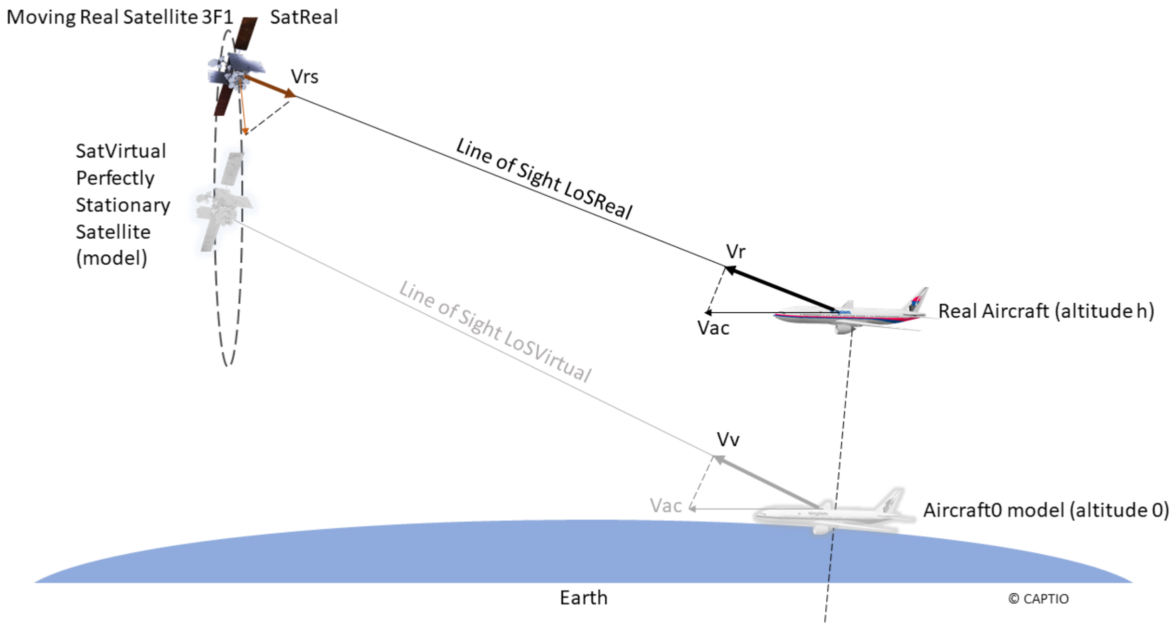

Figure 24: The 4 real physical components of the SuC

3 Honeywell-SATCOM-SDIM-MSC7200-23-20-35-rev-1

2 The geometry and the kinetics of the System under Consideration

2.1 *The geometry of the SuC*

The onboard frequency compensation algorithm uses surrogates of the real aircraft and of the real satellite. Thus, the system under consideration (SuC) comprises 2 subsets of components.

The first set of components includes the real physical objects (cf Figure 25):

1- the Earth, modelled by an ellipsoid as described by [9];
2- the real aircraft (noted Aircraft) with its velocity vector (noted Vac). Since it is assumed that the aircraft flies horizontally at altitude h, Vac is contained in a plane parallel to the plane tangent to the Earth, at distance h from Earth.
3- the real satellite 3F1-IOR (noted SatReal), which, because of its inclined elliptical geo-synchronised orbit is moving around its theoretical stationary position with a velocity Vrs.
4- The corresponding line of sight (noted LoSReal) for the straight line between SatReal and Aircraft;

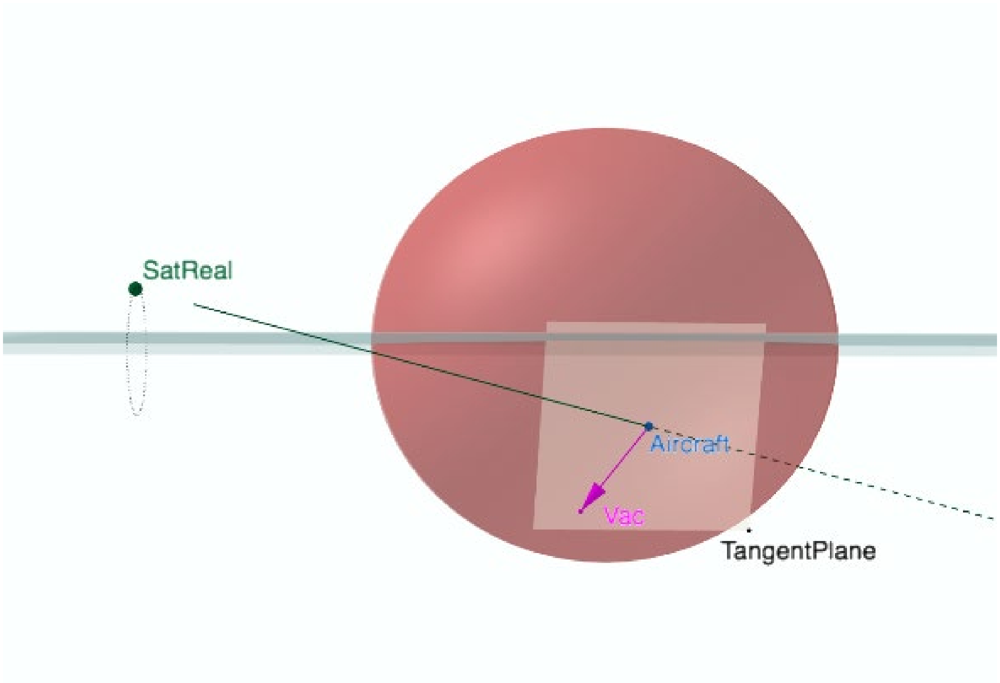

Figure 25: The 4 real physical components of the SuC

The second set of components includes the virtual models associated to real objects (cf Figure 26):

5- the vertical projection of the aircraft on the earth ellipsoid thus at altitude 0 (called Aircraft0) with the same velocity vector Vac (in 1st order approximation) in the tangent plane to the earth at that point i.e. at altitude 0;
6- a model of a perfectly geostationary satellite (called SatVirtual) located in the equatorial plane whose projection on the ground is fixed;
7- the line of sight (noted LoSVirtual) for the straight line between SatVirtual and Aircraft0.

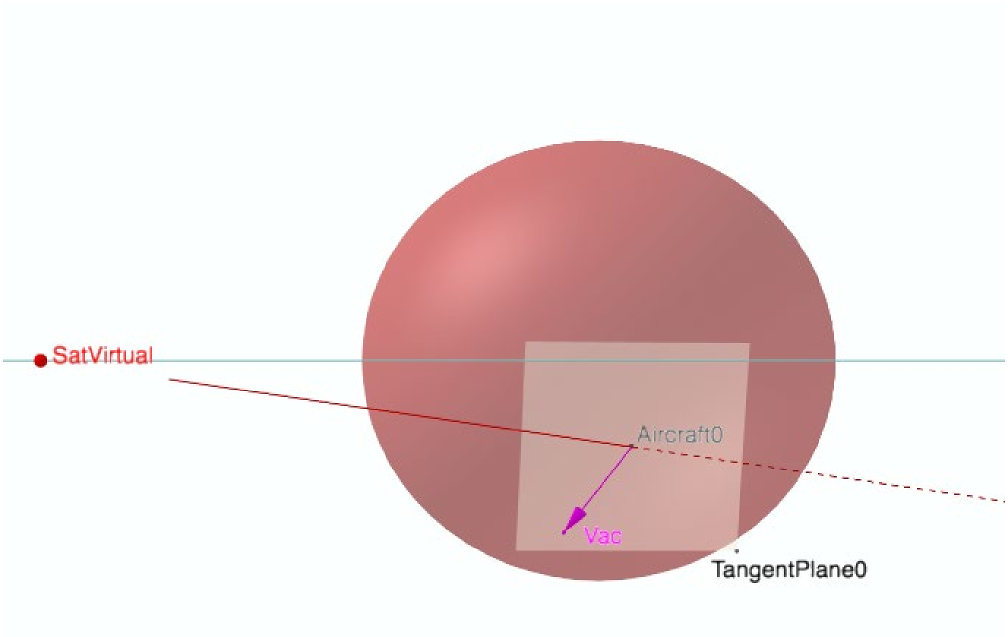

Figure 26: The 3 virtual components of the SuC

Figure 27 illustrates the complete system under consideration with both the set of real objects and the set of modelled virtual objects used by the compensation algorithm.

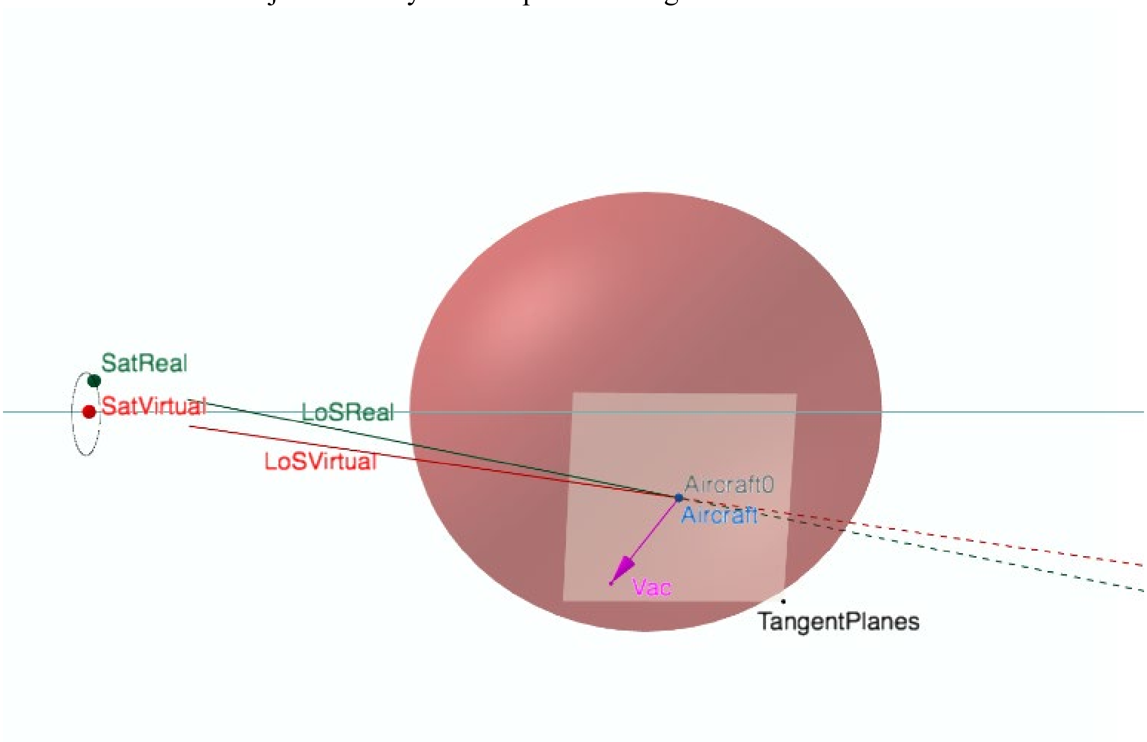

Figure 27: The full System Under Consideration (SuC)

Figure 28 shows a perspective view where one can see that the two Lines of Sight do not necessarily cross each other. In fact, they do not cross at the aircraft geodetic position. It shows also the distinction between Aircraft and Aircraft0 with their respective tangent planes in which the aircraft velocity Vac evolves.

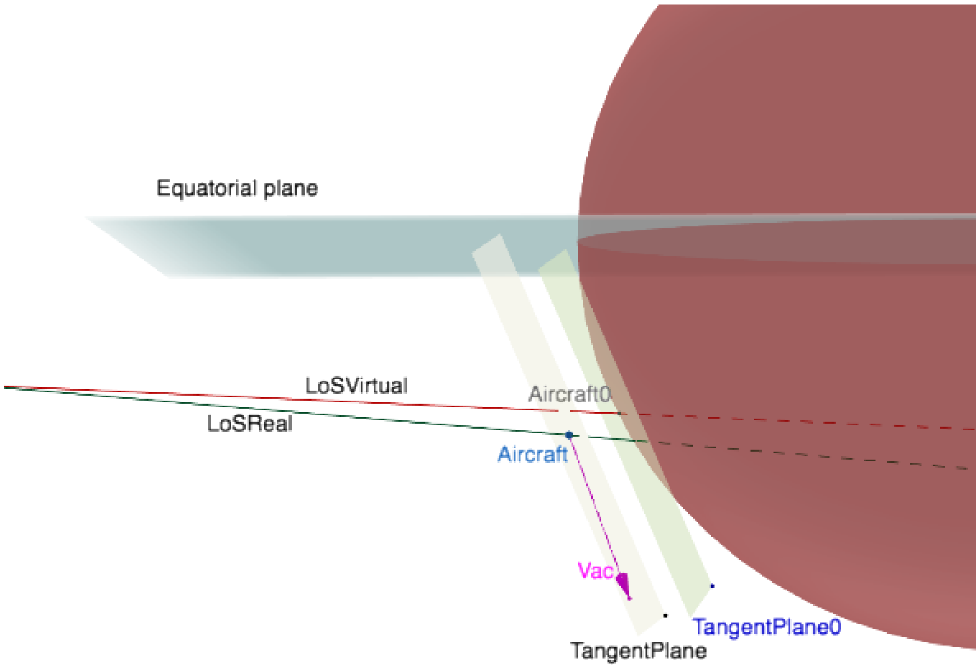

Figure 28: Differences between the real Aircraft and the virtual Aircraft0 geometry

These two sets of components must be considered in turn for the computation of the Doppler effect along each line of sight:

- on the one hand, Vac and the SatReal velocity have to be projected onto LoSReal. The estimated real Doppler component is proportional to the difference of these two projected velocities,
- on the other hand, Vac of Aircraft0 has to be projected onto LoSVirtual. The estimated Doppler correction component is proportional to this projected velocity only since SatVirtual is fixed.

2.2 The kinetics of the SuC

2.2.1 Inmarsat Satellite 3F1 ephemerides

The satellite characteristics are detailed with Figure 8 in [1] which is reproduced below as Figure 29.

This sub-satellite point trajectory comes from the orbit inclination vis-à-vis the equatorial plane and its eccentricity because the satellite does not move around the earth in a circle but in an ellipse.

- due to the inclination, the north-south excursion of the satellite is about 2 414km (2 x ~1207 km) in the tangent but slightly oblique plane at the location of the virtual perfectly stationary satellite,
- due to the eccentricity the west-east excursion is about 96km (2 x ~48km) leading to an excursion ratio with the long axis of ~4%.
- The perigee is at 7h36:42 UTC and the apogee at 19:36:14 UTC leading to a total satellite altitude excursion of ~46km (i.e. 1.9% of the long axis).

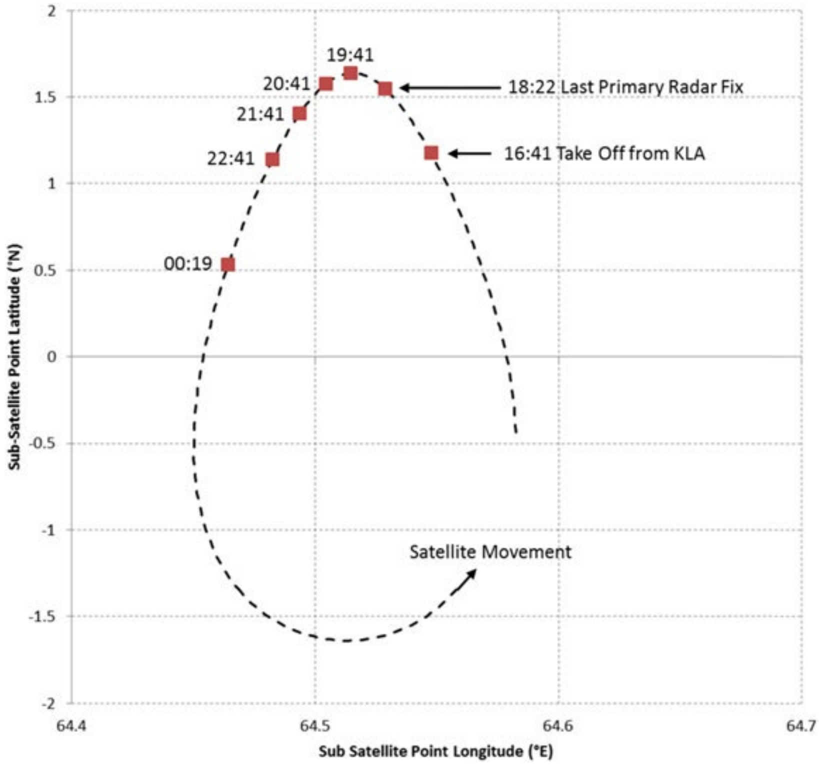

Figure 29: 3F1 Sub-satellite point locations during MH370 Flight (source Inmarsat)

Figure 29 provides a clear view of the ellipsoidal motion of 3F1-IOR. However, this representation is distorted by the difference of scales between the two axes. If one plots the satellite locations on a diagram with orthonormal axes one gets an ellipse highly elongated in the north-south direction as depicted in Figure 30:

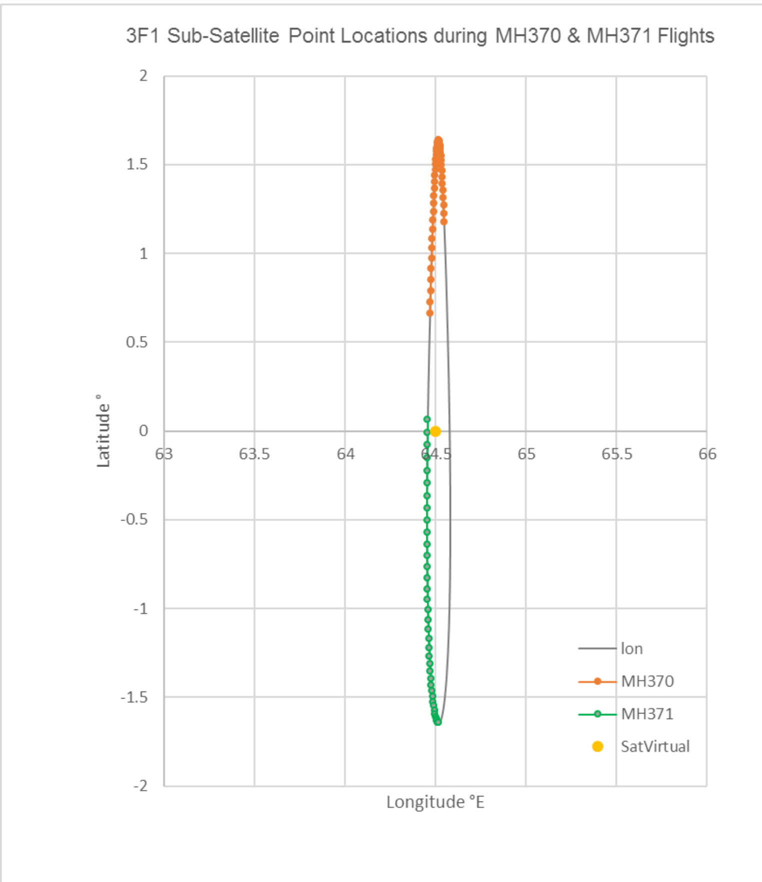

Figure 30: 3F1-IOR Sub-Satellite point locations during MH370 & MH371 flights (orthonormal axes)

One can see that during the MH370 flight, 3F1-IOR satellite occupies a northern position and during the MH371 flight a southern position. This explains the difference between these two flights during the sensitivity analysis as will be seen below.
SatReal does not move orthogonally to LoSReal. Therefore, its velocity Vrs contributes significantly to the Doppler effect and to the change of direction of LoSReal.

2.2.2 Aircraft Movement

For both LoSReal and LoSVirtual, at the aircraft end, Vac is the main contribution to the Doppler effect and must be considered:

- at altitude h for computing the real value Doppler effect (i.e. for the Aircraft), and
- at altitude 0, for the value computed by the compensation algorithm (i.e. for Aircraft0)

The analysis considers the associated Doppler variations in respect of 2 parameters:

1. the true track angle (in the range from 0° to 360°) in the horizontal plane at altitude h and at altitude 0.
2. The value of Vac (in an operationally reasonable range of speeds from 200 to 500kt)

Figure 31 illustrates this analysis with an example.

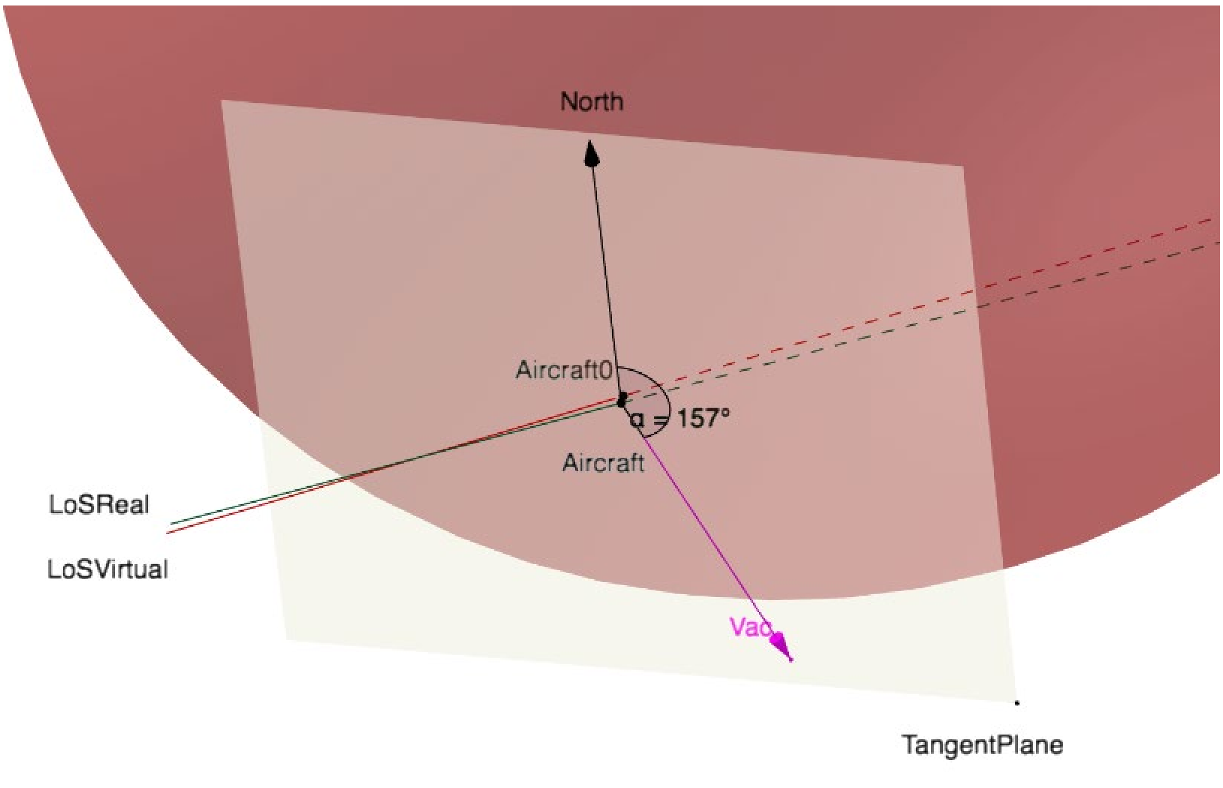

Figure 31: Variables for the study: True track α and magnitude of Vac (example at track 157°)

3 Analytic computation of *Δfup* and *δfcomp*

3.1 *Analytic computation of ΔFup: the Doppler affecting the signal passing from the aircraft to the satellite*

Figure 32 presents an example on how the aircraft and satellite velocity projections onto LoSReal are constructed. The blue plane is the orthogonal plane to LoSReal containing the extremity of the Vac vector and illustrates the direction of the orthoganal projection of Vac.
The orange arrow Vr is this projection of Vac onto LoSReal and is proportional to the Aircraft contribution to the real value of the Doppler.
In the same way, projecting the moving satellite velocity onto LoSReal yields Vrs, proportional to the satellite contribution to the real value of the Doppler.
The green arrow VrTot = Vr - Vrs represents the velocity difference resulting in the real Doppler.
In Figure 32, the chosen example is at 22h41 UTC, the satellite moves southwards and towards its perigee, thus getting closer to the aircraft, Vr and Vrs go in the same direction as aircraft track is chosen towards the south-east. The result of the relative movement of the satellite and the aircraft leads to VrTot being smaller than Vr. This reduces the Doppler contribution compared to the aircraft's alone leading to the green arrow being smaller than the orange arrow.

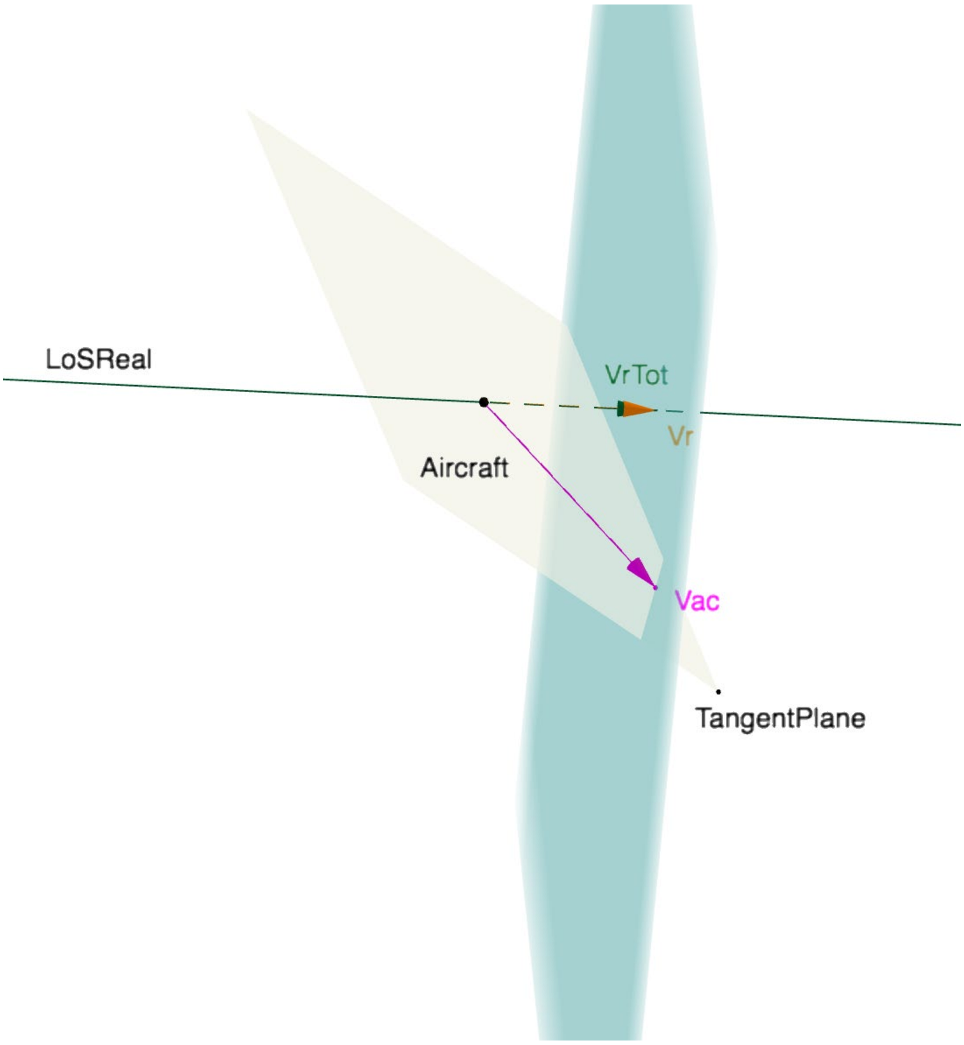

Figure 32: Principle of projection of the aircraft velocity on the line of sight for ΔFup

In the previous example, the aircraft was flying away from the real satellite. By contrast, the example chosen in Figure 33 illustrates the case when the aircraft gets closer to the satellite. Subsequently their relative velocity is increased, as is the Doppler effect (VrTot>Vr).

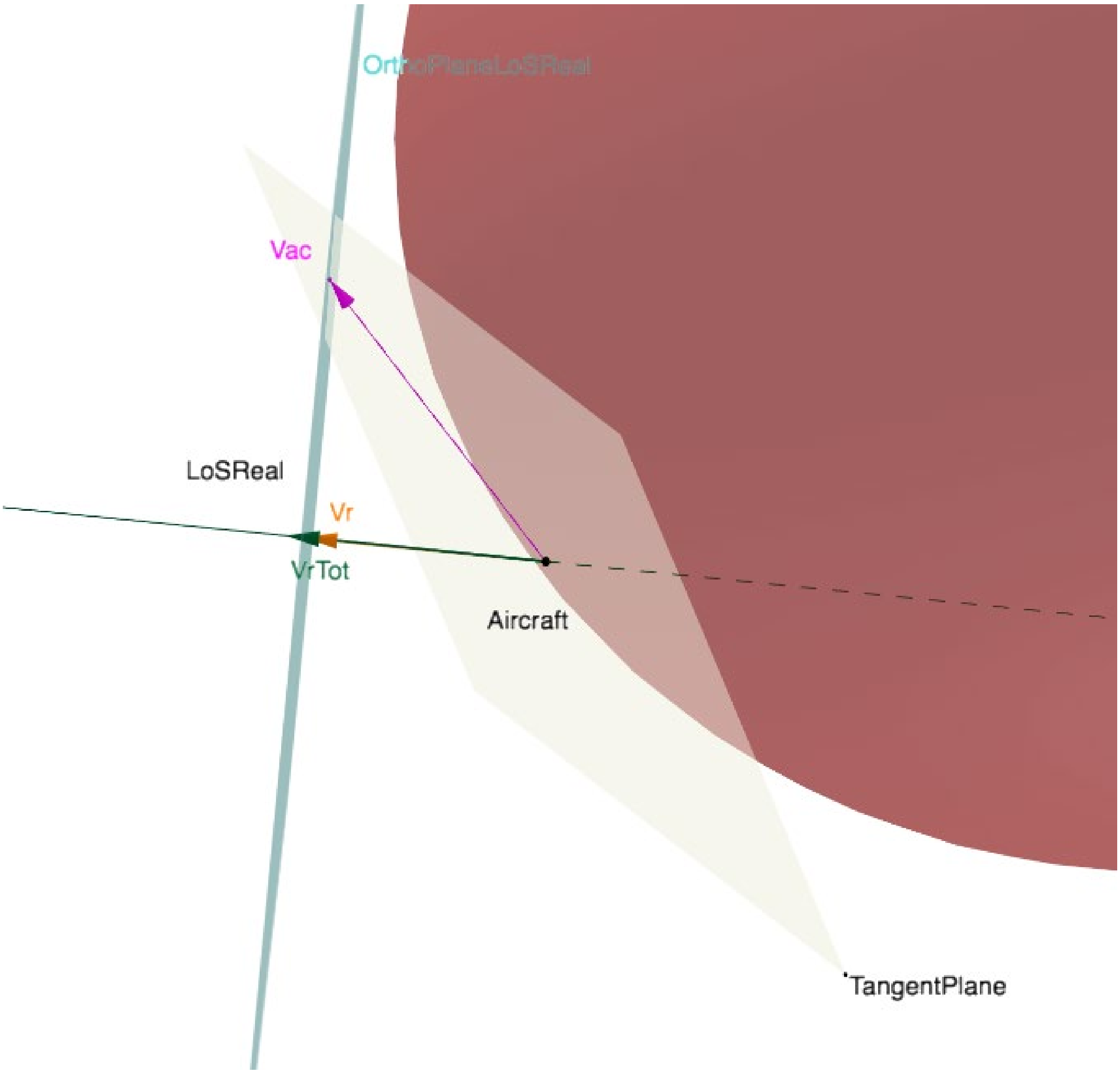

Figure 33: 2nd Example of calculation of velocity projection when the aircraft gets closer to SatReal

ΔFup is the real Doppler frequency shift affecting the signal passing from the aircraft to the real satellite. It is the product of VrTot by the ratio *f/c* where *f* is the uplink carrier frequency and *c* the celerity of light:

$$\Delta Fup = VrTot * f/c \qquad (2)$$

3.2 Analytic computation of δfcomp: the frequency compensation applied by the aircraft

A similar approach is followed to compute the Doppler estimated by the aircraft SatCom system, based on SatVirtual and Aircaft0.
By definition, and in 1st order approximation, the algorithm considers Aircaft0 which flies horizontally at the same ground speed Vac as the Aircraft. Thus, its velocity vector Vac is between the points Aircraft0 and V0ac in the tangent plane at altitude 0 as illustrated in Figure 34.
The considered line-of-sight is now LoSVirtual i.e. the line-of-sight between Aircaft0 and the virtual motionless and perfectly stationary satellite SatVirtual positioned at [0°; 64.5°E] at a slightly higher altitude than the nominal geostationary orbit by a few hundred kilometres as reported by [7].

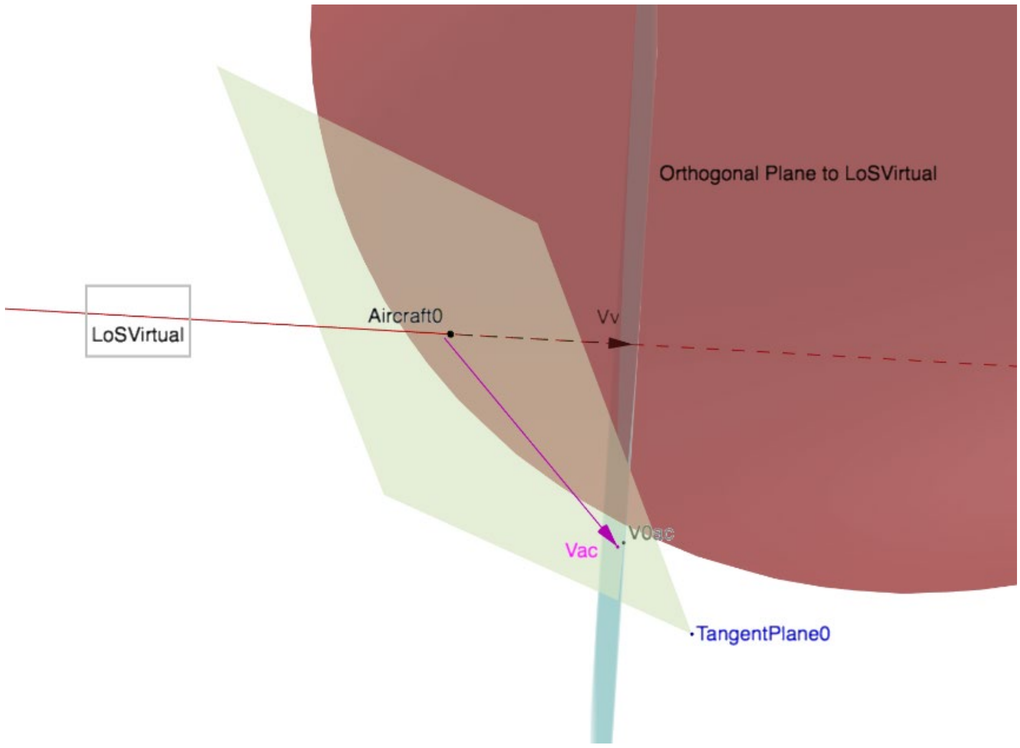

Figure 34: Example of calculation of velocity component pertinent to δfcomp

In Figure 34, the point V0ac is obtained by translating Vac to the new origin Aircaft0. It represents the velocity of Aircraft0.
The Doppler frequency computed compensation *δfcomp* is obtained by multiplying the projection of Vac onto LoSVirtual (noted Vv to denote the Aircaft0 contribution to the estimated Doppler, the SatVirtual contribution being equal to zero by definition) by the same ratio f/c as above.
Thus, the total Doppler component due to the geometry and the kinetics of the System under Consideration is the signed arithmetic sum of the two factors:

$$\Delta Fup + \delta fcomp = (VrTot\text{-}Vv) * f/c \tag{3}$$

Recalling equation *(1)* $BFO = \Delta Fup + \Delta Fdown + \delta fcomp + \delta fsat + \delta fAFC + \delta fbias$ and re-arranging the terms, it becomes

$$BFO = (VrTot\text{-}Vv) * f/c + \Delta Fdown + \delta fsat + \delta fAFC + \delta fbias \tag{3}$$

where the sum ($\Delta Fdown + \delta fsat + \delta fAFC + \delta fbias$) depends only on the time. Thus, at each of the so-called Inmarsat arcs corresponding to a unique time t_i where i corresponds to the nomenclature proposed in [1] this sum is constant i.e. = K_i leading to

$$BFO_i = (VrTot\text{-}Vv)_i * f/c + K_i \tag{4}$$

The term $(VrTot\text{-}Vv)_i$ depends on:

a) the aircraft position (Xac_i, Yac_i, Zac_i) on arc_i and its velocity ($VXac_i$, $VYac_i$, $VZac_i$) which could also be expressed in cylindrical coordinates (Vac_i, α_i, RoC_i)[4] and
b) on the real satellite velocity as the exact satellite position can be known at any time, thanks to its ephemeris and thus is determined at t_i.

Now that the Doppler compensation is characterised, the next step is to analyse the behaviour of the BFOs and BFORs at the crossing of the arcs with an aircraft flying horizontally and following a true track direction α_i from the North.

4 *RoC is the aircraft rate of climb*

4 *ΔFup* + *δfcomp* behaviour when the aircraft track varies from 0° to 360°

Some partial analysis of the BFO and BFOR behaviour as a function of the true track have been performed in [1], [3] and in relation with the antenna reception power diagram in [4], but no variation of the velocity magnitude was analysed nor the specific geometry of the SuC. Chapter IV of [4] presents interesting elements on the BFOR sensitivity with respect to the geodetic position along a specific arc$_i$.
Recalling the Doppler frequency shift at arc$_i$, equation (4) is the object of the study

$$BFO_i = (VrTot\text{-}Vv)_i * f/c + K_i$$

The term $(VrTot\text{-}Vv)_i$ can be developed as $(Vr\text{-}Vrs\text{-}Vv)_i$ where Vrs is the projection of the real satellite SatReal onto the line of sight LoSReal between this real satellite and the aircraft. As the aircraft position is chosen on arc$_i$ a priori, Vrs is fixed for this specific position and can be transferred into the constant part of the equation. Thus, the variability of BFO_i comes from the remaining terms leading to a simplified expression:

$$BFO_i = (Vr\text{-}Vv)_i * f/c + K'_i \qquad (5)$$

where K'_i includes all the components having a fixed value because of the fixed position of the aircraft.
Figure 35 illustrates the different elements taken into account for the BFO[5] computation. Vac and the track α which can vary from 0 to 360° from the North will be the only two variables.

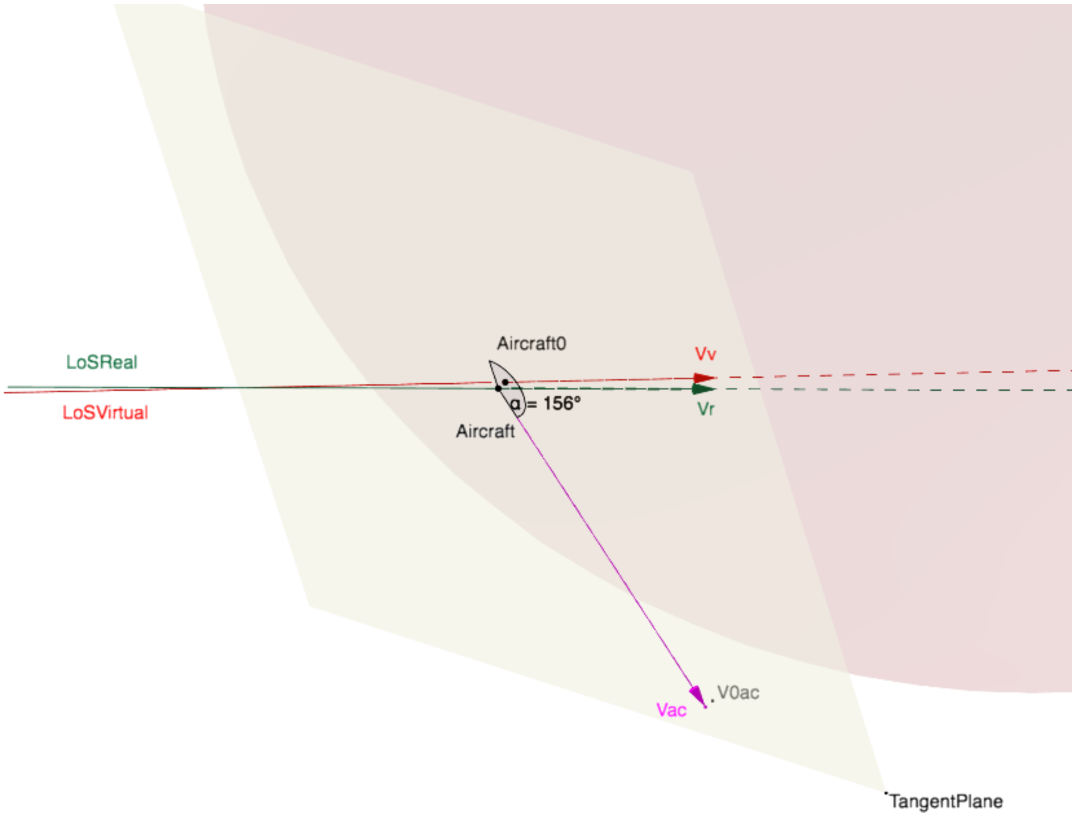

Figure 35: Aircraft velocity projections on the two lines of sight LoSReal and LoSVirtual at Arc 5 for example at track 156°

For a given Vac, making the track direction α varying continuously from 0° to 360 allows to analyse the continuous evolution of Vr and Vv.

5 *in the rest of the analysis, the index i will be ignored as the study is generic at each arc i.*

***Note**: In the following figures, the velocity magnitude values had to be chosen enlarged for illustrative purpose within GeoGebra [10]. They are not to scale.*

Figure 36 highlights four remarkable positions of such a rotation of the aircraft velocity direction: two where the relative velocity difference is 0 (wrt to GeoGebra precision) and two at his maximum. One can see the cyclic evolution of the velocity vectors projections (green and orange arrows).

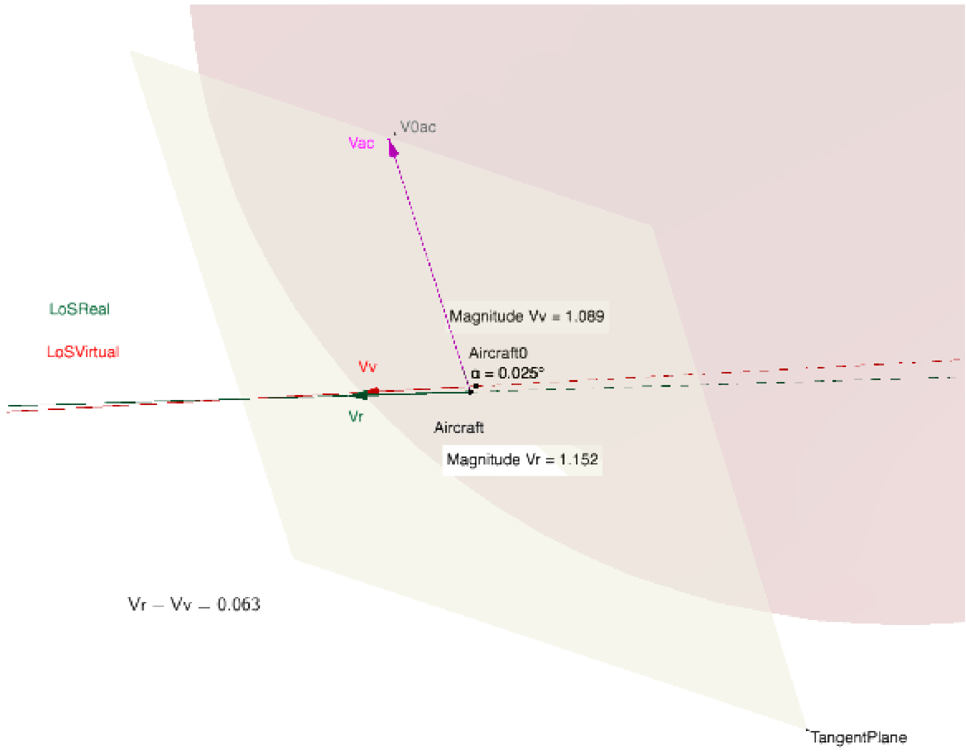

Aircraft velocity direction at 0° (difference at maximum)

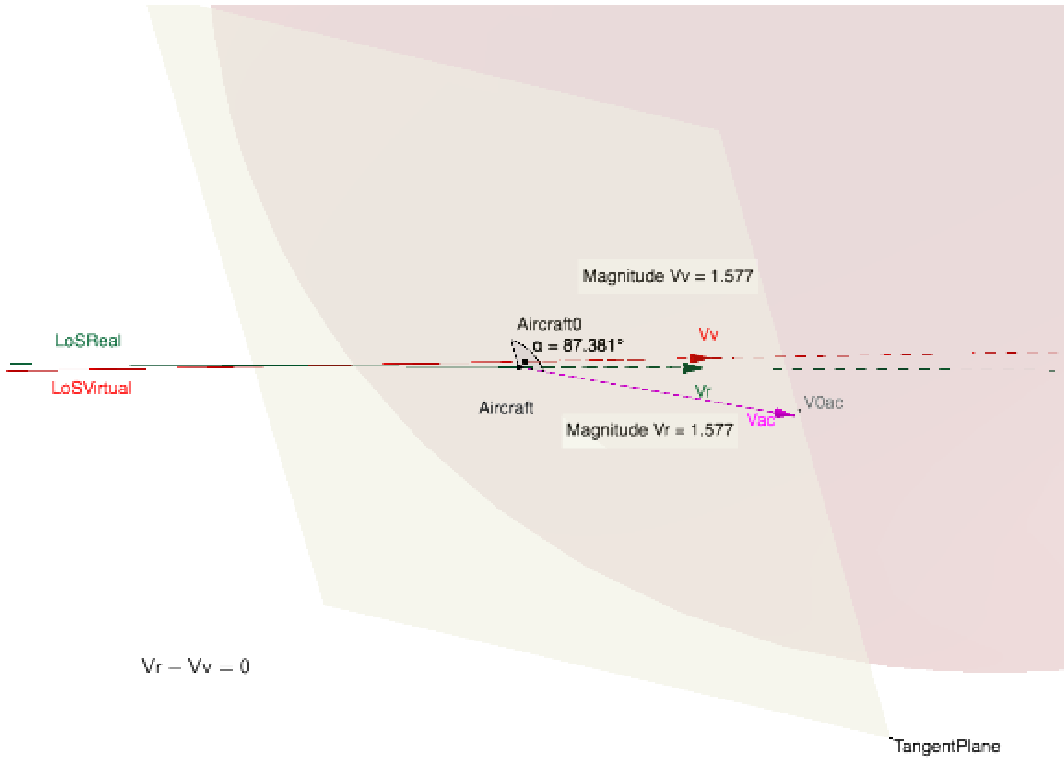

Aircraft velocity direction at 87° (difference at minimum)

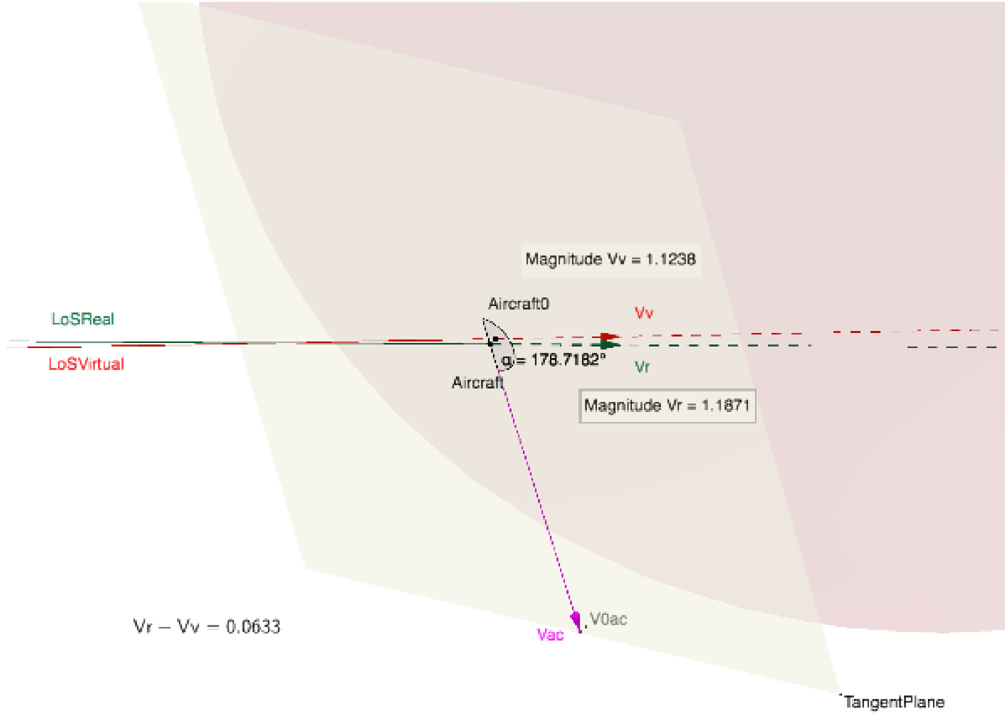

Aircraft velocity direction at 179° (difference at maximum)

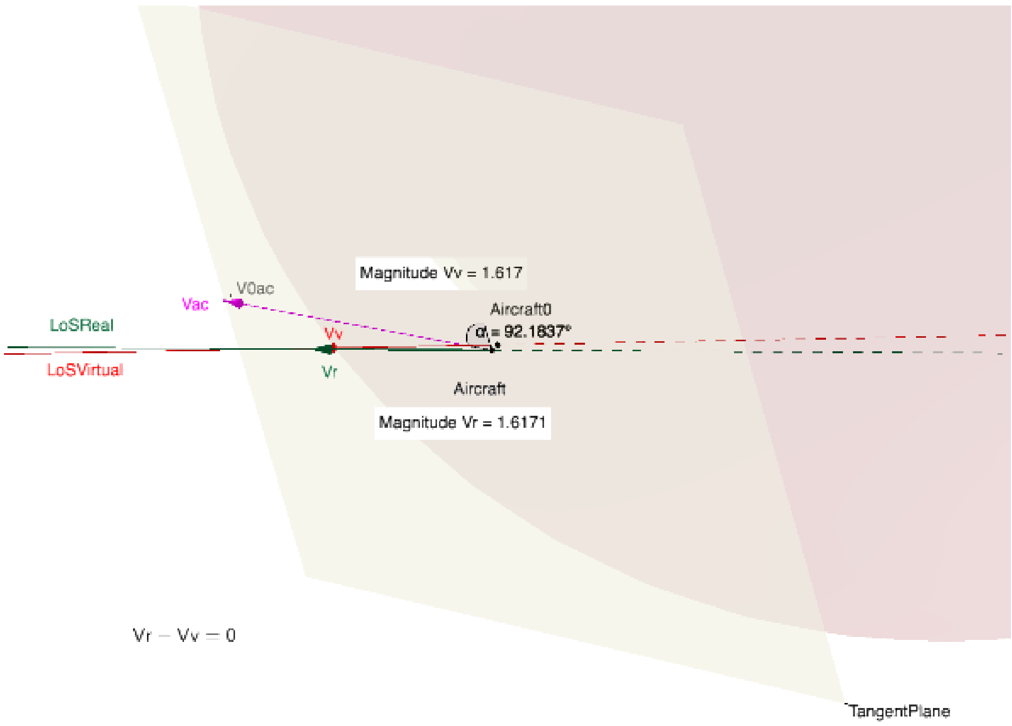

Aircraft velocity direction at 268° (difference at minimum)

Figure 36: Rotation of the aircraft velocity direction on Arc 5

Two values of the track direction α induce a null value for Vr-Vv, the arithmetic difference of the magnitude of these projections i.e. at angle ~87° and ~268° (equivalent to -92° in Figure 36d). This is remarkable, as this occurs for any value of the real aircraft velocity magnitude Vac. Thus, the Doppler correction in these two directions is **independent of Vac.**
One can conclude that the West (~268°) and East (~87°) directions are intrinsically privileged directions of the SuC as the subsequent BFO values will be identical independently of the aircraft

velocity and they will form a cross-node point of the family of BFO residual curves (cf below Figure 37) for these two particular directions.

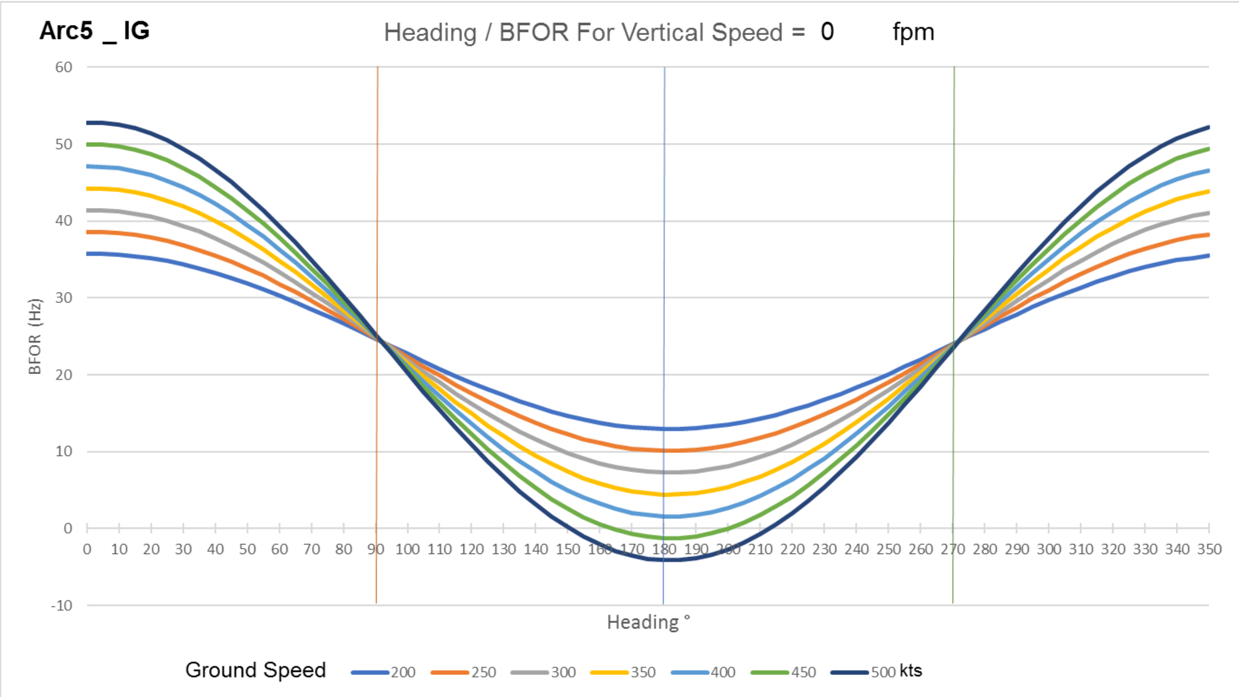

Figure 37: Rotation of the aircraft velocity direction at Arc 5 for example

The other two remarkable positions are very close to 0° and 180° which maximise the difference between the velocity projections magnitude. Unlike the East-West case, the difference of the magnitude of these projections is directly proportional to the magnitude of the aircraft velocity Vac (cf Figure 37).
These four specific directions are visible in Figure 38 below representing the aircraft Doppler components (i.e. Doppler on the LoSReal and Doppler on LoSVirtual) sinusoid shaped curves obtained when varying the aircraft velocity direction (0° to 360°) for two different velocity magnitudes (here 485kt and 200kt). The blue curve is the difference between the green and the purple curves. The green and purple curves are plotted with a scaling factor of 1/10 to allow the blue curve to be readable on the same graph. The zero crossings and the extrema of the blue sinusoid shaped curve represent these four peculiar directions.

***Note**: Computations by CAPTIO Constraint Assessment Tool as described in [2].*

The amplitude of the difference of the aircraft Doppler components is (by definition) proportional to the magnitude of the aircraft velocity as illustrated in Figure 38. One can thus conclude that the larger the magnitude of the aircraft velocity is, the more sensitive the Doppler difference.
Another important conclusion can be drawn using the gradient of the difference of the aircraft Doppler components versus the velocity direction. This gradient being zero for directions ~0° and ~180° and slowing varying around these angles, the sensitivity will be much smaller at these angles than at 87° and 268°. This means that **the larger the given tolerance interval (for ex +/-7 Hz), the larger the interval for acceptable velocity directions**. This will have an impact on the finding of acceptable trajectory solutions for a given BFO.

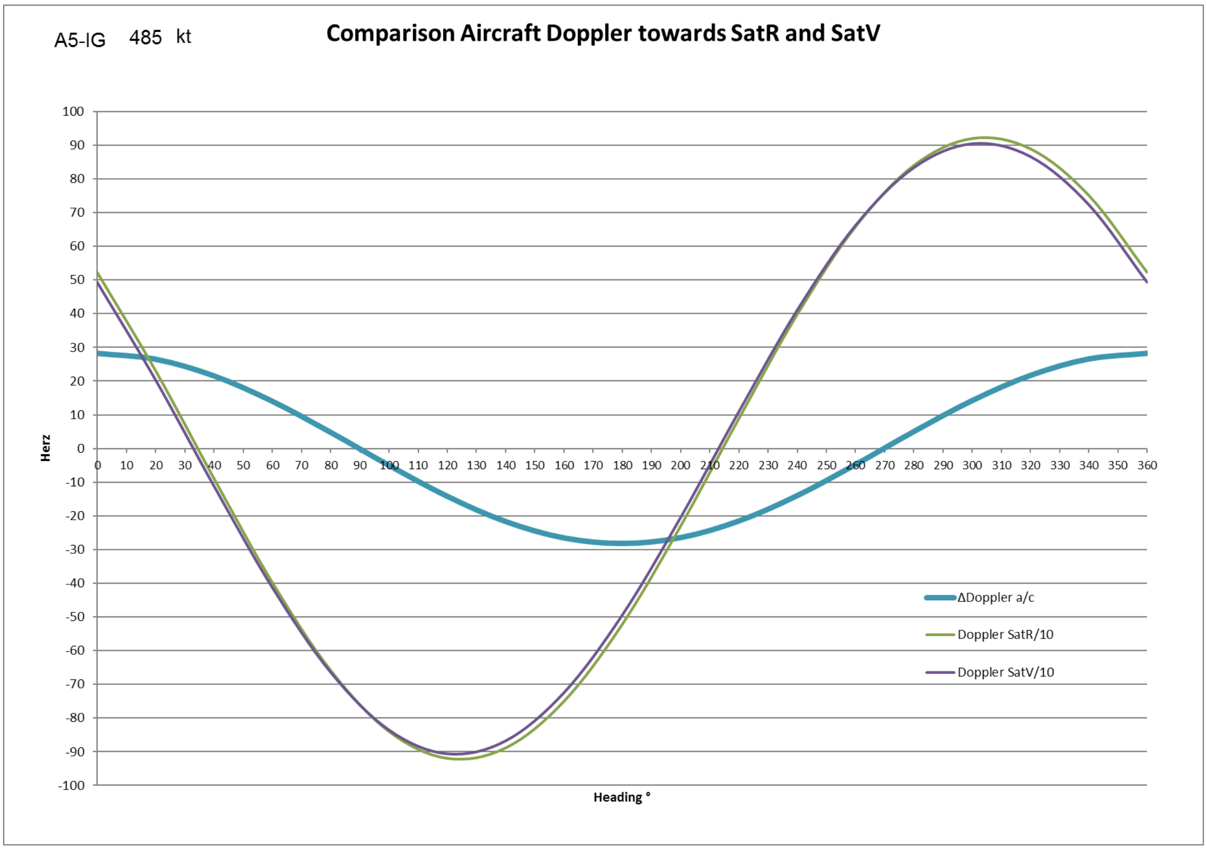

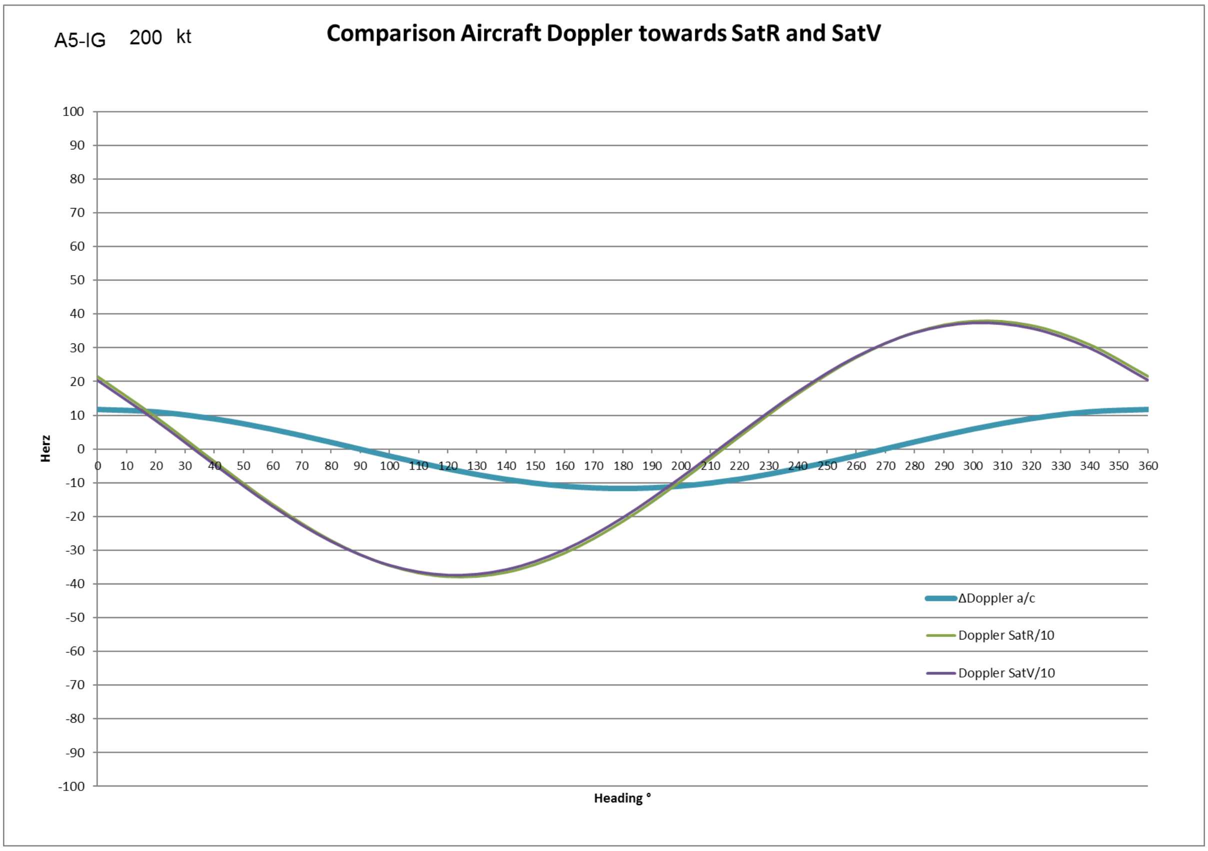

Figure 38: Evolution of aircraft Doppler contribution vs aircraft velocity direction at Arc 5.

Vac=485kt (top) and Vac=200kt (bottom)

Note: a scaling factor= 1/10 is applied to Doppler curves to make the figure more readable.

5 BFO & BFOR behaviour versus aircraft velocity and direction

So far only the aircraft component was analysed. It was seen that the Aircraft Doppler components difference drives the difference ($\Delta fup + \delta fcomp$) following Equation (3) because

$$VrTot = Vr - Vrs$$

where Vrs is constant vis-à-vis the aircraft velocity direction at any given aircraft position. Including all the components of the *BFO Equation (1)* and computing the BFO residual BFORs, one can see that, as expected, the term ($\Delta fup + \delta fcomp$) is shaping the BFORs curve as illustrated in *Figure* 39 as it differs only by a constant value leading to a vertical translation between them (see differential blue curves).

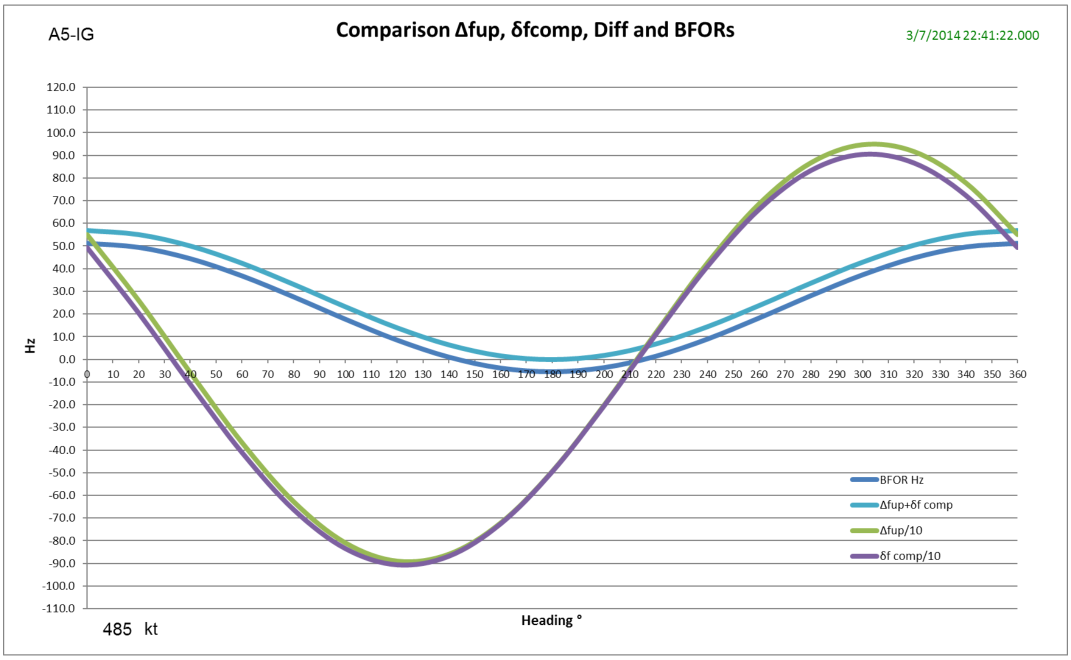

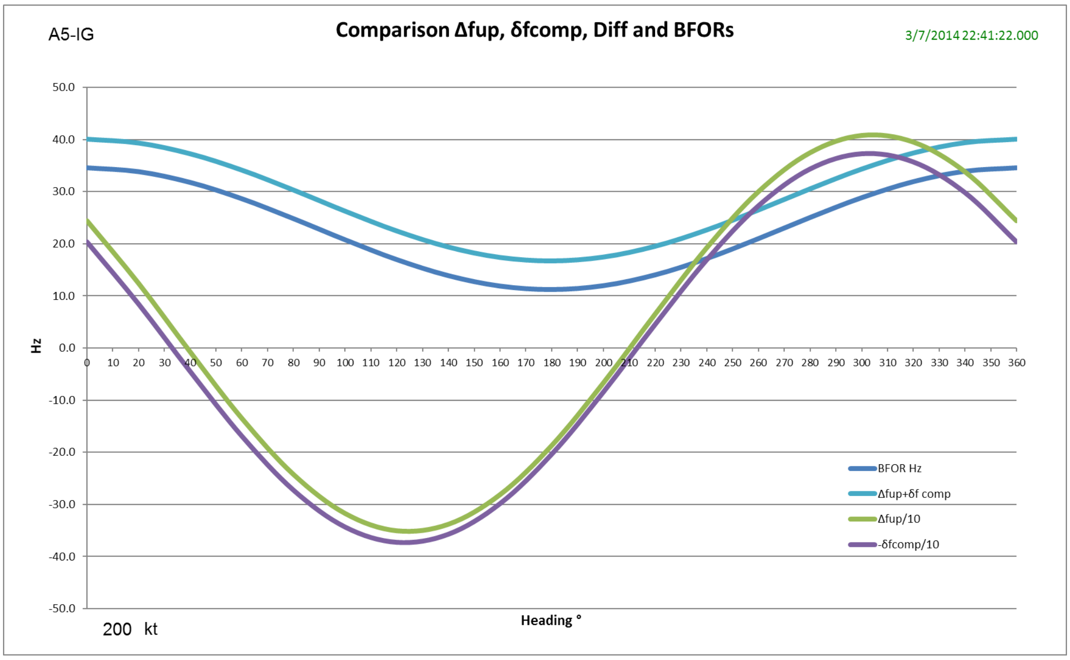

Figure 39: Evolution (Δfup+δfcomp) compared to BFORs vs aircraft velocity direction at Arc 5

All BFO components are included.

Note: a scaling factor= 1/10 is applied to Doppler curves to make the figure more readable.

Gathering the family of plots of BFORs at the selected aircraft position example for a velocity magnitude ranging from 200kt up to 500kt, one can see the four remarkable velocity directions. The nodes close to 87° and 268° at BFOR~24 Hz illustrate that these BFORs are indeed independent of the aircraft velocity magnitude while the extrema at 0° and 180° indicate a higher sensitivity to the velocity magnitude as the curves separate more from each other at these points. The gradient behaviour around 0° and 180° is more slowly varying allowing an increased relaxation on the track angle sensitivity.

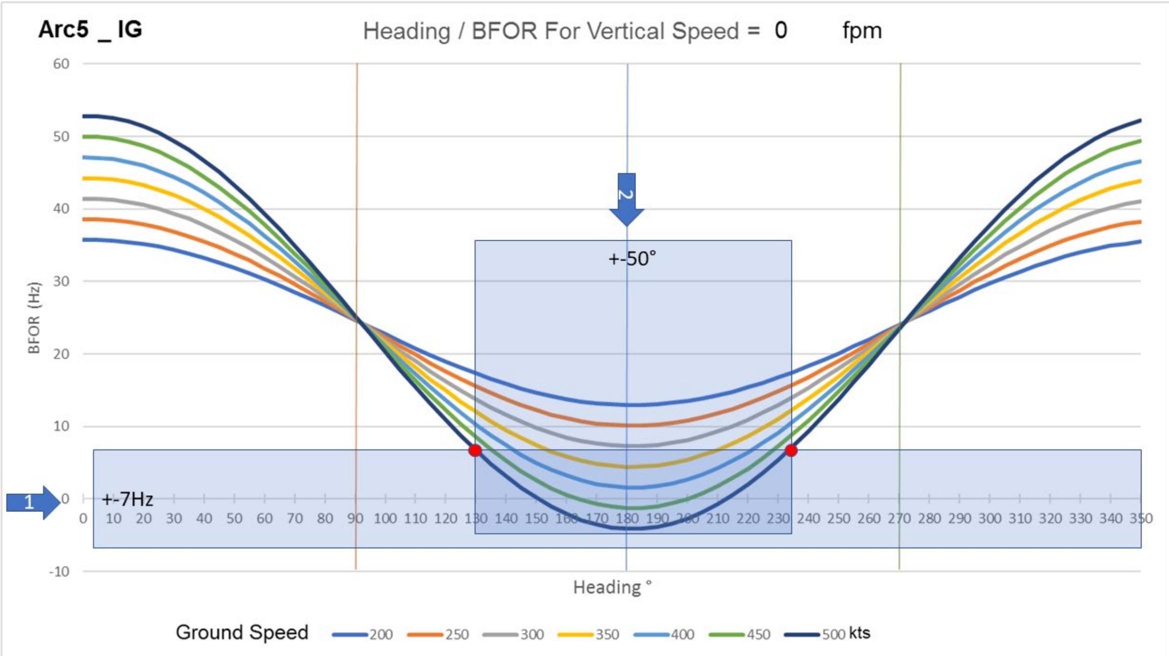

Figure 40: Acceptable aircraft velocity direction interval at Arc 5 IG [-21.42 ; 93.79]

Figure 40 should be read with extreme cautious to avoid misinterpretation. As seen above, the shape of the curve is driven by the geometry and kinetics of the MH370 system. What can be said at this stage is that, for example, a velocity of 485kt would lead to two best directions at ~153° and ~210° where the BFOR=0. But as the BFO uncertainty is set in [1] at +/-7 Hz, the interval of all equally acceptable solutions is in fact the full range from ~130° to ~235° i.e. a ~105° wide interval.
Figure 41 illustrates another example at a different location where the interval of acceptable solutions is in fact the full range from ~135° to ~228° i.e. a ~93° wide interval. In a hypothetical case of a vertical speed of -2000 fpm, considering the acceptable solutions around true track angles of 80° and 270°, the width of the intervals is reduced to ~20°.

As a conclusion and considering the Inmarsat +/-7Hz uncertainty interval, 0° and 180° angles are the angles where the BFORs are the least sensible to the aircraft velocity direction changes because of the low gradient values.

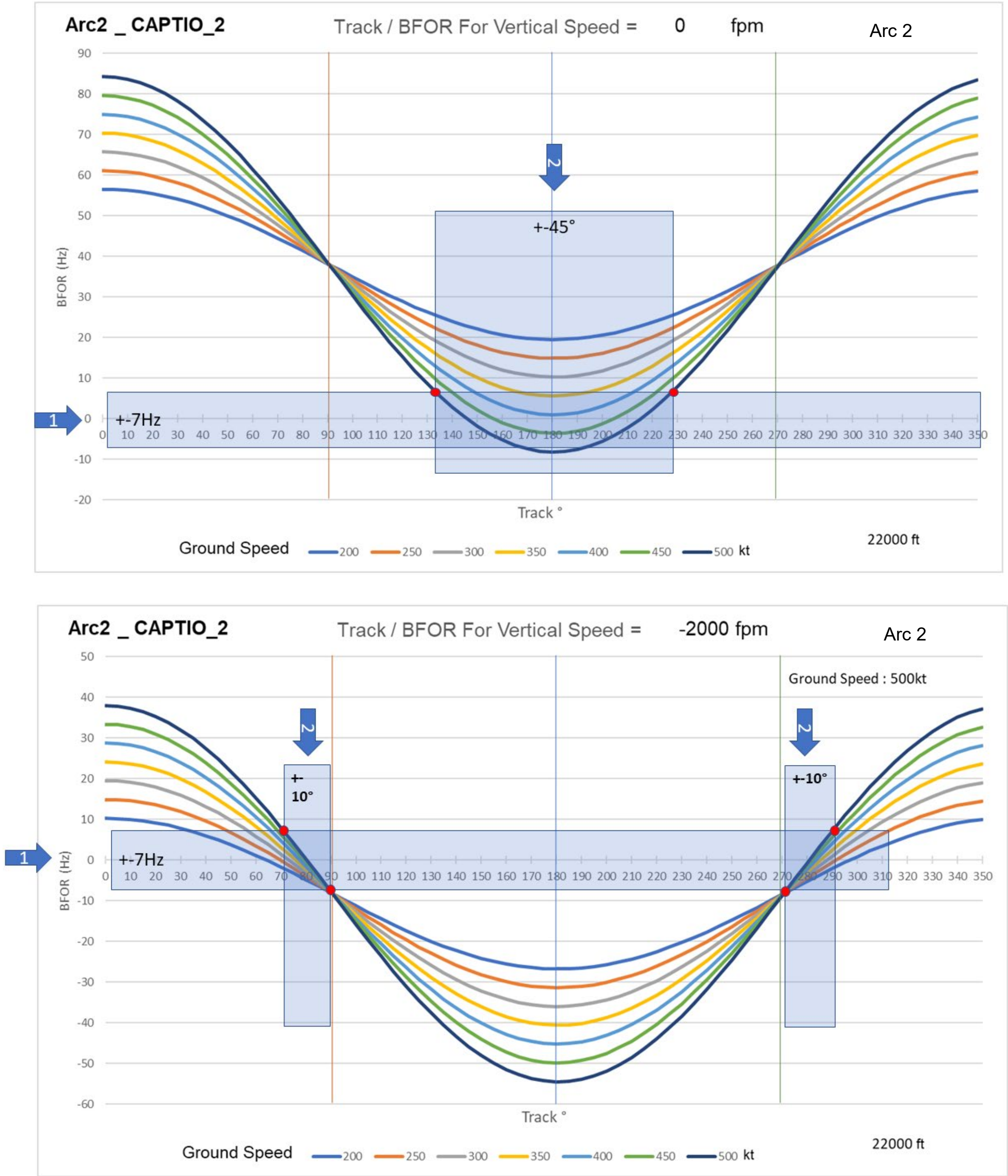

Figure 41: Acceptable aircraft velocity direction interval at Arc 2 CAPTIO

Thus, a caveat must be posted when selecting a trajectory: the presence of an extremum at ~180°, which would seem to indicate an optimisation point with a low BFOR is a false indication. The shape of the BFOR curve is in fact driven by the geometry and kinetics of the SuC due to these elements and their relative position:

1- The location of the aircraft in Northern or Southern Hemisphere
2- And subsequently the orientation of the tangent plane at the aircraft location
3- The location of the real Satellite relative to the equatorial plane
4- The direction of the velocity of the satellite
5- The orientation of the lines of sight to real and virtual satellites

6 Sensitivity analysis for MH370 flight

The MH370 flight started in the northern hemisphere flying northwards with the real satellite moving northwards above the equatorial plane. Then it is supposed to have flown southwards in the south hemisphere when the satellite was still above the equatorial plane but moving southwards. These "twisted" or "flip-over" characteristics over location and time counter act each other such that an identical shape of the BFOR curves is observed along the full flight in both hemispheres as illustrated by Figure 42 from arc1 to arc 7.

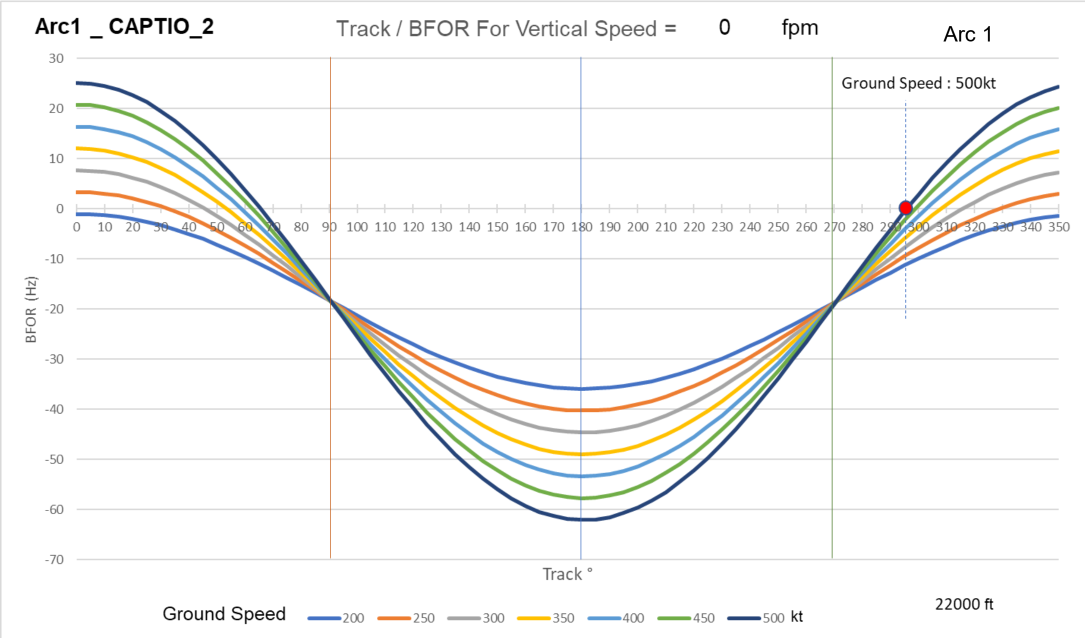

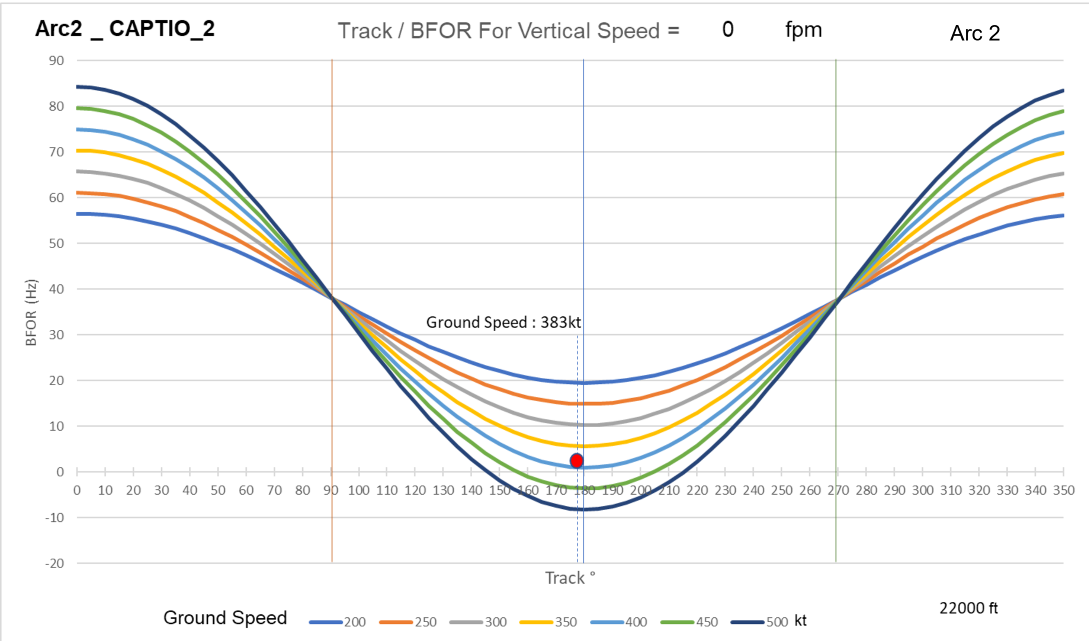

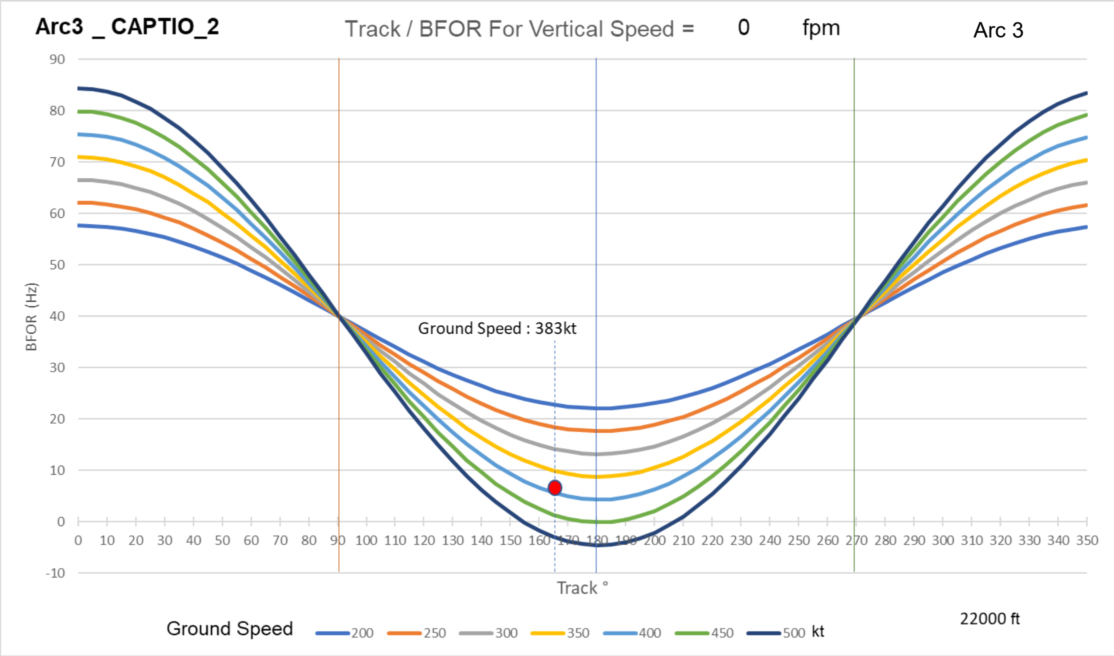
Arc3 _ CAPTIO_2
Track / BFOR For Vertical Speed = 0 fpm
Arc 3
BFOR (Hz)
Ground Speed : 383kt
Track °
Ground Speed 200 250 300 350 400 450 500 kt
22000 ft

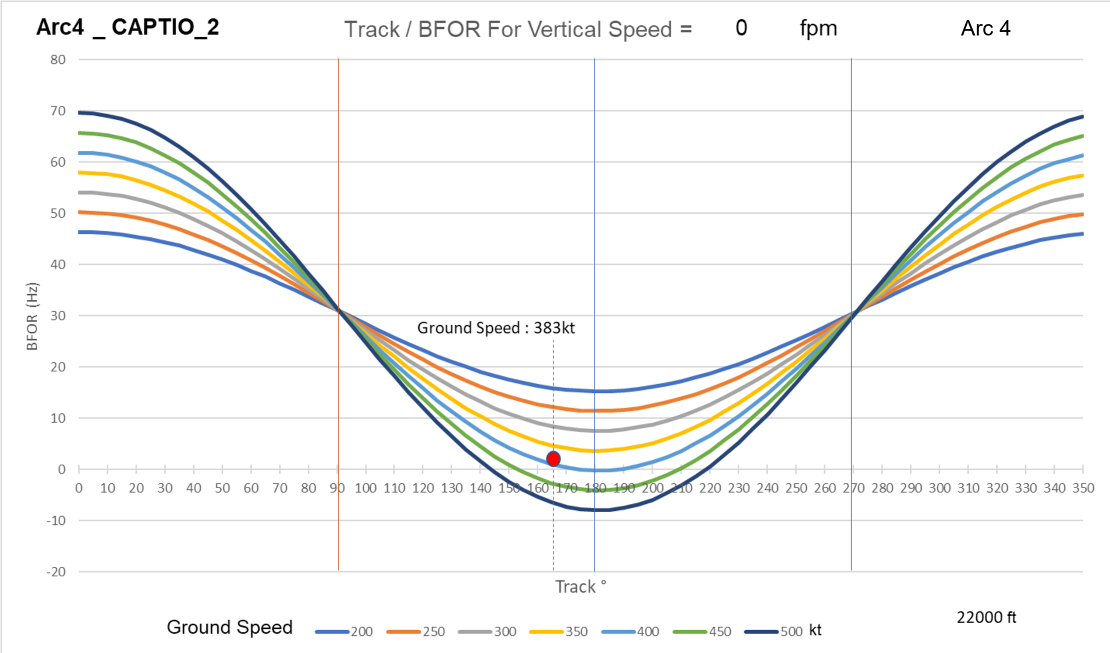
Arc4 _ CAPTIO_2
Track / BFOR For Vertical Speed = 0 fpm
Arc 4
BFOR (Hz)
Ground Speed : 383kt
Track °
Ground Speed 200 250 300 350 400 450 500 kt
22000 ft

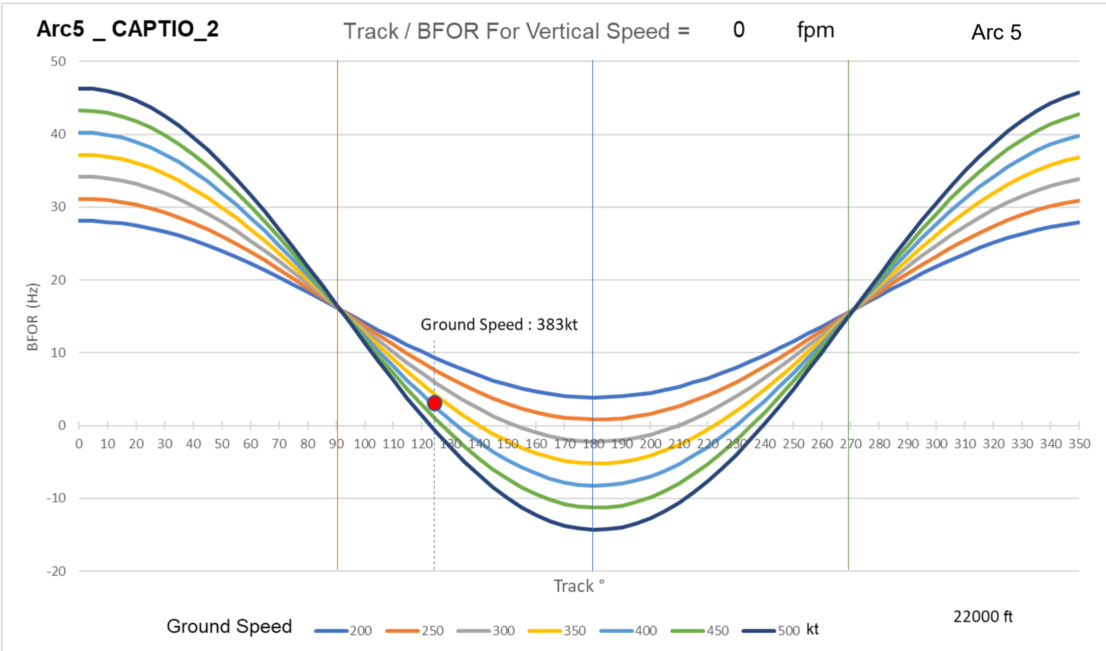
Arc5 _ CAPTIO_2
Track / BFOR For Vertical Speed = 0 fpm
Arc 5
BFOR (Hz)
Ground Speed : 383kt
Track °
Ground Speed 200 250 300 350 400 450 500 kt
22000 ft

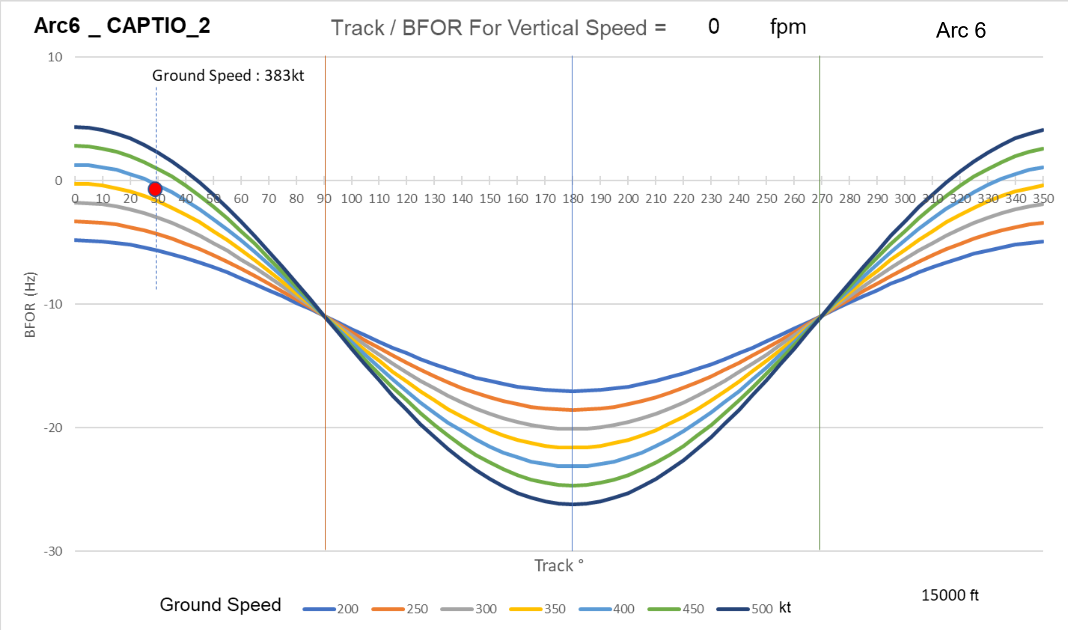

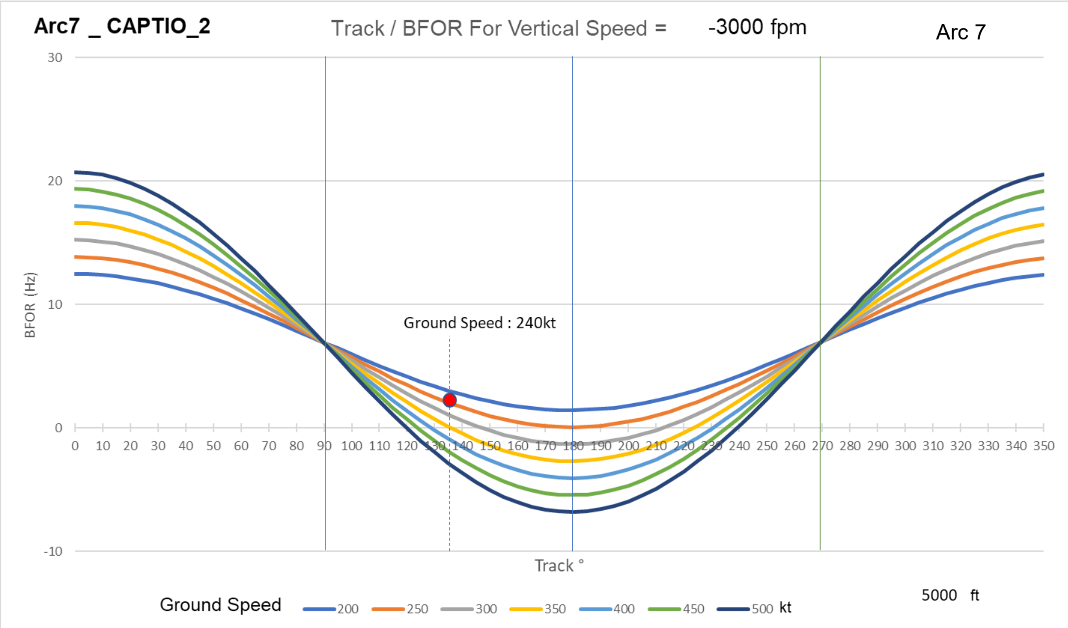

Figure 42:BFORs behaviour versus aircraft velocity direction for CAPTIO at arc1 to arc7.

The shape is similar along the full CAPTIO trajectory. The red spot represents CAPTIO trajectory BFORs at each arc. At arc7 the range of candidate tracks is wide as explained above. The chosen vertical speed is noticeably within the range of a controlled descent. CAPTIO selected a track in coherence with a head-wind ditching.

7 Sensitivity analysis for MH371 flight

Having analysed MH370 BFORs, an interesting follow-up question is: do we observe the same characteristics for MH371 BFORs?

MH371 flight, from Beijing to Kuala Lumpur on the same day, was 9M-MRO aircraft preceding flight. It took place entirely in the northern hemisphere with the satellite basically under the equatorial plane and always moving southwards. These constant characteristics are different from MH370 and lead to an inverse effect compared to MH370 BFORs such that the shape of the observed curves along the full flight is of a bell shape type as illustrated by the sketched Figure 43 from arc2 to arc11. These data come from the Inmarsat measured MH371 BTOs and BFOs compared to the computed estimations from our CAT model.

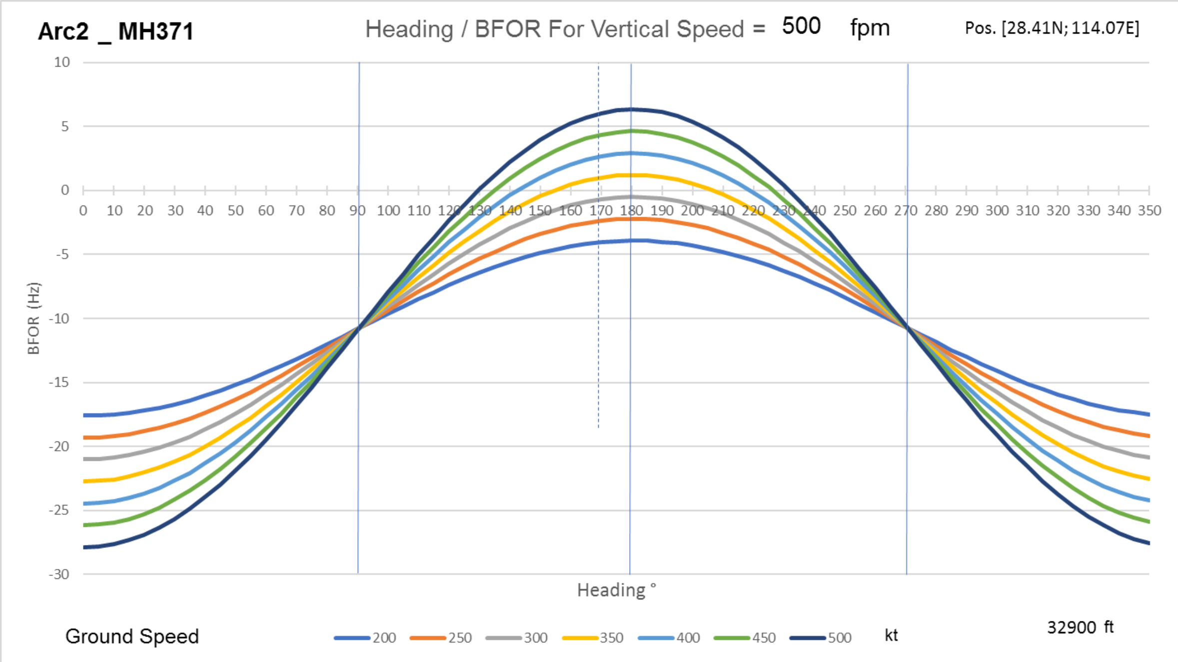
Arc2 _ MH371
Heading / BFOR For Vertical Speed = 500 fpm
Pos. [28.41N; 114.07E]
BFOR (Hz)
Heading °
Ground Speed
200 250 300 350 400 450 500 kt
32900 ft

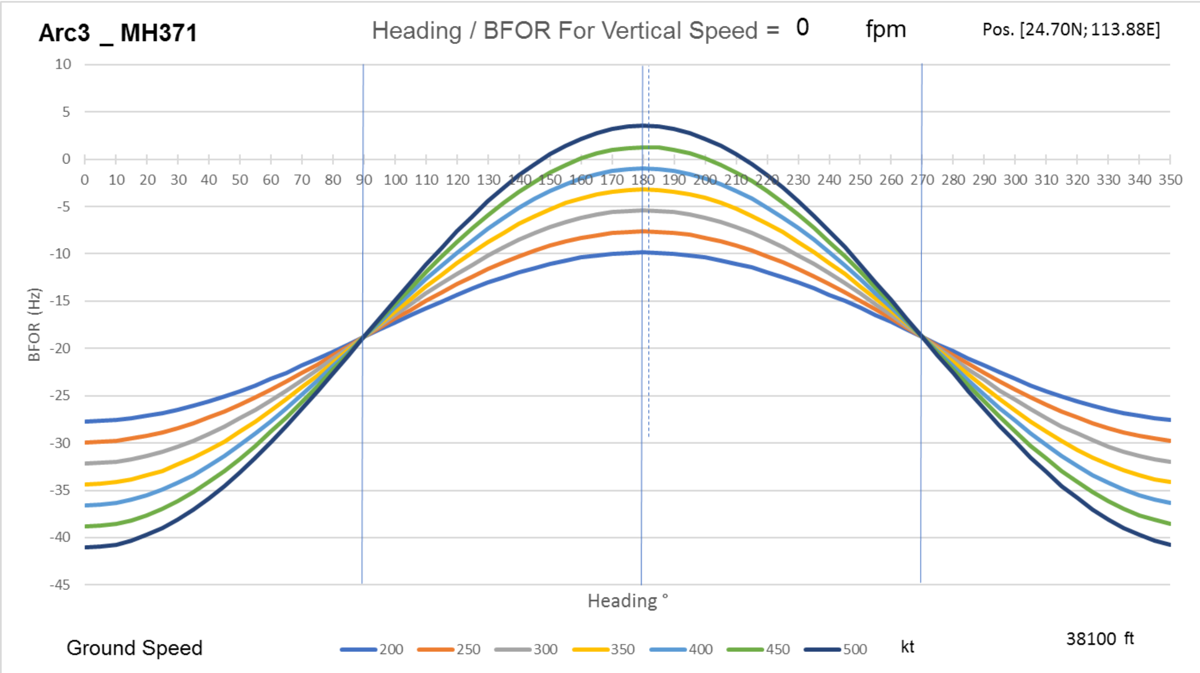
Arc3 _ MH371
Heading / BFOR For Vertical Speed = 0 fpm
Pos. [24.70N; 113.88E]
BFOR (Hz)
Heading °
Ground Speed
200 250 300 350 400 450 500 kt
38100 ft

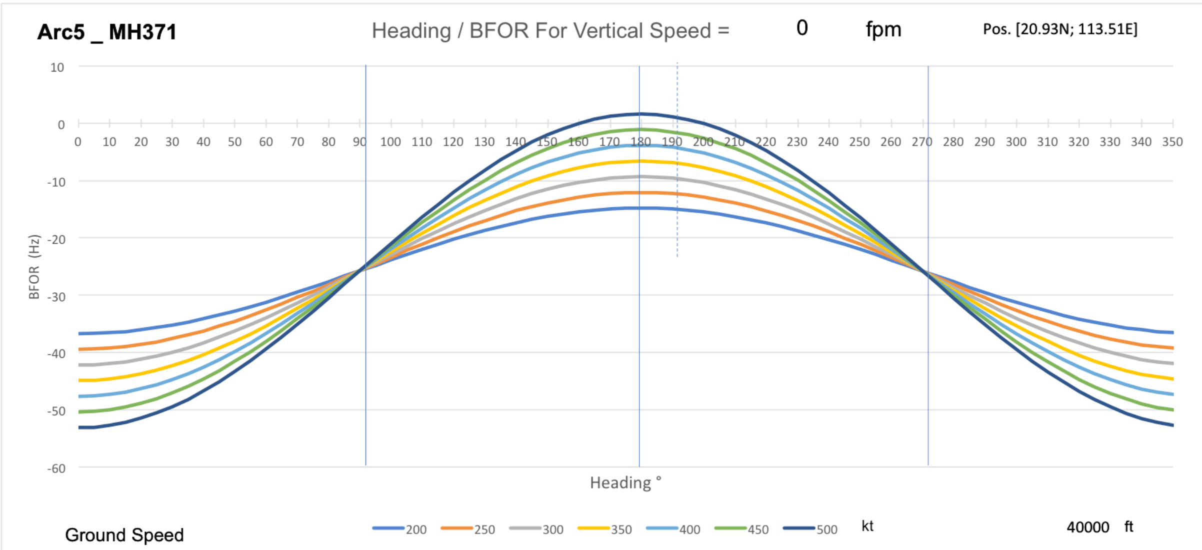
Arc5 _ MH371
Heading / BFOR For Vertical Speed = 0 fpm
Pos. [20.93N; 113.51E]
BFOR (Hz)
Heading °
Ground Speed
200 250 300 350 400 450 500 kt
40000 ft

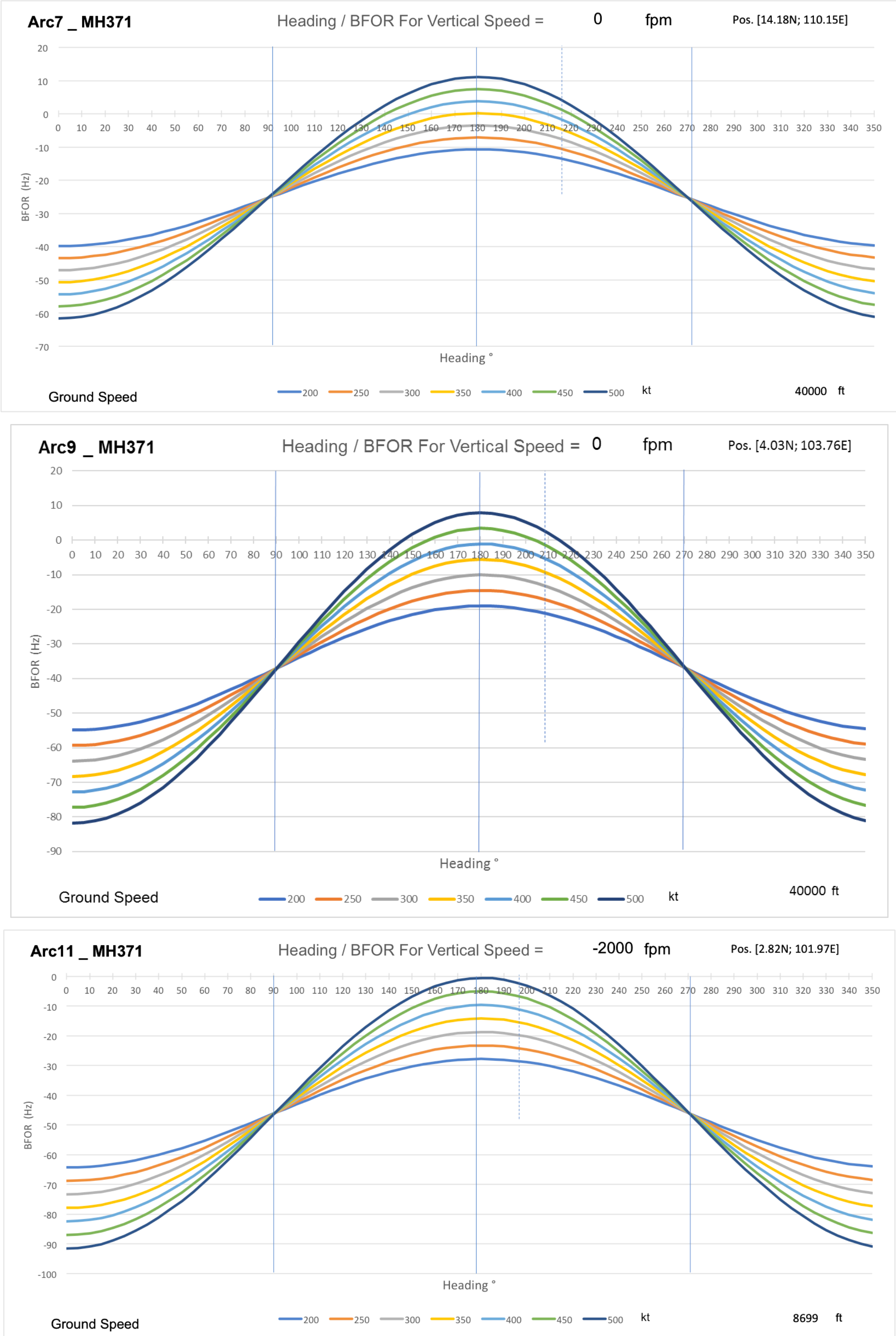

Figure 43: BFORs behaviour versus aircraft velocity direction for MH371 at some of its arcs.

The shape is similar along the full MH371 trajectory.
The blue vertical dotted lines indicate the flown true track at the geodesic position of the crossing of the arcs.
The four remarkable velocity directions are present but the sensitivity of the BFORs to the heading is different as foreseen because of the SuC geometry and kinetics. Here again, 0° and 180° directions are

thus artificially attracting the attention while the key question is position of the BFOR curves - scaled by the velocity - vis-à-vis the uncertainty interval +/-7 Hz.

Figure 44 illustrates the dependency of the BFORs behaviour to the geometry of the SUC. It represents the BFORs values at 1:39 on March 7th UTC when 3F1-IOR satellite crosses the equatorial plane. This demonstrates a strong sensitivity on the geometry of the SuC. One can see that the "nodes", maxima and minima are in the move for a 90° shift as explained above.

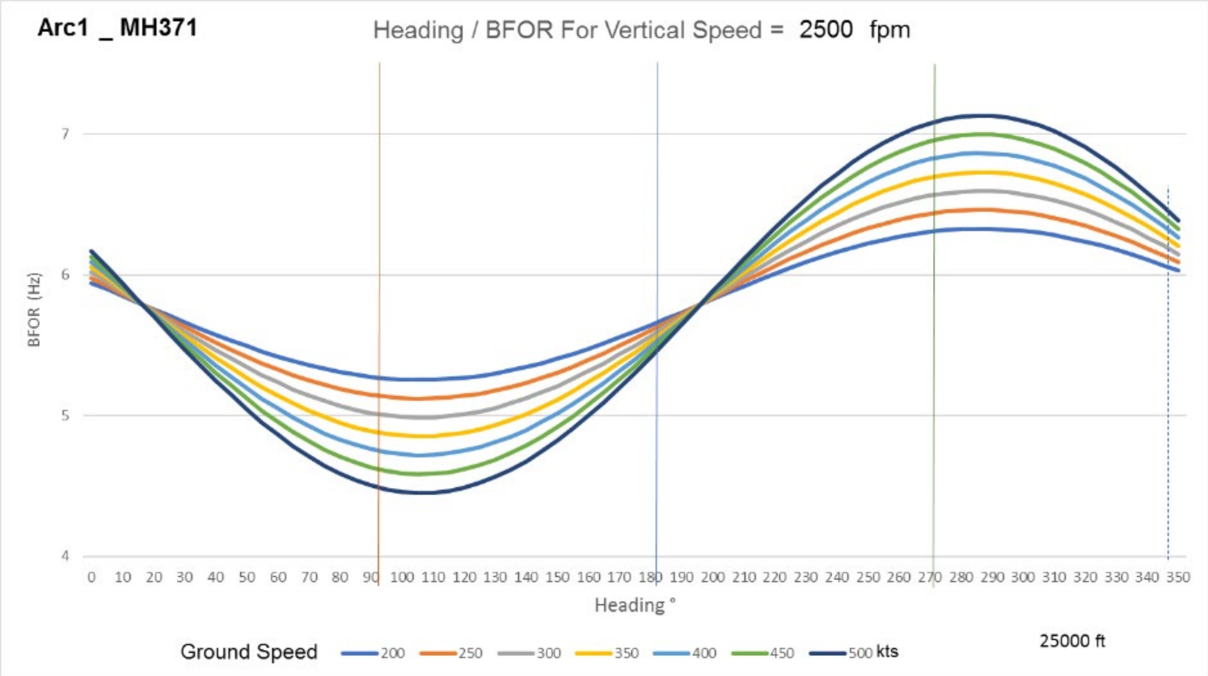

Figure 44: BFORs behaviour versus aircraft velocity direction for MH371 at 1:39 on March 7th UTC.

8 What if the satellite had a West-East excursion?

So far, the considered locus of the sub-satellite point was the actual very elongated ellipse with a North-South oriented major axis as depicted in Figure 30. To further explore the dependency of the BFORs on the SuC geometry and kinetics, let's ask the question: what if the real satellite had a motion around the nominal position [0°; 64.5°E] with completely different characteristics?
One could design a hypothetical different satellite locus of the sub-satellite point as presented in Figure 45, which has been simulated in modifying the satellite orbit inclination and eccentricity for the sake of demonstration. The simulated locus includes the same shape and same proportions as the actual one but with a major axis rotated by 90° in a West-East direction in the equatorial plane and with the corresponding kinetics. The journey of the satellite is illustrated at the corresponding periods when the two flights MH371 and MH370 took place in orange and green colours respectively.

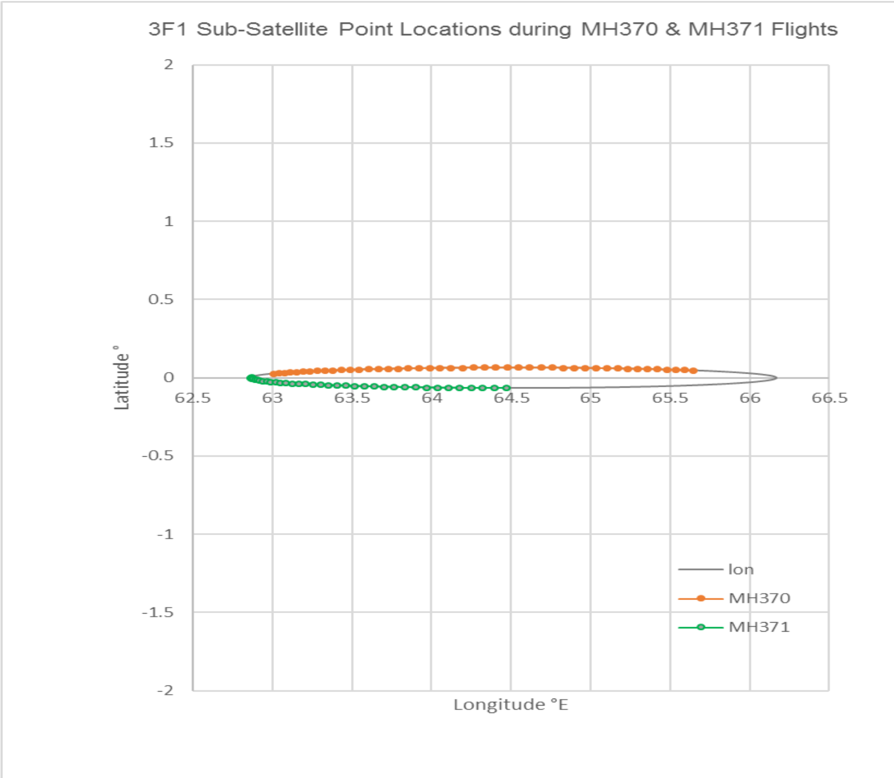

Figure 45:Model of a hypothetical West-East oriented satellite ephemeris.

In Figure 46, the results of the computation of the subsequent BFOs and BFORs show that the different geometry configuration – here the rotation of the satellite motion major axis - modifies the shape of the BFORs curves. The four remarkable directions have swapped roles: 0° and 180° directions become the nodes where all BFORs are independent of the aircraft velocity magnitude while ~90° and ~270° directions become the extrema of the BFORs plots.

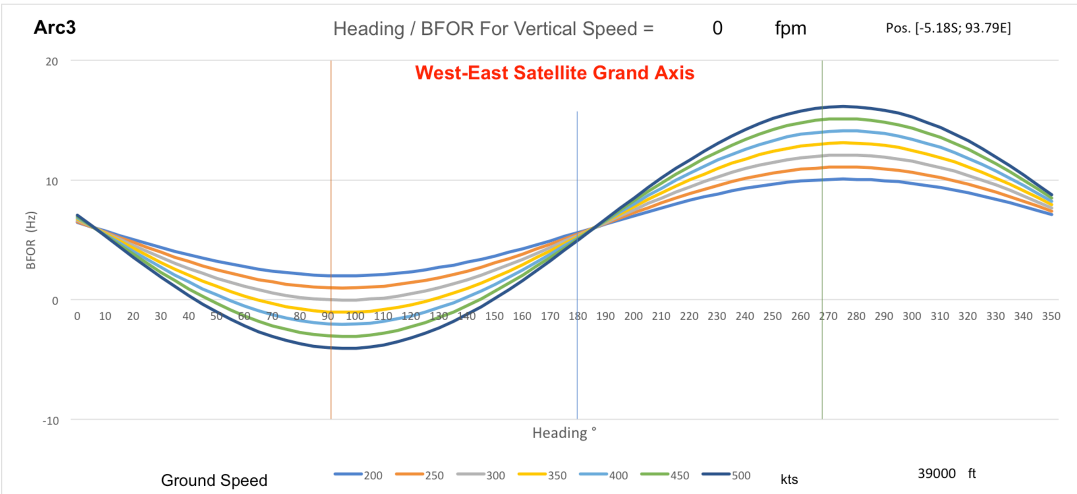

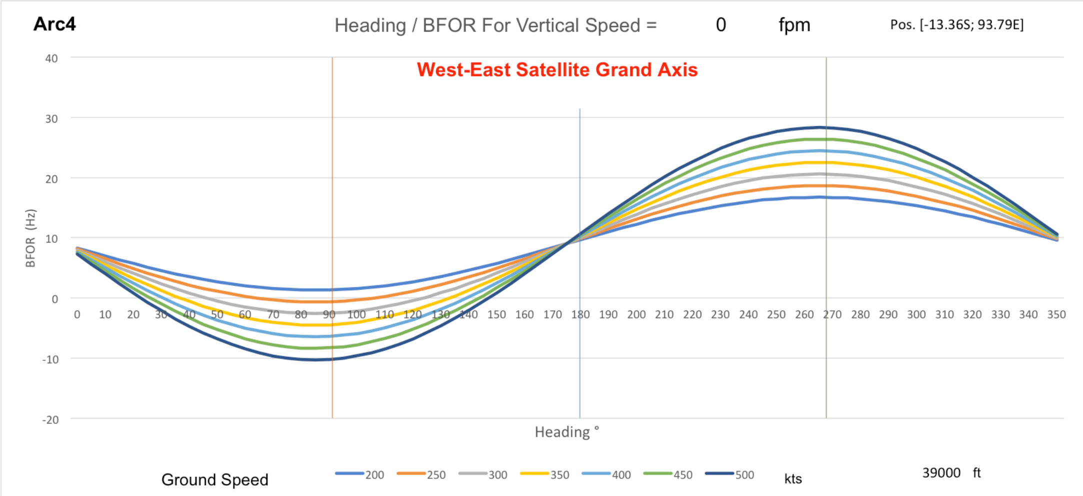

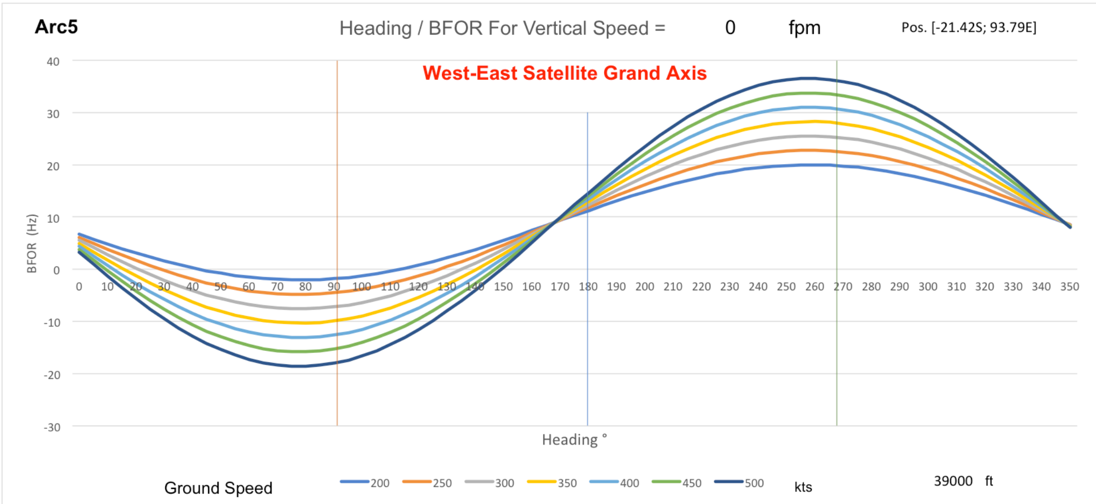

Figure 46: BFORs behaviour versus aircraft velocity direction at selected points on MH371 arc3 to arc5. (The sub-satellite point locus' major axis is in the equatorial plane).

The shape of the curves of the BFORs as function of the true track shows a translation by an angle of approximately ~ -90° to the left.
In these simulations, the "simulated" measured BFOs had to be arbitrarily chosen because no actual measurement exists in such a hypothetical geometry. As explained in the first part of this analysis, measured BFOs contribute only via a constant term in the BFORs computation, which simply vertically translates the BFORs curves along the frequency (Hz) axis of the plots. But the shape of the curves is not affected by this fixed shift. Consequently, from this analysis, a valid conclusion can still be drawn on the impact of the geometry and kinetics of the SuC.

References:

[1] The Search for MH370, Chris Ashton, Alan Shuster Bruce, Gary Colledge and Mark Dickinson, (Inmarsat), THE JOURNAL OF NAVIGATION (2015), 68, 1–22

[2] A Plausible Trajectory for MH370", CAPTIO Team, Dec. 2017, www.mh370-captio.net

[3] Ian-D-Holland -1702.02432.pdf, The Use of BFO in the search of MH370

[4] Peter O. Large, A meta-analysis of geospatial estimates in the case of the Malaysian Airlines Flight MH370, Dissertation, May 2019, ProQuest 13857090

[5] The Final Resting Place of MH370, B. Ulich, R. Godfrey, V. Iannello and A. Banks, 7th March 2020

[6] Henrik Rydberg, "MH370: Finding the Path", 3 June 2014, http://bitmath.org/mh370/mh370-path.pdf

[7] Bayesian Methods in the Search for MH370, S. Davey, N. Gordon, I. Holland, M. Rutten & J. Williams, Defence Science and Technology Group Australia, Springer Verlag, ISBN 978-981-10-0378-3 (2016)

[8] Analytic Equations for the Orbit of 3-F1, sk999 (Jul 3, 2014)

[9] Wikipedia, https://en.wikipedia.org/wiki/Geographic_coordinate_conversion

[10] Graphics and equations modelled in GeoGebra https://www.geogebra.org

9 Annex A: Inmarsat sensitivity analysis complement

This section offers some complementing aspects to the sensitivity analysis performed by Inmarsat in Section 5.5 of [1]. In Figure 46, the BFORs curves are plotted at the Inmarsat selected time t_i=17:07 when the last ACARS message was received a short while after MH370 Top of Climb. Table 7 in [1] was built in considering a limited symmetrical interval +/-25° for the velocity direction around the known true track of 25° i.e. [0°; 50°]. The striking results came from the asymmetrical behaviour of the BFORs limits, which is explained below.

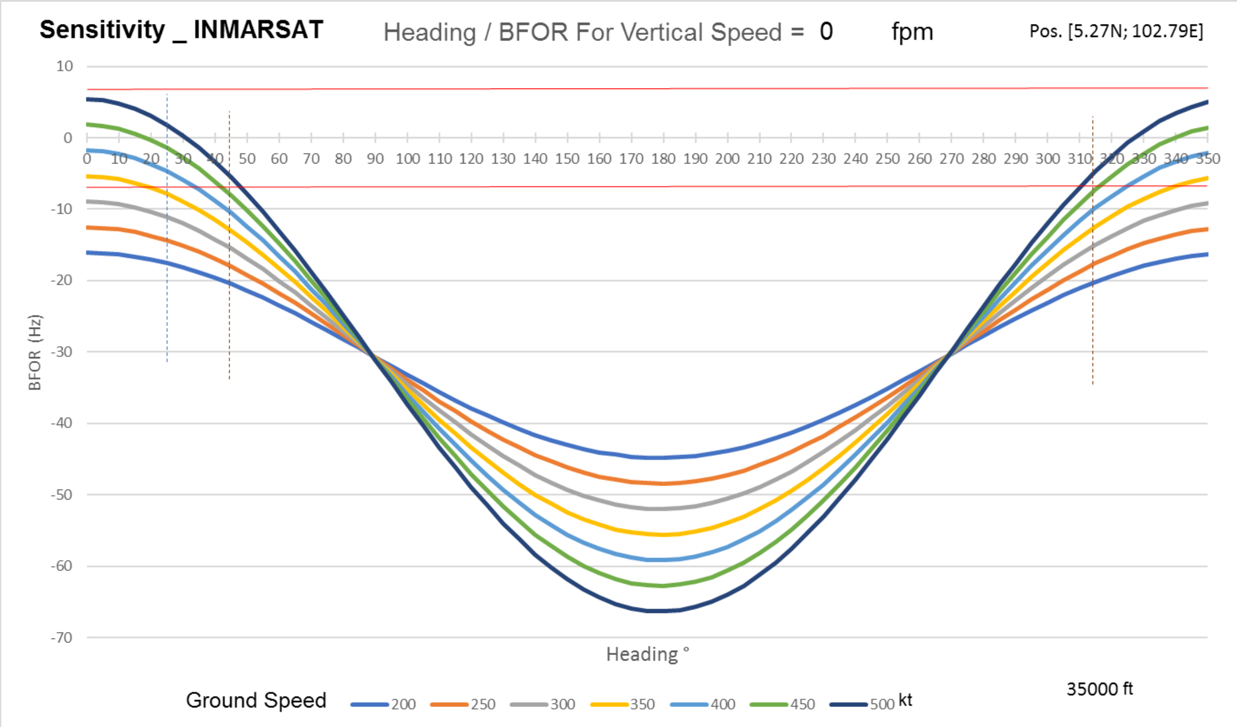

Figure 47: BFORs Sensitivity to aircraft track errors at 17:07 after Top of Climb.

In Figure 47, the blue dotted vertical bar indicates the true track corresponding to the actual velocity of 470kt. The two horizontal red lines represent the +/-7 Hz uncertainty interval around the true track BFOR. The two brown dotted vertical bars indicate the upper and lower boundaries of the track angle at this speed. Thus, Inmarsat Table 7 should be enhanced with Table 9 below.

Measurement Parameter		True Track		Notes
BFOR (Hz)	-7	-1	-7	BFOR never above +7Hz
Track	313°	25°	45°	In [1] the choice of the high track direction was = true track +25°. This led to a |BFOR| = 10.9 Hz > 7 Hz

Table 9: BFORs Sensitivity to aircraft track errors (complement of Table 7 in Inmarsat paper [1])

The range of possible track directions within the given uncertainty interval is thus ~92° wide, but not centred on the true track. The sensitivity Hz/Degree should thus be expressed for each side of the extremum and separately.

10 Annex B: Vertical Motion of the Aircraft:

Recalling the initial boundaries of the study, the vertical motion of the aircraft has been considered to be zero up to now i.e. no climb and no descent. Only horizontal Vac_i and α_i, have been considered as input variables for the sake of analysing flat trajectories.
But what is the impact of a non-zero rate of climb RoC_i on the BFORs behaviour?
Considering the geometry, a RoC_i is by definition the vertical component of the aircraft velocity Vac_i. Thus, it is orthogonal to the tangent plane as defined in Figure 28. In addition, it does not contribute to the computation of the Doppler compensation by the aircraft by design of the algorithm.
Thus, the contribution of RoC_i impacts solely the velocity VrTot by its projection on the line-of-sight LoSReal between the real satellite and the aircraft. This projection adds to VrTot on top of the projections Vrs and Vr onto LoSReal.
Consequently, its contribution to the behaviour of the BFORs via the BFOs is a shift of the curves along the frequency axis (Y vertical axis) as illustrated in Figure 48 by 3 examples of different RoC_i at Arc2. The amplitude peak to peak stays constant at 78.92Hz. This shift is an important adjustment variable in order to “make the BFORs fit within the Inmarsat +/-7Hz interval” when deriving a possible trajectory.
Due to its angle with the LoSReal (elevation angle), the more obtuse this angle is the more influencing is a non-zero RoC_i . This can be said another way: the closer the trajectory is to the satellite the more a non-zero RoC_i will impact the BFOs and thus the BFORs and vice-versa for the horizontal component of Vac (Vr). The farther from the satellite the trajectory is the more Vr influences the value of the BFOs.

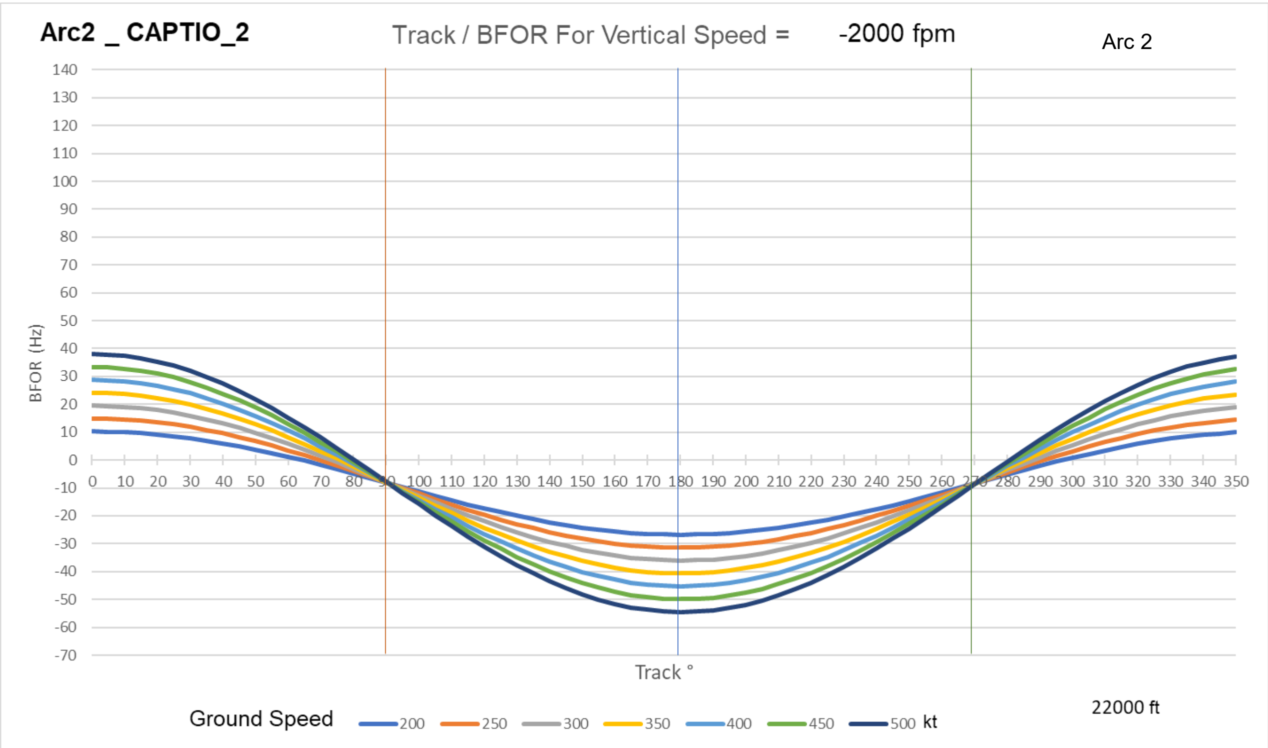

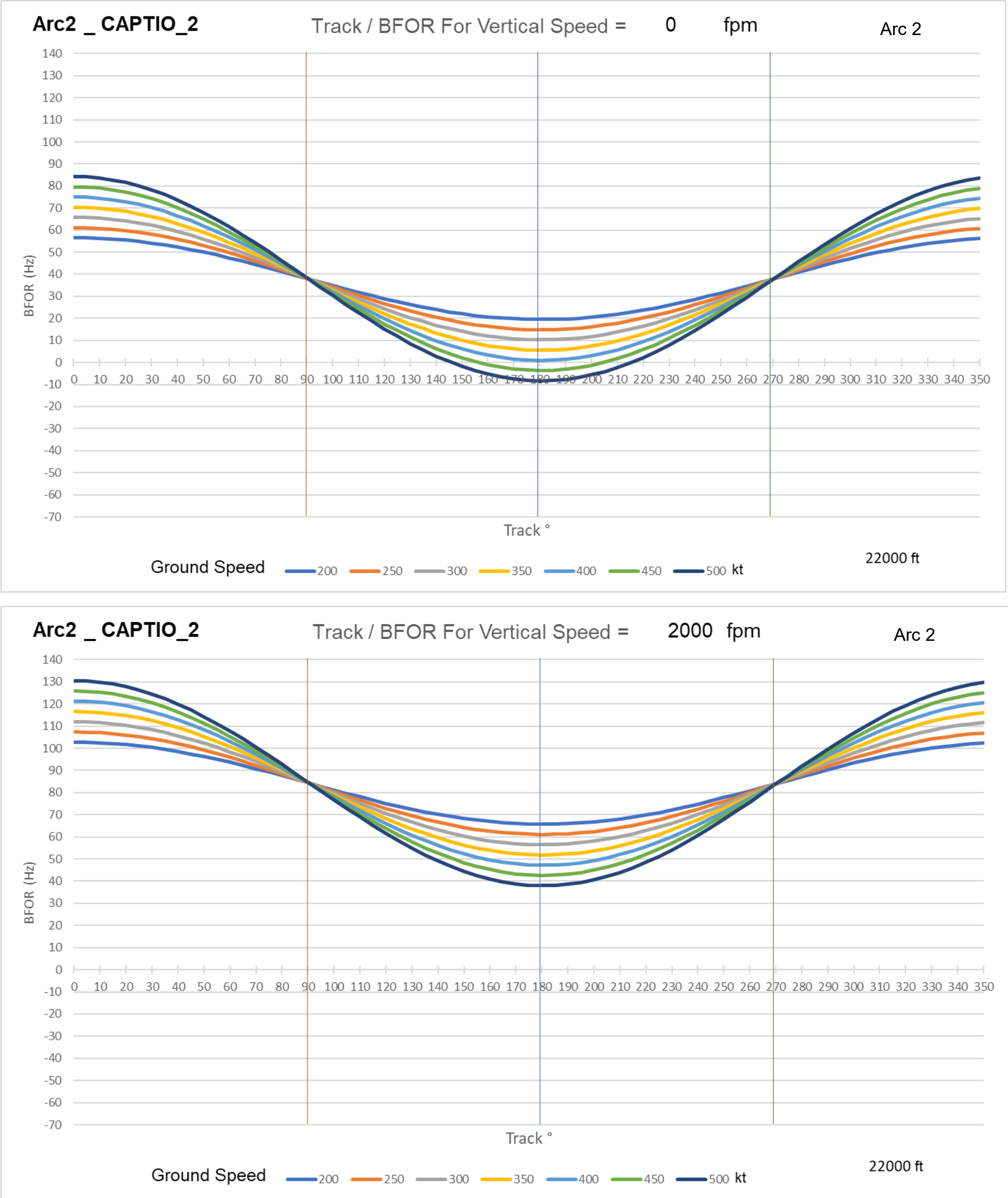

Figure 48: Example of BFORs behaviour versus aircraft RoC at 19:41.

This explains why CAPTIO trajectory derives an acceptable negative RoC_i at arc 7 compatible with a glided path compared to other hypotheses on Arc7 BFO which favour a free fall of the aircraft. In fact, at this geographic location, the geometry and kinetics of the SuC lead to a range of candidate RoC in the fpm range of [-2500; -4000] as depicted in Figure 49. The operational choice of a controlled ditching calls for a choice of a heading facing the wind, dwell permitting. This naturally selects a RoC of ~ -3000fpm leading to a BFOR of about -2Hz.

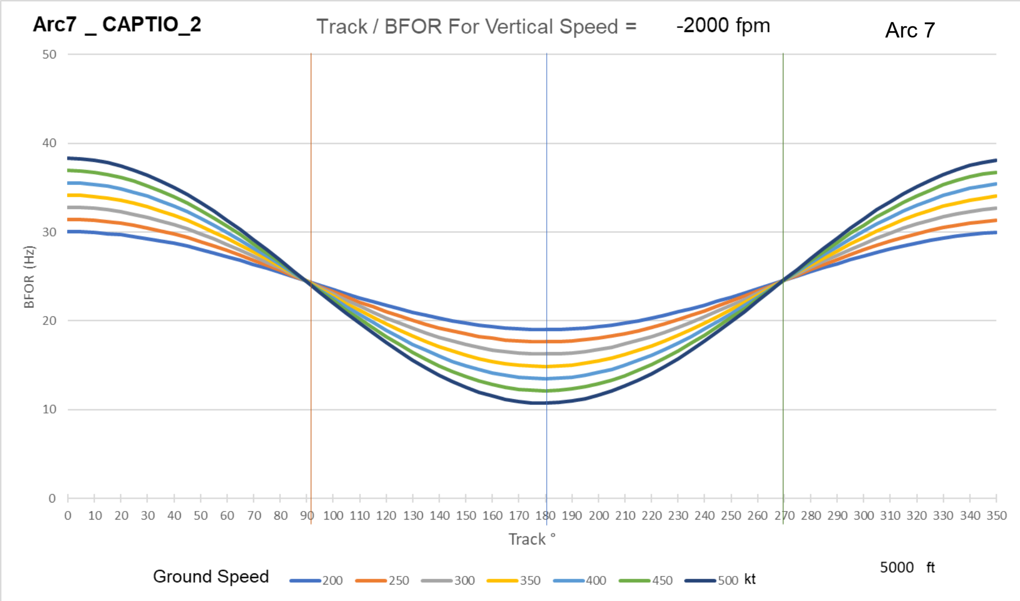

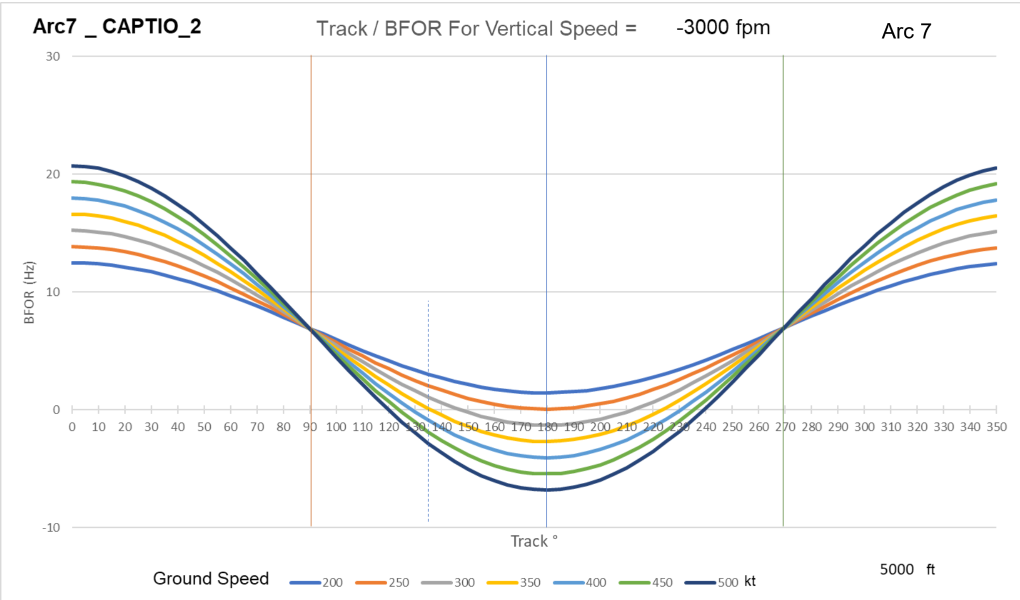

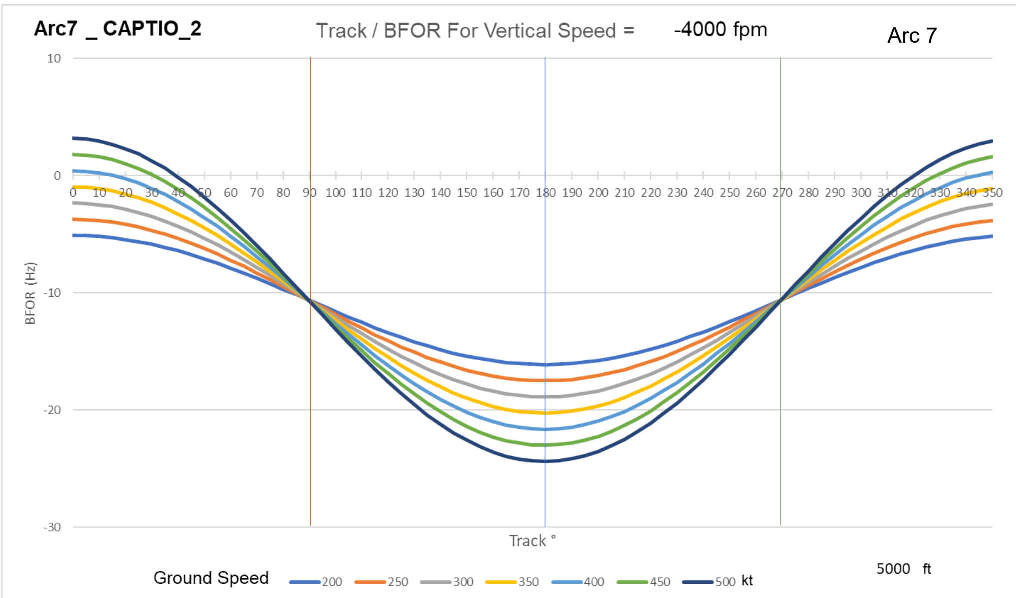

Figure 49: CAPTIO RoC selection at Arc 7 at 00:19:29.

For this analysis, our computations are based on two software tools. The first one is an excel workbook initially created by Prof. Yap F. Fah, NTU, Singapore (Version4) that we have gradually enhanced as our knowledge progressed (now our own is Version 6). In particular, we have included SK999-Satellite Model which nicely compares with Inmarsat and Duncan Steel's models. The second tool, the Constraint Assessment Tool (CAT) is a homemade software developed in parallel encompassing similar functions as Version 6 with all required complementary operational data (fuel consumption, meteo, arc generation, etc.) to allow us to estimate the flight characteristics in conditions closer to reality.

Satellite

Quoting SK999 satellite ephemeris model which is publicly available [8]:

For the limited time that MH370 was flying, one can approximate the orbit of satellite Inmarsat 3F1 by a traditional Keplerian ellipse and achieve good accuracy. Further, because the orbit is nearly circular, the conversion from Keplerian ellipse parameters to a Cartesian coordinate system can be expressed by some fairly straightforward equations.

"Two Line Element" (TLE) sets are produced by NORAD from optical and radar tracking systems and are the main source of orbital elements for Earth-orbiting satellites. Satellite operators like Inmarsat presumably have much more accurate orbital information, but such information is not readily available, nor is it necessary for this study purposes.

The TLE set for 3F1 is updated every few days. Here is the TLE set used for MH370:

1 23839U 96020A 14066.96754476 -.00000012 00000-0 10000-3 0 2640

2 23839 1.6371 73.1994 0005326 270.3614 234.8362 1.00274124 65669

But the orbital parameters in a TLE set do not give the actual parameters for an orbit at epoch, but rather represent parameters of some mean orbit, to which additional terms must be added to account for various perturbations due to the non-spherical shape of the earth and the influence of the moon and sun. The "sgp4" model is used to compute and apply these corrections. It turns out that the "long term periodic" corrections are the only ones of significance. The ascending node increases by about 0.8 degree and the argument of perigee decreases by about the same amount

In the ATSB report on "Definition of Underwater Search Areas", Inmarsat has tabulated, in Table2, the position and velocity of 3F1 in ECEF coordinates for a number of times during the flight. This information can be used to refine the orbital parameters. The derived values are as follows:

epoch = 14066.9675 = year and day number for which the elements are computed

M = 234.836 = mean anomaly at epoch

ω = 269.550 degrees = argument of perigee

Ω = 74.011 degrees = right ascension of ascending node

n = 1.00274 = mean motion (revolutions/solar day)

e = 0.00054 = eccentricity

i = 1.6401 degrees = inclination

lsat = 64.516 degrees: nominal latitude

rs = 42164.7 km = radius

Using these elements and the above equations, Inmarsat's table values are reproduced within 1 km in position and 0.7 km/s in velocity worst-case error. The remaining derived parameters are as follows:

ut0 = 13.620 hours = UT of ascending node passage

utp = 7.607 hours = UT of perigee passage

κ = 15.041 degrees/hour = angular rate

BFO/BTO

Our computation of the BTO and BFO are based on our own improved formulas in version 6 of our software.

We have enhanced these formulas in introducing SK999 satellite model, in enhancing the perfect satellite model, and in re-modelling and extending the two Inmarsat figures n°10 Calculated Pilot Frequency doppler Offset and n° 11 on the Measured Pilot Frequency Error (After conversion) published in [1]. To our knowledge no digital values have been made publicly available by Inmarsat.

Figure 50 and Figure 51 illustrate the plot of the new polynomial modelling and tabulation of these two curves in orange and in red dotted line.

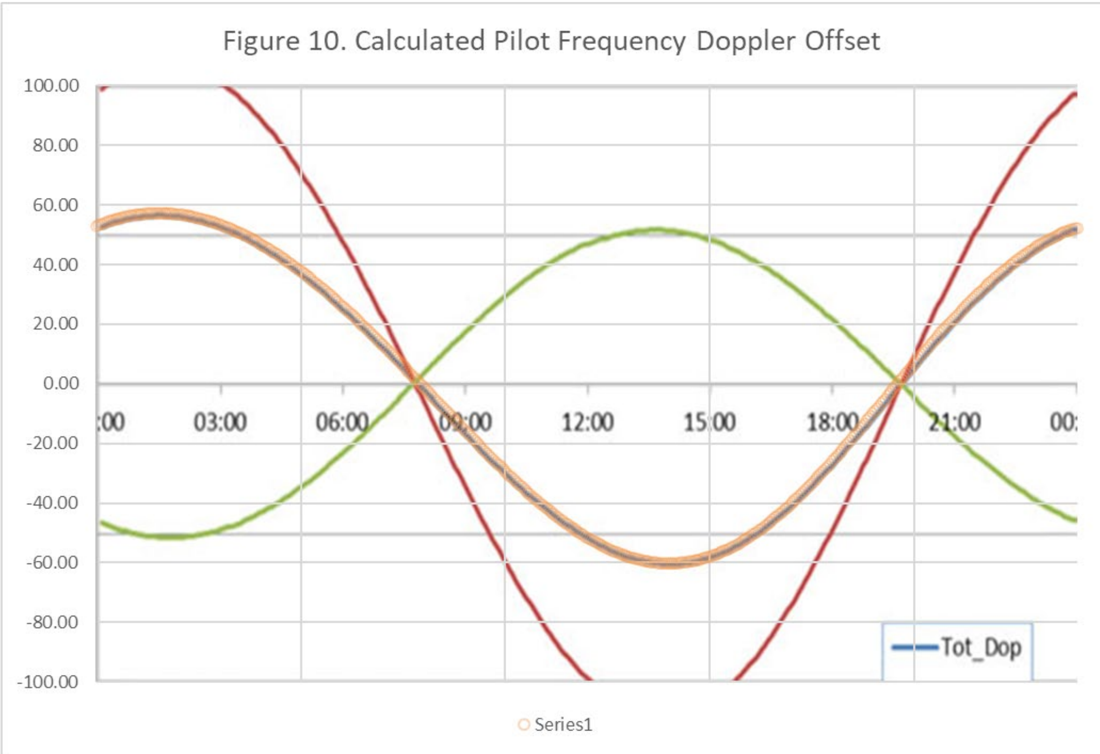

Figure 50: Enhanced modelling of the Calculated Pilot Frequency Doppler Offset

(Orange plot above the original blue)

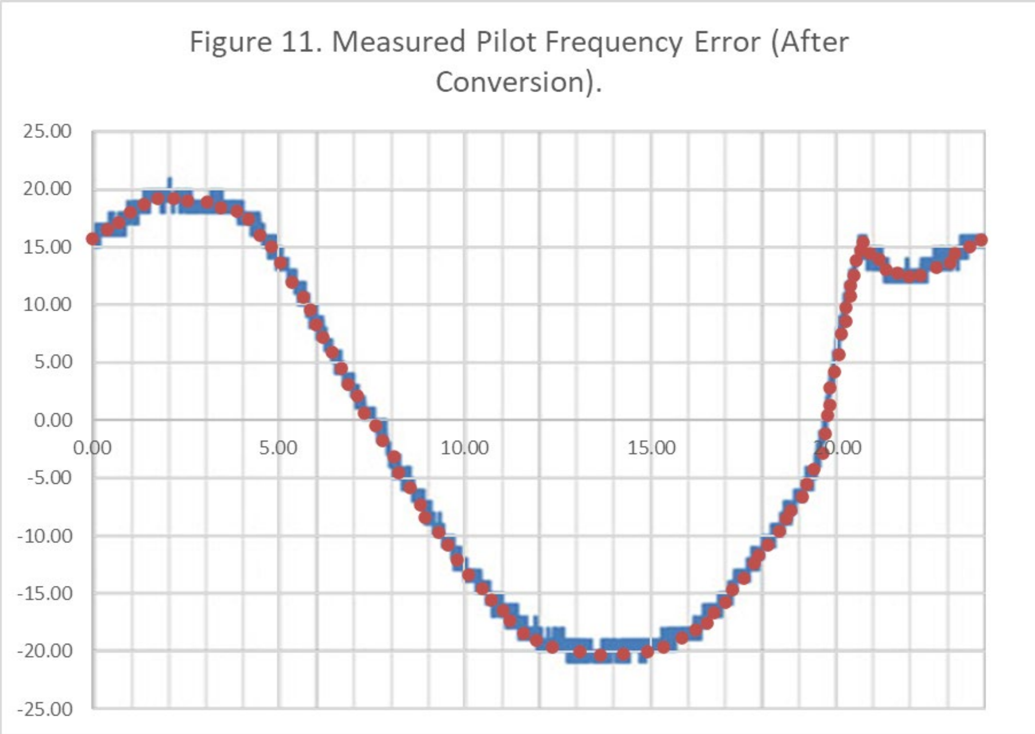

Figure 51: Enhanced modelling of the Measured Pilot Frequency Error (Red)

Please note that in order to be comparable with Inmarsat paper findings a δf bias of 150Hz should be used. Today and after their signal processing analyses, the Independent Group recommends to use 152Hz.

Our computation results for the exact same four Inmarsat first points of Table 9 in [1] show the quality of our tools. They do compare well with Inmarsat figures.